Cocaine Esterase: A pharmacokinetic approach to treating cocaine addiction

by

Joseph Alexander Nichols

A dissertation submitted in partial fulfillment
of the requirements of the degree of
Doctor of Philosophy
(Pharmacology)
in The University of Michigan
2017

Doctoral Committee:

Professor Roger K. Sunahara, Co-Chair
Professor John J.G. Tesmer, Co-Chair
Professor John Traynor
Assistant Professor Barry Grant

Dedication

This thesis is dedicated to all those who try and fail…then get up and try again.

This is also dedicated to all those who struggle with addiction. Though there is no substitute for focus and discipline, everybody needs a helping hand once in a while.

Acknowledgements

Thank you to my mentor Dr. Roger Sunahara. You were a guardian angel and scientific advisor, and you gave me the space and time to develop into whatever it is that I am now.

Thank you to my committee Drs. John Tesmer, John Traynor, and Barry Grant, and past members Drs. Shivaraj Shivamakrisnan and James Woods. You all contributed to this project and my scientific development in so many different ways that I will never be able to say thank you enough.

To the Sunahara Lab, past and present: Drs. Diwahar Narasimhan and Remy Brim, and the great Jimmy Chan, Team CocE! What a great honor it was to work together and share that time and place. Drs. Elin Edwald, Diane Calinski, and Gissele Velez Cruz Ruiz all made coming to the lab a welcoming place and I appreciate all the encouragement to return to graduate school. Dr. Jake Mahoney and (Soon to be Dr.) Osvaldo Cruz, the original members of the Wolf Pack, never forget.

Dr. Nicolas Villanueva: Dr. Villanueva spearheaded the crystallographic efforts contained in this thesis. Without your guidance, support, and sense of humor this whole thing would have been a giant steaming pile of…well, you get the point. So, thank you.

Dr. James Woods: Until our relocation to UCSD, Dr. Woods was my Co-Chair, and he stayed plugged in to me and the project even well after the *in vivo* work was completed. I thank you for all that you did for me, as a technician and as a graduate student. Dr. Woods' lab conducted the *in vivo* experiments contained in Chapter 2 of this thesis. His lab members, Drs. Greg Collins and Holden Ko, as well as, Yong Gong Shi, Erin Gruley, Collette Cremeans all performed the actual mice work, and trained me on mice handling.

Table of Contents

List of Figures

List of Tables

List of Abbreviations

5-HT: 5-hydroxy-tryptamine (serotonin)

BChE: human butyrylcholinesterase butyrylcholinesterase

CocE: Bacterial Cocaine Esterase

CCRQ-CocE: G4C/S10C/T172R/G173Q Cocaine Esterase

CNS: Central nervous system

CPP: Conditioned Place Preference

DA: dopamine

DAT: dopamine transporter

FDA: United States Food and Drug Administration

FPLC: Fast protein liquid chromatography

Hr: Hour

IP: intraperitoneal

IPTG: isopropyl β-D-1-thiogalactopyranoside

IV: intravenous

K_M: concentration of substrate needed to achieve an enzyme velocity one-half the maximum value

MAP: Mean arterial pressure

Min: minute

NE: norepinephrine

NET: norepinephrine transporter

PBS: Phosphate-buffered Saline, pH 7.4

PEG: Poly(ethylene glycol)

PLGA: Poly(lactic-co-glycolytic acid)

RA: Resorufin Acetate

RQ-CocE: T172R/G173Q Cocaine Esterase

SERT: serotonin transporter

SDS-PAGE: sodium dodecyl sulfate-polyacrylamide gel electrophoresis

$t_{1/2}$: half-life

V_{max}: maximum enzyme velocity

WT: wild-type

Abstract

Cocaine's impact on society spans several thousand years, yet its adverse effects due to the toll of addiction have only imposed a global problem during the last hundred years. After cocaine was isolated from its natural source, leaves of a coca plant, it proved to be a "miracle drug" with numerous pharmacological effects. Its potential for abuse quickly became so prevalent that it became one of several drugs targeted by the war on drugs. A standard treatment for cocaine addiction remains elusive though multiple research efforts are currently developing a number of candidates. The majority of pharmacological approaches to treating cocaine addiction offer limited benefits that treat symptoms of addiction and do not curb long term drug seeking behavior once the treatment is over. A number of protein-based therapeutics have shown promise in their ability to hydrolyze cocaine and provide a more pharmacokinetic approach to cocaine addiction. In this thesis, the continued development of a bacterial enzyme - cocaine esterase – will be explored. More specifically, through PEGylation of CocE, the *in vivo* activity of the drug has been extended to over three days of complete protection against a lethal dose of cocaine in mice, providing the best protection to date. Also, through crystallographic studies and mutation of CocE's primary structure, a mutant with the highest velocity of cocaine hydrolysis has been engineered. The results of these studies

demonstrate how CocE continues to prove worthy for the application of cocaine addiction treatment.

Chapter 1

Introduction

Cocaine addiction began in this country soon after it was made available to the public around the end of the 1800s. Since this time, the prevalence of cocaine addiction in society has fluctuated based on the current tastes of drug seekers, but its grip on society has remained entrenched in the population. The ramifications of addiction cover loss of productivity at work and school as well as money spent on treatment and rehabilitation. Unfortunately, no single successful treatment currently exists that can curb cocaine craving in addicts. Providing a readily available and universally accepted treatment would reduce the overall cost of addiction and provide the addicts with a tool to help them return to the state of their lives prior to cocaine craving taking over.

In order to provide a treatment for cocaine addiction, researchers have pursued several different approaches to this problem. Behavioral reconditioning can be effective if addicts adhere to their chosen mode of distraction from drug seeking patterns. Relapse rates remain too high to allow this approach to stand-alone. Advancements in addiction science and pharmaceutical development expand the potential field of treatments from small molecules to protein-based therapeutics. Ingesting higher amounts of cocaine and relying on adherence to treatment regimens now constitute an Achilles heel in both of these approaches

to treatment. For over 10 years we have been developing an enzyme that can address both cocaine toxicity and addiction. This enzyme not only provides immediate reduction of cocaine levels in circulation, but its ability to hydrolyze cocaine rapidly enough will prevent animals conditioned to seek out cocaine stimulation from continuing to pursue this drug. Though this enzyme has passed phase two clinical trials as a treatment for cocaine toxicity, its application as an addiction treatment means that a couple of aspects need addressing. In order to address these deficiencies, a more thorough evaluation of cocaine, its pharmacology, and current modes of treatment should first be evaluated.

Coca plant – discovery and use

Indigenous people from the northwest region of South America found that chewing coca leaves energized their mind and body. The leaves of the *Erythrozyla* genus plants synthesize an alkaloid stimulant, today known as cocaine, and humans began to utilize the leaves several thousand years ago. The *Erythrozylon* coca plant, in particular, produces the most cocaine, but only grows in a specific climate like that found in the northwest region of South America. The financial and cultural importance of these coca leaves caused them to be distributed well outside of this region. [2]

The coca plant's initial importance to human civilization revolved around religion, sex, and war [3-5]. Early Inca mythology surrounding the origins of the coca plant claimed that the first coca plant grew from the remains of a woman that lived a promiscuous life [3]. Her conspicuous actions and lifestyle clashed

with that of her community, ultimately ending in her murder and dismemberment prior to burial. Both the woman and the plant were referred to as “Mama Coca”. A legend inspired by this event alleges that the men of the community would carry bags of coca leaves with them but could partake in the leaves only after engaging in sexual congress with a woman. Another religious account from the area of modern day Columbia, states that early humans sprang forth from the Milky Way the story claims that the first two humans came to earth in a canoe containing three plants - cassava, caapi, and coca. [2, 6]

Coca leaves have been found in the graves of many nobles, warriors, and priests who were interred around the northwestern area of South America. Accounts from the Incan expansion throughout this region tell tales of warriors chewing the coca leaves prior to and during battle. Ancient carvings of the warriors and gods contained swollen cheeks depicting the ritual of coca leaf consumption. [2] Archeological excavations uncovered containers with coca leaf remnants and vessels containing lime (calcium carbonate from roasting shells of shellfish) indicating that ancient Moche and Quimbaya tribes consumed the leaves as early as 4000 years ago. [2]

Amerigo Vespucci, the famous Italian cartographer, noted the swollen cheeks of the first indigenous people he had sighted in the New World. Coca cultivation and usage were initially recorded and published in Europe by Vespucci when he detailed his initial travels to the New World in 1505. [5]

Outside of the religious, battlefield, and bedroom customs, coca leaves were consumed as part of the daily life of the indigenous peoples, either as a tea

or by chewing them throughout the day. Both of these methods of consumption alleviate hunger and provide an energy boost to farmers and laborers. Throughout the Spanish colonization of South America, slaves and indentured servants were given daily allowances of coca leaves to help them work in the gold and silver mines, as well as, on the coca plantations themselves. Taxes collected by the European governors in these areas were often paid in the form of coca leaves, which the self-appointed government officials would then in turn dispense to the locals as payment for services rendered [2].

Though the ritual of chewing coca leaves continues to the present day, the alkaloid compound responsible for all physiological and psychological effects was sought out by a new generation of consumers in Europe shortly after its introduction to the area. Cocaine, [methyl (1*R*,2*R*,3*S*,5*S*)-3- (benzoyloxy)-8-methyl-8-azabicyclo[3.2.1] octane-2-carboxylate], was isolated in the mid-19th century, and soon after, was being synthesized by laboratories and companies looking to profit from cocaine's various effects on the body and mind.

Isolating cocaine

Soon after Europeans gained an appreciation for coca leaves, research efforts began to understand the molecular basis of coca leaves' physiological effects. The cocaine molecule was isolated in 1859 by the German chemist Albert Niemann during his doctoral thesis work. He wrote of the alkaloid's "colourless transparent prisms" and said that, "Its solutions have an alkaline reaction, a bitter taste, promote the flow of saliva and leave a peculiar numbness,

followed by a sense of cold when applied to the tongue." Because of the alkaloid classification of the compound, Niemann named the molecule "cocaine" [7]. Tragically, only one year after his isolation of cocaine, Niemann died due to a lung condition possibly from inhaling the sulfur mustards used during this dissertation research. After Niemann's death in 1861, his colleague, Wilhelm Lossen, continued the research on cocaine and was able to identify the chemical formula of cocaine [4].

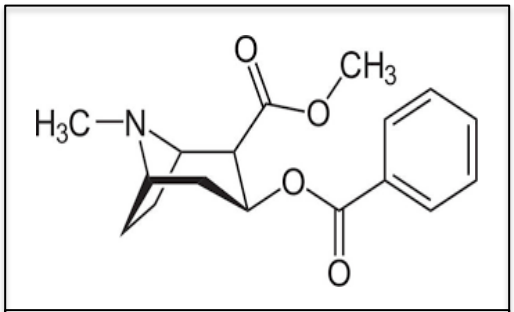

Figure 1.1: Structure of cocaine methyl (1*R*,2*R*,3*S*,5*S*)-3-(benzoyloxy)-8-methyl-8-azabicyclo[3.2.1] octane-2-carboxylate

Cocaine, (2-β-carbomethoxy-3-β-benzoxytropane), contains one internal ester bond shown to be a site of hydrolysis during bodily processing of the drug. The synthesis of cocaine can be achieved through reacting starting materials ecgonine and benzoyl chloride, a process discovered by Richard Willstätter in 1901, with an additional step to add the methyl ester on the tropane ring. Sir Robert Robinson perfected a more efficient method with higher yield in 1917 [3, 8].

Cocaine's use in Europe and in the United States exploded after Dr. Karl Köller demonstrated the use of cocaine as a topical local anesthetic agent for eye surgery in 1884. Due to the success of the surgery, cocaine became available almost overnight throughout the western world and was produced by many pharmaceutical companies. Prior to Dr. Köller's experiment, cocaine was rarely available in the US and was sold, where it could be found, for around one dollar per grain (~65 milligrams). By 1887, the drug was readily available in most drug stores and could be purchased for two cents per grain [4]. Cocaine was added to wines and elixirs designed to promote, enliven, and 'tonify' the mind of consumers. It was even an ingredient in the early forms of the popular beverage CocaCola™.

The two branches of pharmaceutical companies at that time, ethical and patent medicine, produced cocaine both in its powder form and also as a key ingredient to many medical remedies. Most of these remedies came in the form of a liquid tonic that claimed to cure a wide range of disorders from all sorts of physical, mental and emotional natures. Ironically, one of the first uses of cocaine was as a curative treatment for opiate addiction [4].

As the availability and acceptance of cocaine grew, so did its potential for abuse. Doctors found other uses for the drug through its anesthetizing abilities, but they too began to abuse the drug. While some physicians treated ether, alcohol, and opiate addictions with cocaine, more problems arose due to cocaine addiction as a result of these treatments. The transition of cocaine from "miracle

drug" to evil destroyer of society was evident when the drug was included in the Harrison Narcotic Act of 1914 [3, 4].

Though cocaine has never been decriminalized since that time, its use in the United States has never disappeared entirely, and its resurgence in popularity has helped shape popular culture. During the 1950s and 60s, cocaine use increased with the beat and hippie generations iconoclastic approach to "square" living. Drug use had been demonized by society and as these generations began questioning society's view of right and wrong, their exploration of new perspectives included experimenting with mind-altering substances [3].

By the end of the 60' s and through the 70s, cocaine use slackened, around the time that US President Richard Nixon enacted the new federal policy of the "War on Drugs". Cocaine once again became popular in the 1980's club culture. Its widespread use surpassed that of the previous generation, primarily due to the establishment and maturity of South American drug cartels and expanding the production and availability of cocaine. During this time, production in Columbia grew to all-time highs and the illegal supply in this country grew larger than it had ever been [9].

The 1980s also saw the next generation of cocaine evolve as cocaine was formulated into crack cocaine, and the drug took on a whole new face of addiction. When cocaine is mixed with a base (usually ammonia or sodium bicarbonate) and heated it converts to its free base form, and can be smoked

rather than inhaled or injected. This new form of cocaine gives a stronger and faster high compared to the traditional modes of cocaine usage. Crack cocaine is less expensive compared to the powder form and its widespread use amongst the poor and homeless further entrenched the problem in this society [9].

The latest statistics provided by the National Institute of Drug Abuse website show a steady number of people using cocaine in this society over the last several decades. In the 'Monitoring The Future' study, performed at the University of Michigan on public high school children who voluntarily report illicit drug use, almost 30,000 8th grade students (~0.5%) during the 2015 academic year reported using cocaine in the month prior to the study. Respondents who reported using cocaine within the last month are classified as the group most likely to be addicted to cocaine. The number of students using cocaine during the same period increases to over 58,000 students by the 12th grade (~1.1% of all 12th graders nationally) [10].

The Monitoring The Future study has been conducted annually since 1975, and reveals that the percentage of students using cocaine has remained steady for years [10]. To address the larger point, there is a steady number of teenaged students who continue to seek out this drug.

Looking at the US population as a whole, a 2012 study conducted by the Substance Abuse And Mental Health Administration (SAMHA) found that over 1.5 million people, aged 12 and over, used cocaine during the month prior to the study. Over 39 million people in the same age group reported using cocaine at

least once in their lifetime where men are almost twice as likely as women to use cocaine in any form [11].

In 2013, the US government dedicated almost 24 billion dollars on its attempt to control drug use, ranging from treatment and prevention strategies to law enforcement and incarceration for illicit drug use. This amount has climbed to over 30 billion dollars in 2016 [12]. Though this money is primarily focused on dealing with the opiate abuse epidemic in this country, the statistics in the previous paragraphs demonstrate the continued need for drug treatment for cocaine addiction and abuse.

Since its discovery, cocaine consumption has evolved to have several routes of administration - from chewing the leaves, to inhaling the isolated compound, to smoking the free base form. The magnitude of its effect on the body is directly correlated to the concentration that is ingested. This drug has multiple effects on the body, acting on both the brain and the periphery.

Cocaine pharmacology –

The sites of action of cocaine are complex due to it binding at several targets in the body based on the local concentration of the drug ranging from ion channels to monoamine transporters. At lower concentrations cocaine binds to voltage-gated Na^+ channels, blockage of sodium currents in neurons and thus yielding a local anesthetic effect [13]. At higher concentrations, cocaine can inhibit Na^+-dependent monoamine transporters for dopamine, serotonin, and norepinephrine, resulting in sustained high neurotransmitter levels in the synaptic

cleft [14-17]. The reinforcing effects of cocaine are believed to work primarily through the dopaminergic stimulation, but there are several other physiological effects as well.

Ion channel blockade –

Cocaine has been reported to modulate the activity of several voltage-dependent cation channels on neurons, namely sodium, potassium and calcium [18]. Each blockade produces a different physiological response, but the most pronounced is that of the sodium blockade that imparts cocaines local anesthetic activity. Interestingly, researchers have found that cocaine can block sodium channels in several of their recognized conformations: resting, open, or active, unlike most sodium channel modulators that bind and stabilize specific conformations[19]. Although cocaine can bind sodium channels in various conformational states, it prefers the inactive conformation (with resting requiring the highest concentration with a K_i of 328 μM, and the active and inactive states being inhibited at 19 and 8 μM, respectively) [13]. Indeed, binding and stabilization of the inactive state of the channel leads to channel blockade and in heart leads to cardiac arrest, the major toxic effect of acute cocaine overdose [19].

Cocaine has the opposite effect at calcium channels. At pharmacological doses, cocaine enhances calcium current by increasing the channel opening and preventing the closing of the ion channel [20].

Monoamine re-uptake inhibitor

Most of the behavioral effects of cocaine derive from its potency at the sodium-dependent family of monoamine transporters, the primary mechanism of neurotransmitter removal in synaptic termini within the mesocorticolimbic system. Each of the monoamine transporters targeted by cocaine - dopamine (DAT), serotonin (SERT), and norepinephrine (NET) are responsible for removing the specific monoaminergic neurotransmitter from the synapse back in to the presynaptic neuron, arresting signaling at the postsynaptic neuron and maintain proper tone throughout the nerve. The main transporter responsible for cocaine's euphoric properties is DAT; however, its ability to block re-uptake of serotonin and norepinephrine is well established[15, 17, 21-23]

SERT – Cocaine inhibition of SERT has a combination of effects that lead to both the rewarding and aversive aspects of cocaine use [24]. Though cocaine's effect on SERT is not completely understood, rodent knockout models of the serotonin transporter show altered responses to cocaine compared to wild-type animals [25]. More specifically, $SERT^{-/-}$ mice display delayed hyperactivity after cocaine treatment compared to wild type mice, while the same cohort of mice show enhanced conditioned place preference (CPP) compared to WT mice. Taken together, the researchers suggest that cocaine action at SERT contributes to the anxiety and nervousness that accompanies the euphoria of the cocaine

high [26]. The significance of these data, however, are in question as the same group of researchers was unable to repeat the CPP results in SERT KO mice in another study [27].

NET – The potency of cocaine at the NET was demonstrated by transfecting HeLa cells with a functional mutant form of NET. The transporter could perform its role in NE reuptake, and still be bound by certain psychoactive substances previously shown to bind to NET. This triple mutant (NET:F101C-A105G-N153T) displayed the greatest loss of sensitivity to cocaine treatment compared to the other drugs in the experiment seen as a rightward shift in the dose response curve (>1.5 orders of concentration) [28]. The behavioral effect of cocaine through action at NET was demonstrated through NET KO mice. The NET-deficient mice showed hypersensitivity to cocaine treatment compared to WT controls. When NET KO mice receive cocaine treatment, they display increased levels of activity compared to WT mice. Prior to being given cocaine, the NET KO mice showed less activity compared to WT controls [29]. These results suggest that NET plays a role in cocaine addiction, but due to expression of NET in the body, the overall influence NET is believed to affect the cardiac and circulatory response to cocaine.

DAT – The rewarding effects of cocaine arise primarily through the mesocorticolimbic dopamine (DA) system, making the DAT a strong candidate target for the behavioral actions of cocaine . This circuitry is composed of DA

neurons originating in the ventral tegmental area (VTA) of the brain and extending into the nucleus accumbens (NAc), amygdala and prefrontal cortex (PFC) [18, 30]. DAT blockage by cocaine and ensuing increases in dopamine concentration within the synapse produces feelings of euphoria. By repeatedly subjecting the synapse to higher dopamine levels, whether voluntary or not, the dopaminergic tone is reinforced and the animal becomes conditioned to the altered level of synaptic dopamine [18]. Such conditioning reinforces (cocaine) seeking behavior that defines the addictive state.

Although DAT is thought to be the primary target of cocaine that leads to reinforcing behavior in addiction, ablation of the transporter does not completely curb cocaine cravings as seen in work with DAT KO mice. After genetically removing the dopamine transporter in C57Bl6 mice, researchers found that the mice could still be trained to self-administer cocaine, suggesting that other transporters may also be involved [23]. The promiscuity of what is often referred to as a “dirty drug”, through binding several partners ranging from transporters to ion channels, make treating cocaine addiction extremely challenging. From small molecules to entire multimeric protein complexes, the current state of cocaine addiction treatments encompasses a plethora of molecules. Each treatment focusese on either pharmacokinetic or pharmacodynamic approaches, since this section dealt with PD treatments, the next section will focus on PK based therapies.

Cocaine metabolism –

Several enzymes can breakdown cocaine once it is distributed throughout the blood. Human liver carboxyl esterase will convert cocaine into benzoylecgonine through demethylation of the methylester at the 2 position on the tropane ring. This enzyme can also perform a transesterification of cocaine into the toxic metabolite cocaethylene when ethanol is also present in the blood. [31, 32] Cytochrome P450 processing by CYP 3A4 produces norcocaine through demethylation at the nitrogern on tropane. The majority of cocaine metabolism occurs by human butyrylcholinesterase (hBChE). [33] Through hydrolysis of the esterbond connecting the tropane ring to benzoate, BChE produces ecgonine methyl ester and benzoic acid.

Though cocaine can be processed into several different metabolites depending on which enzyme it binds, the fate of the product can be more toxic than cocaine itself. As mentioned above, the combination of cocaine and ethanol can produce cocaethylene that has previously been shown to pose risk to nerve and cardiac cell functioning, as well as, being an immune suppressant. [34, 35] Methylecgonidine can be produced when cocaine is ingested as its free-base form, crack cocaine. This toxic metabolite has shown to be detrimental to smooth muscle functioning in the respiratory tract. [36, 37] Due to the toxicity of certain cocaine metabolites, it is crucial to not only to clear cocaine after ingestion, but avoiding generation of the toxic metabolites is also important in metabolizing this drug.

Treatment for cocaine addiction –

Two distinct approaches to treating cocaine addiction currently exist. The first, and most commonly used, approach involves correcting the addict's behavior by reconditioning them to seek constructive hobbies and pastimes when the urge to use cocaine arises. Since the behavioral reconditioning approach involves a non-pharmacological method to treat cocaine, it will not be considered further in this thesis. While only pharmacologically based addiction treatments will be explored, it is important to note that the effective treatment of cocaine addiction will likely involved the combined use of therapeutics and behavioral reconditioning. The pharmaceutically based treatments can be divided into small molecule therapies that target specific receptors to interfere with cocaine's ability to bind or its effect after binding, and protein-based therapies that can either sequester or metabolize cocaine in the peripheral circulatory system.

Small Molecule therapies

Due to cocaine's ability to bind monoamine transporters, a multitude of drugs have been developed to either interfere with the reuptake inhibition or correct the altered tone of a specific neurotransmitter pathway. This *pharmacodynamic* approach focuses primarily on preventing the body's response to cocaine either by simply inhibiting cocaine binding to its sites of action or by altering neurotransmitter function (mainly dopamine) that leads to reinforcement.

The following list of molecules is not meant to be exhaustive, but more to give an overview of the field's diversity.

L-Dopa: Since the euphoric feelings of cocaine are primarily attributed to the change in dopaminergic tone, correcting this alteration has a considerable amount of attention in the efforts to develop a drug to treat cocaine addiction. Levodopa (L-Dopa)-carbidopa combination therapy has been proposed in order to treat the dopamine deficiency seen in long-term cocaine addicts. L-dopa is converted to dopamine in DA neurons, a process that is enhanced through carbidopa's capacity to decrease L-dopa metabolism. Treatment with dopamine precursors (L-dopa), was therefore thought to reverse the hypdopaminergia in addicts [30]. Unfortunately, this approach showed no clinical efficacy compared to placebo in a double-blind, randomized, human clinical trials, and was not pursued further [38].

Dextroamphetamine (D-AMPH): D-AMPH can also correct hypodopaminergia with the added effect of decreasing post-synaptic dopamine D_2 receptor (D_2DR) activity where enhanced binding of DA at D_2DR is seen in chronic cocaine users [39]. Like cocaine, D-AMPH acts at DAT and inhibits reuptake of DA and increases synaptic DA levels. D-AMPH also efficiently binds the other monoamine transporters, in addition to vesicular transporters as well as trace amine receptors[40]. Other transporter inhibitors that display higher selectivity for DAT over SERT or NET have been shown to correct hypodopaminergia, but

have not proven effective due to abuse liability since their overall physiologic effect mimics that of cocaine itself [39, 41, 42]

Doxazosin: Doxazosin is a long-acting, selective alpha-1 adrenergic antagonist that reduces central NE activity. This molecule will limit the behavioral effects of cocaine and attenuates cocaine-induced reinstatement of cocaine seeking behavior in rats [43, 44]. Though this drug shows promise, it suffers one of the most common problems associated issues with small molecule therapies, compliance. Each drug has to be taken willingly by the addict, and failure to take the drugs to curb addiction often result relapse into cocaine seeking behavior.

Disulfiram (Antabuse): Disulfiram is a copper chelator that is mostly associated with treatment of alcohol addiction through inhibiting acetaldehyde dehydrogenase, the enzyme that converts alcohol metabolite acetaldehyde to acetic acid. Disulfiram also inhibits dopamine-beta-hydroxylase (DβH), an enzyme in the DA synthesis pathway. Disulfiram administration reduces NE levels in the brain that, in turn, reduces stimulation of α1A-adrenoceptors. Reduction of NE tone results in modulation of cocaine reinforcement and decreased cocaine use [45-47]. Unfortunately, more recent studies showed mixed results where some cohorts treated with disulfiram had no better adherence to abstinence versus placebo [46].

Nepicastat: Another NE altering drug, Nepicastat (SYN 117), is a selective DβH inhibitor. This drug attenuates reinstatement of cocaine-seeking behaviors in rats following exposure to several reinstatement protocols, namely – cocaine-

related cues, food prompts, and stress [48]. Oddly enough, this drug showed efficacy in rats but not in squirrel monkeys and the effects of SYN 117 in humans is mixed[49]. While it is capable of attenuating the subjective effects of cocaine, it does not curb craving behavior[50].

Modafinil: Modafinil, another DAT and NET antagonist, increases extracellular glutamate, and decreases cocaine reward and reinstatement [51-53]. In a head-to-head comparison with two other therapeutic approaches, L-dopa/carbidopa and naltrexone, modafinil failed to show a significant decrease in cocaine use compared to controls or between groups [54].

Topiramate: The gamma amino butyric acid (GABA) pathway is involved in decreasing the tone of several neurotransmitters that fluctuate after cocaine use. Topiramate, a GABAa receptor agonist, effectively reduced cocaine craving and use in humans [55-57]. Similarly, vigabatrin, an irreversible GABA aminotransferase inhibitor, showed an ability to inhibit cocaine-induced increases in nucleus accumbens in rats [58, 59]. These approaches have shown the most promise among the small molecule therapeutics.

Others: Research into the serotonergic pathway found that serotonin receptor subtype 5-HT2A is involved in cocaine's physiologic effect. Antagonists at this receptor have shown attenuated cocaine-induced reinstatement of cocaine-seeking behavior; however, the issue of complying with drug treatment has lessened the impact of these findings [60].

Protein-based therapeutics

As promising as some of the above molecules may be, the limitations of therapeutic compounds stem from abuse liability and compliance with treatment [30]. As small molecule therapeutics continue to be investigated, another approach to treating cocaine addiction has come to the forefront of the addiction treatment genre. Biologically derived therapeutics have gained much interest due to their ability to be produced without multiple synthesis steps, production yield, and ability to alleviate compliance issues due to persistence in circulation.

The application of biologics to address cocaine addiction focuses not on the capacity to directly alter the pharmacodynamics of cocaine, but rather to alter cocaine's pharmacokinetics. Small molecule-based therapeutic approaches that attempt to alter the pharmacodynamics of cocaine face the challenges reversing or altering the activity of many of cocaine's molecular targets. The difficultly in dealing with the 'dirty drug' properties of cocaine in itself has complicated the therapeutic approaches have thus yielded limited effectiveness in treating this complicated disease in humans. The focus on altering the pharmacokinetics of cocaine, either through antibody or vaccine-mediated chelation or by accelerating the metabolism and elimination of cocaine, surpasses the multiple-target challenges.

Vaccine: A cocaine vaccine (TA-CD) was developed that contains a cocaine hapten conjugated to inactivated cholera toxin B [61]. This antibody based therapeutic generates an immunologic response that sequesters or chelates cocaine in the circulating periphery. The cocaine is then cleared by endogenous esterases in circulation and then by renal elimination. Though this approach initially showed promise in correcting addictive behavior in lab rats, this strategy is overcome by ingesting larger quantities of cocaine [62].

Enzyme-based metabolism:

Monoclonal 15A10: A cocaine-hydrolyzing monoclonal antibody – 15A10 – displayed the capacity to bind and hydrolyze cocaine to inactive metabolites benzoic acid and ecgonine methylester, the same metabolites that the endogenous enzyme, butyrylcholinesterase, produces. Administration of 15A10 effectively suppressed cocaine self-administration in a rodent model [63, 64]. 15A10 was also capable of attenuating the increase in mean arterial pressure (MAP) in response to cocaine injection, suggesting that the catalytic antibody may also be used as an antidote for cocaine toxicity [65]. Unfortunately the catalytic properties of 15A10 were poor, owing to the slow off-rate of enzyme products (ecgonine methyl ester and benzoic acid) from 15A10. In this paradigm 15A10 behaved as both an enzyme to accelerate cocaine metabolism but also, effectively as a cocaine chelator making the stoichiometry of cocaine:antibody a limitation. Like vaccine treatment the effect of 15A10 was surmountable with higher concentrations (or doses) of cocaine. Due to this

inability to process cocaine efficiently, this approach was deemed not viable as a therapeutic for cocaine addiction [66].

Butyrylcholine esterase: Butyrylcholine esterase (BChE), the enzyme that breaks down the majority of cocaine in circulation, has been extensively pursued as a potential therapeutic[67, 68]. The initial hurdle for this enzyme stems from its poor kinetics for the active sterioisomer of cocaine, (-)-cocaine (~ 4 moles of cocaine per minute). Through several mutagenesis approaches the selectivity for the (-) enantiomer over the inactive (+) enantiomer was substantially improved, as well as improvements in the catalytic properties of the enzyme. As with many protein-based therapeutics, and perhaps more apparent with BChE, the protein itself is extremely difficult to produce in large quantities in a cost-effective manner. In addition, increases in BChE activity is linked to neurodegenerative disorders and the toxicity of Beta-amyloid production [69, 70].

Although more efficient BChE mutants have recently been developed as recombinant molecules with long-term viability, the over-reaching limitation of this enzyme, however, stems from the potential for an immune response directed at the host BChE due to mutations in the BChE protein in circulation [33]. The potential to develop an autoimmune response against host BChE may ultimately limit the usefulness of this biologic in human subjects.

Cocaine Esterase – Evolution, discovery, and development into human therapeutic

While searching for a protein to develop into a biosensor for detecting trace amounts of illicit drugs, a group from the University of Cambridge, England stumbled upon a cocaine-hydrolyzing enzyme during a genetic screen of various bacteria [71]. The enzyme, cocaine esterase (CocE), is expressed in the bacterium *Rhodococcus* MB1. These particular bacteria grow in the soil surrounding the roots of the *Erythrozylon* coca plant, and have evolved to use cocaine as a nitrogen and carbon source after the initial breakdown of cocaine by the cocaine esterase enzyme. Once the gene encoding CocE was isolated and cloned, the initial studies determined the kinetic profile of the enzyme [71]. The first expression of CocE was performed in *E. coli*, and the soluble protein was purified using affinity chromatography.

The purified CocE gene product effectively hydrolyzed cocaine, with a K_M of 1.3 +/- 0.085 μM for cocaine based on HPLC analysis [71]. Subsequent studies determined the kinetic constants of cocaine hydrolysis by CocE to be a k_{cat} of 470 min^{-1} and K_M of 640 nM [72]. This exceptionally high activity toward cocaine is approximately 800-fold higher than the activity of wildtype, endogenous BChE. The actual kinetics of CocE have been a point of contention throughout in the recent literature and has partially focused on the different assays utilized to assess the enzymatic reaction. These two initial reports have a discrepancy of about 4 orders of magnitude. A major difference in the described values relates to the integrity or stability of the enzyme itself. As described below, wildtype CocE is extremely labile at higher temperatures making measurement of enzymatic activity more challenging. In our laboratory,

we have commonly found that freshly prepared wildtype CocE has a K_M for cocaine of about 25 μM with a V_{max} of about 2500 min^{-1}. Outside of the differences in kinetics found by experimentation and enzyme stability (see below), CocE has proven to be the most efficient naturally occurring enzyme able to hydrolyze cocaine.

Structural analysis of CocE by x-ray crystallography suggests that the enzyme is a member of the α/β hydrolase superfamily of proteins. It has three domains in its overall structure – Domain I is the α/β hydrolase fold, Domain II contains seven helices, and Domain III has a jelly roll structure[72]. The

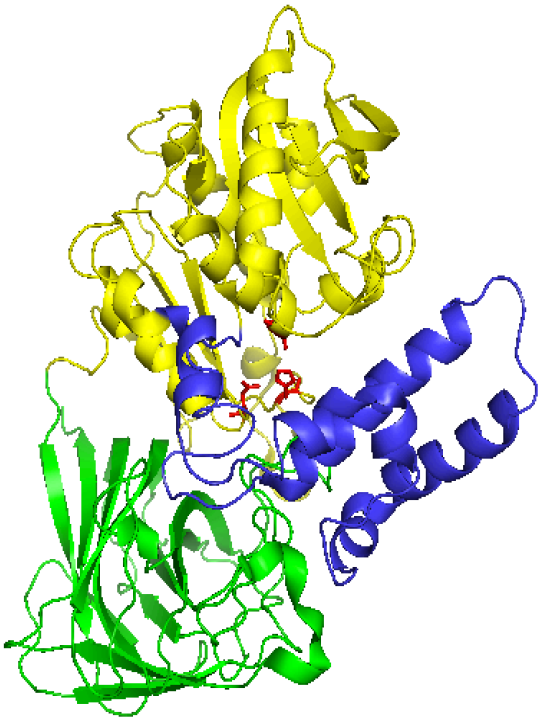

Figure 1-2: Structure of cocaine esterase. The three domains of the CocE monomer are shown in yellow (Domain I), blue (Domain II) and green (Domain III). The catalytic triad is shown in red sticks.

catalytic triad is sandwiched in between the three domains and helix 2 and 3 of Domain II, which form a lid over the triad with their antiparallel orientation. The protein is functional as a dimer, although initial reports claimed that the protein exists as a 65 kDa monomer[71, 73].

The kinetics and production of CocE provide evidence of its potential as a therapeutic candidate for treating cocaine addiction. The recombinant CocE molecule can be expressed as a soluble protein in *E. coli*, reaching yields of 100-200 mg/ml in shake flask cultures. Scaling-up to small fermentation formats (i.e. 10 L) yield of reaching 2-3 g/L can be easily obtained. This is in sharp contrast to the production of recombinant BChE that must be expressed in insect cells cultures (1 mg / L of culture) [74] or in goats milk (0.1 – 5 g / L) [75], the latter requiring the production of a transgenic goat expressing BChE mutants. The superior catalytic properties of CocE and the lower potential to elicit an autoimmune response to this bacterial protein, coupled with the facile production and purification of the enzyme make CocE a far more attractive candidate than BChE.

Thermostability of CocE

Though CocE is a relatively efficient enzyme at hydrolyzing cocaine our laboratory in collaboration with Dr. James Woods (University of Michigan) and Donald Landry (Columbia University) performed the initial *in vitro* activity assay with WT CocE and found it has a half-life of about 12 minutes at 37°C in

phosphate buffered saline (PBS) [76]. This thermolability thus presented significant setbacks to the development of CocE in *in vivo* studies and for it to be considered for use as a therapeutic in humans. We also demonstrated the capacity of CocE to protect rats against a lethal dose of cocaine (180mg / kg), and found the enzyme only showed a protective advantage immediately after CocE administration [77]. We subsequently determined that the enzyme's *in vivo* half-life was approximately 12 minutes [76].

In an attempt to improve the thermostability of CocE our laboratory in collaboration with Dr. Changuo Zhan (University of Kentucky) utilized computational approaches using available x-ray crystallographic data [76]. This analysis demonstrated that the two helices in Domain II conferred the instability of this protein. Following a survey of residues in Domain II by site-directed mutagenesis, we focused on three residues (L^{169}, T^{172} and G^{173}) and that when mutated displayed significant thermal stability. Combining mutations T172R, and $G^{173}Q$ produced an enzyme (RQ-CocE) with a $\tau_{1/2}$ at 37°C of approximately 5.5 hours, using an *in vitro* assay in PBS [76]. Similar time courses were observed using the *in vivo*, protection against cocaine-induced lethality assays. The improvement in $\tau_{1/2}$ at 37°C was approximately 25-27-fold raising the potential of this protein-based therapeutic for the treatment of cocaine addiction and overdose.

While developing the thermostable mutants we further determined that CocE is a dimer, based on size-exclusion column (SEC), as well as x-ray crystallography [78]. We determined that the major dimer interface was located

at enzymes extreme N-termini where beta-strands from each protomer interacted in an anti-parallel fashion and together completed a beta sheet spanning both monomers (Figure 1.3). To stabilize this interface we generated mutant mutants containing two cysteine residues (S^4C & $S^{10}C$) at the N-terminus of each protein, engineered to form two disulfide bonds spanning the dimer interface and effectively crosslinking the two monomers together (CC-CocE). This new engineering effort yielded a enzyme that is stable for over 4 days at 37°C *in vitro*.

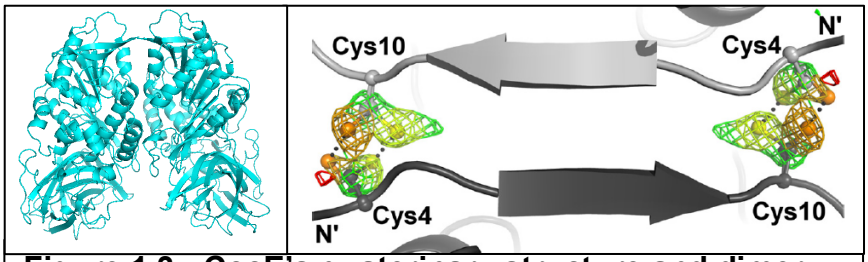

Figure 1.3: CocE's quaterinary structure and dimer interface Left panel shows the dimer form of CocE with monomers facing each other. Right panel - Alignment of CocE's N-termini. The antiparallel beta strands were mutated to cysteine and Fo-Fc electron density demonstrates that thiol groups in opposite strands lie in close enough proximity to form disulfide bonds between the two monomers[1]. (taken from Narasimnhan et al, 2011)

To further enhance the thermostability of CocE, we combined the CC-CocE and the RQ-CocE mutants to generate CCRQ ($S^4C/S^{10}C/T^{172}R/G^{172}Q$-CocE). Combining these mutations provided an unprecedented level of stability at 37°C of over 40 days in saline buffer, and representing an almost 5000-fold improvement over the wild-type enzyme . The sustained duration of *in vitro*

activity of CCRQ at 37°C prompted the *in vivo* studies in various rodent paradigms. The initial studies with CCRQ showed the same level of protection that was observed in earlier CocE studies, where protection against a lethal dose of cocaine was seen immediately after administration but unfortunately no protection was seen after 24-hours of administration [1, 79].

To extend the *in vivo* residency of CocE our laboratory, in collaboration with Dr. Victor Yang (University of Michigan) reported that covalent modification of CocE with polyethylene glycol polymers afforded enhanced activity *in vivo* [80]. We subsequently determined that covalent attachment of PEG (PEGylation) onto CCRQ provided protection of rodents against lethal doses of cocaine for 48 hours post CocE administration using two rodent models of protection against cocaine-induced lethality (Figure 1.4, [1])

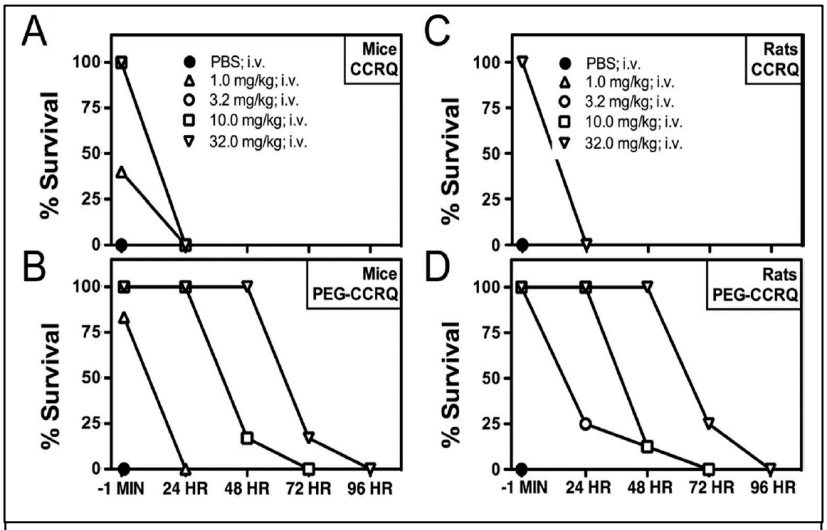

Figure 1.4: Survival curves comparing the *in vivo* results of CCRQ-CocE compared to PEG-CCRQ-CocE. No protection against a lethal dose of cocaine (180 mg/kg) were shown in mice or rats dosed with CCRQ-CocE. All rodents were protected from the same lethal dose of cocaine for 48 hours after administration of PEG-CCRQ.

These exciting data prompted more thorough analysis of the PEGylation of CocE and the effect on *in vivo* life-time. This analysis is the subject of the first Specific Aim of this thesis work. For CocE is to be used as a viable human therapeutic for cocaine addiction, it will require full *in vivo* activity sustained for as many days as possible, to provide the most efficient dosing regimens, minimize compliance issues and reduce production costs.

The kinetics of cocaine hydrolysis by CocE

While developing the thermostable CocE, one combination of point mutations ($L^{169}K$, $G^{173}Q$-CocE, or KQ-CocE) hydrolyzed cocaine two to three times faster than wildtype and the other thermostable mutant, RQ-CocE

(V_{max}~6500 min^{-1} for KQ-CocE versus 2500 min^{-1} for RQ-CocE) [81]. We interpret the increase in thermostability to the Nζ atom of K^{169} where new hydrogen bonding partners with active site waters and new van der Wals interactions with the hydroxyl of Y^{44} are formed which together stabilize the two helices in DOM2. Combined with $G^{173}Q$ there is an overall improvemt in thermostability and an accompanying increase in Vmax through allowing for faster product release and therefore a higher maximal velocity. While this interpretation explains the enhanced V_{max} of KQ-CocE, it does not provide an explanation for the increase in K_M for substrate cocaine.

The enhanced V_{max} of KQ-CocE demonstrated that a more efficient enzyme could be engineered and inspired a more rational structure-based approach to construct a form of the enzyme with even higher catalytic activity. In trying to develop CocE into a potential therapeutic for cocaine abuse, having the most efficient enzyme possible would be highly desirable in order to reduce the dose needed. To that end, we formulated an interrogation of the enzymes active site, assessing the contributions of residues that interact directly with the cocaine substrate. Our goal is to enhance the affinity of the substrate (lower the K_M) or increase catalysis (K_{cat}, or V_{max}) by optimizing the chemistry of catalysis and/or through increasing product release.

Early crystallographic analysis of CocE by Larson and coworkers found electron density in the active site that at the time was modeled as a benzoic acid partial product [72]. Both the high resolution of the structure (1.6Å) and the coordination of this molecule by several aromatic residues suggested that this

density was indeed benzoic acid. Together with the structure of CocE bound to a transition-state analogue (phenylboronic acid), an approximation of the active site, and potentially the substrate-binding site, could be made. While these two structures were informative, it does not quite help us to place the tropane ring of cocaine, arguably the most important moiety that contributes to substrate specificity. Moreover, analysis of the active site reveals a rather large binding pocket that could either accommodate substrates that are considerably larger than cocaine, or alternatively serve as a docking site for cocaine or cocaine-like molecules to bind and transition toward the active site where hydrolysis occurs.

Toward attaining a better understanding the nature of the actual binding site for cocaine we endeavored to generate a high resolution data set and model of CocE bound to non-hydrolyzable cocaine-like molecules. The two compounds, WIN 35065-2 and RTI-150, both contain methylated tropane rings like cocaine, both bind and inhibit DAT, and also behave like cocaine in self-administration models of addiction [82, 83]. In addition we attempted to utilize catalytically compromised mutants of CocE to see if we could trap cocaine bound to the active site(s). Once validated these structures would be extremely valuable for not only delineating the catalytic mechanism of this enzyme but also useful in engineering more catalytically active mutants.

In an attempt to find which residues lay in close enough proximity to the cocaine substrate, we reasoned that a crystallographic image of either cocaine analog bound in the active site would provide this information. After obtaining data sets with either analog bound, and generating a structural models of the

compounds bound to CocE we proceeded to first validate the model by site-directed mutagenesis and then, based on this model identify, several residues that may enhance the enzymes catalytic properties.

We were also fortunate to obtain a high resolution data set of a catalytically impaired mutant CocE ($D^{259}N$) bound not to substrate cocaine but as a transition state bound as a covalent intermediate to the catalytic serine S^{117}. This real intermediate, as opposed to the previously reported transition-state mimic, phenylboronic acid, reveals a significantly different microenvironment around the active site. Using these data we were able to obtain a nice model for the catalytic mechanism of CocE and test this by mutagenesis. Moreover, these data, together with the cocaine analog structures have directed further mutagenesis studies with the goal of engineering a better enzyme.

The crystallography, biochemistry, and enzymology with the goal of creating a more catalytically efficient enzyme are covered in the Second Aim of this thesis.

Specific Aims

Specific Aim 1: Extending the in vivo enzymatic activity of CocE via PEGylation

Due to the short *in vivo* half-life of CocE, covalent attachment of polyethylene glycol (PEG) polymers was performed and shown to extend the duration of *in vivo* protection against cocaine-induced lethality (<24 hours

compared to ~48 hours, with PEG). By first ascertaining the location of what turned out to be a single site of attachment attempts to further extend the *in vivo* activity by adding additional PEGs were successfully performed. Through utilizing a structure-based strategy for targeting specific residues with PEG polymers, we were able to produce mutants displaying longer *in vivo* enzymatic activity.

Specific Aim 2: Active site analysis of CocE using non-hydrolysable cocaine analogs and active site mutants

One of the major goals of research on cocaine esterase as a potential therapeutic for cocaine addiction is to enhance the catalytic efficiency of the enzyme itself. Our observation that one thermostable mutant, KQ-CocE, has a V_{max} that is three times the velocity of our other CocE mutants has inspired us to propose that the catalytic capacity of CocE may be tuned. Structural analysis of the residues within the "binding pocket" that contains the active site triad, provide hints about the location of substrate binding. Though we do not have a structure of cocaine bound in the active site, we have procured two different non-hydrolysable cocaine analogs (WIN 35065-2 and RTI-150) and delineated their structures bound to CocE. To validate this structural model mutations were made at the analog-protein interface and tested for their capacity to alter the catalytic efficient of CocE on cocaine. Using the validated model of the cocaine analog-bound CocE we designed new mutants with the intention of altering (enhancing) the interaction between enzyme and substrate/product with the

hopes of generating a more efficient enzyme. Since the two cocaine analogs are non-hydrolyzable, they serve as inhibitors of CocE. This aim also analyzes the type of inhibition generated by both molecules.

References

1. Narasimhan, D., et al., *Subunit stabilization and polyethylene glycolation of cocaine esterase improves in vivo residence time.* Mol Pharmacol, 2011. **80**(6): p. 1056-65.
2. Karch, S.B., *A Brief History of Cocaine, Second Edition*. 2005: CRC Press.
3. Grinspoon, L. and J.B. Bakalar, *Cocaine: a drug and its social evolution*. 1985: Basic Books.
4. Gootenberg, P., *Cocaine: Global Histories*. 2002: Taylor & Francis.
5. Plowman, T., *Cocaine: A Drug and Its Social Evolution. Lester Grinspoon , James B. Bakalar.* The Quarterly Review of Biology, 1987. **62**(2): p. 224-225.
6. Straughan. *The history of the extraction and study of cocaine*. 2001; Available from: (http://www.chm.bris.ac.uk/webprojects2001/straughan/2.htm).
7. Niemann, A., *Über eine neue organische Base in den Cocablättern: Inaug.-Diss. von Göttingen*. 1860: Huth.
8. Dragon, P. *Puff the Mutant Dragon*. Science on crack: the chemistry of illegal drugs, 1 2011; Available from: https://puffthemutantdragon.wordpress.com/2012/07/22/science-on-crack-the-chemistry-of-illegal-drugs-1/.
9. Reinarman, C. and H.G. Levine, *Crack in America: Demon Drugs and Social Justice*. 1997: University of California Press.
10. Johnston, L.O.M., Patrick. Miech, Richard. Bachman, Jerald. Schulenberg, John., *Monitoring the Future: National Survey Results on Drug Use.* 2016.
11. *<NSDUH-FRR1-2014.pdf>.*
12. Policy, O.o.t.N.D.C., *National Drug Control Budget: FY 2017 Funding Highlights.* 2016.
13. Crumb, W.C., Craig., *Characterization of cocaine-induced block of cardiac sodium channels.* Biophys. J. **57**: p. 10.
14. Beaulieu, J.M. and R.R. Gainetdinov, *The physiology, signaling, and pharmacology of dopamine receptors.* Pharmacol Rev, 2011. **63**(1): p. 182-217.
15. Hall, F.S., et al., *Molecular mechanisms underlying the rewarding effects of cocaine.* Ann N Y Acad Sci, 2004. **1025**: p. 47-56.
16. Howell, L.L. and K.A. Cunningham, *Serotonin 5-HT2 receptor interactions with dopamine function: implications for therapeutics in cocaine use disorder.* Pharmacol Rev, 2015. **67**(1): p. 176-97.
17. Howell, L.L. and H.L. Kimmel, *Monoamine transporters and psychostimulant addiction.* Biochem Pharmacol, 2008. **75**(1): p. 196-217.
18. Johanson, C.E. and M.W. Fischman, *The pharmacology of cocaine related to its abuse.* Pharmacological Reviews, 1989. **41**(1): p. 3-52.

19. O'Leary, M.E. and M. Chahine, *Cocaine binds to a common site on open and inactivated human heart (Na(v)1.5) sodium channels.* The Journal of Physiology, 2002. **541**(Pt 3): p. 701-716.
20. Premkumar, L.S., *Selective Potentiation of L-Type Calcium Channel Currents by Cocaine in Cardiac Myocytes.* Molecular Pharmacology, 1999. **56**(6): p. 1138-1142.
21. Uhl, G.R., F.S. Hall, and I. Sora, *Cocaine, reward, movement and monoamine transporters.* Mol Psychiatry, 2002. **7**(1): p. 21-6.
22. Jayanthi, L.D. and S. Ramamoorthy, *Regulation of monoamine transporters: Influence of psychostimulants and therapeutic antidepressants.* The AAPS Journal, 2005. **7**(3): p. E728-E738.
23. Rocha, B.A., *Stimulant and reinforcing effects of cocaine in monoamine transporter knockout mice.* European Journal of Pharmacology, 2003. **479**(1-3): p. 107-115.
24. Sora, I., et al., *Cocaine reward models: Conditioned place preference can be established in dopamine- and in serotonin-transporter knockout mice.* Proceedings of the National Academy of Sciences of the United States of America, 1998. **95**(13): p. 7699-7704.
25. Fox, M.A., et al., *A pharmacological analysis of mice with a targeted disruption of the serotonin transporter.* Psychopharmacology (Berl), 2007. **195**(2): p. 147-66.
26. Sora, I., et al., *Molecular mechanisms of cocaine reward: combined dopamine and serotonin transporter knockouts eliminate cocaine place preference.* Proc Natl Acad Sci U S A, 2001. **98**(9): p. 5300-5.
27. Hall, F.S., et al., *Cocaine conditioned locomotion in dopamine transporter, norepinephrine transporter and serotonin transporter knockout mice.* Neuroscience, 2009. **162**(4): p. 870-880.
28. Wei, H., E.R. Hill, and H.H. Gu, *Functional mutations in mouse norepinephrine transporter reduce sensitivity to cocaine inhibition.* Neuropharmacology, 2009. **56**(2): p. 399-404.
29. Xu, F.R.R.G., William C. Wetsel2, Sara R. Jones1, Laura M. Bohn1, and Gary W. Miller1, Yan-Min Wang1 and Marc G. Caron, *<Xu_2000_mice lacking NET are supersensitive to phsychostimulants_neurosci.pdf>.* Nature Neuroscience, 2000. **3**(5): p. 7.
30. Shorter, D., C.B. Domingo, and T.R. Kosten, *Emerging drugs for the treatment of cocaine use disorder: a review of neurobiological targets and pharmacotherapy.* Expert Opin Emerg Drugs, 2015. **20**(1): p. 15-29.
31. Brzezinski, M.R., et al., *Human Liver Carboxylesterase hCE-1: Binding Specificity for Cocaine, Heroin, and their Metabolites and Analogs.* Drug Metabolism and Disposition, 1997. **25**(9): p. 1089.
32. Andrews, P., *Cocaethylene toxicity.* J Addict Dis, 1997. **16**(3): p. 75-84.
33. Lockridge, O., *Review of human butyrylcholinesterase structure, function, genetic variants, history of use in the clinic, and potential therapeutic uses.* Pharmacol Ther, 2015. **148**: p. 34-46.
34. Dinis-Oliveira, R.J., *Metabolomics of cocaine: implications in toxicity.* Toxicol Mech Methods, 2015. **25**(6): p. 494-500.

35. Farooq, M.U., A. Bhatt, and M. Patel, *Neurotoxic and cardiotoxic effects of cocaine and ethanol.* J Med Toxicol, 2009. **5**(3): p. 134-8.
36. el-Fawal, H.A. and R.W. Wood, *Airway smooth muscle relaxant effects of the cocaine pyrolysis product, methylecgonidine.* J Pharmacol Exp Ther, 1995. **272**(3): p. 991-6.
37. Chen, L.C., et al., *Pulmonary effects of the cocaine pyrolysis product, methylecgonidine, in guinea pigs.* Life Sci, 1995. **56**(1): p. Pl7-12.
38. Mooney, M.E., et al., *Safety, tolerability and efficacy of levodopa-carbidopa treatment for cocaine dependence: two double-blind, randomized, clinical trials.* Drug Alcohol Depend, 2007. **88**(2-3): p. 214-23.
39. George, T.P., T.A. Kosten, and T.R. Kosten, *The potential of dopamine agonists in drug addiction.* Expert Opinion on Investigational Drugs, 2002. **11**(4): p. 491-499.
40. Jing, L. and J.X. Li, *Trace amine-associated receptor 1: A promising target for the treatment of psychostimulant addiction.* Eur J Pharmacol, 2015. **761**: p. 345-52.
41. Tanda, G., A.H. Newman, and J.L. Katz, *Discovery of Drugs to Treat Cocaine Dependence: Behavioral and Neurochemical Effects of Atypical Dopamine Transport Inhibitors*, in *Advances in Pharmacology*, S.J. Enna and W. Michael, Editors. 2009, Academic Press. p. 253-289.
42. Bisgaard, H., et al., *The binding sites for benztropines and dopamine in the dopamine transporter overlap.* Neuropharmacology, 2011. **60**(1): p. 182-90.
43. Zhang, X.Y. and T.A. Kosten, *Prazosin, an alpha-1 adrenergic antagonist, reduces cocaine-induced reinstatement of drug-seeking.* Biol Psychiatry, 2005. **57**(10): p. 1202-4.
44. Zhang, X.Y. and T.A. Kosten, *Previous exposure to cocaine enhances cocaine self-administration in an alpha 1-adrenergic receptor dependent manner.* Neuropsychopharmacology, 2007. **32**(3): p. 638-45.
45. Shorter, D., et al., *Pharmacogenetic Randomized Trial for Cocaine Abuse: Disulfiram and α(1A)-adrenoceptor gene variation.* European neuropsychopharmacology : the journal of the European College of Neuropsychopharmacology, 2013. **23**(11): p. 10.1016/j.euroneuro.2013.05.014.
46. Carroll, K.M., et al., *Efficacy of disulfiram and Twelve Step Facilitation in cocaine-dependent individuals maintained on methadone: a randomized placebo-controlled trial.* Drug Alcohol Depend, 2012. **126**(1-2): p. 224-31.
47. Baker, J.R., P. Jatlow, and E.F. McCance-Katz, *Disulfiram Effects on Responses to Intravenous Cocaine Administration.* Drug and alcohol dependence, 2007. **87**(2-3): p. 202-209.
48. Schroeder, J.P., et al., *The selective dopamine beta-hydroxylase inhibitor nepicastat attenuates multiple aspects of cocaine-seeking behavior.* Neuropsychopharmacology, 2013. **38**(6): p. 1032-8.
49. Cooper, D.A., et al., *Effects of Pharmacologic Dopamine β-Hydroxylase Inhibition on Cocaine-Induced Reinstatement and Dopamine*

Neurochemistry in Squirrel Monkeys. The Journal of Pharmacology and Experimental Therapeutics, 2014. **350**(1): p. 144-152.
50. De La Garza, R., 2nd, et al., *Evaluation of the dopamine beta-hydroxylase (DbetaH) inhibitor nepicastat in participants who meet criteria for cocaine use disorder.* Prog Neuropsychopharmacol Biol Psychiatry, 2015. **59**: p. 40-8.
51. Ballon, J.F.D., *A Systematic review of modafinil.pdf>.* J Clin Psychiatry, 2006. **67**(4): p. 12.
52. Ferraro, L., et al., *The effects of modafinil on striatal, pallidal and nigral GABA and glutamate release in the conscious rat: evidence for a preferential inhibition of striato-pallidal GABA transmission.* Neuroscience Letters, 1998. **253**(2): p. 135-138.
53. Ferraro, L., et al., *The Vigilance Promoting Drug Modafinil Increases Extracellular Glutamate Levels in the Medial Preoptic Area and the Posterior Hypothalamus of the Conscious Rat: Prevention by Local GABAA Receptor Blockade.* Neuropsychopharmacology, 1999. **20**(4): p. 346-356.
54. Schmitz, J.M., et al., *A two-phased screening paradigm for evaluating candidate medications for cocaine cessation or relapse prevention: modafinil, levodopa-carbidopa, naltrexone.* Drug Alcohol Depend, 2014. **136**: p. 100-7.
55. Reis, A.D., et al., *Craving decrease with topiramate in outpatient treatment for cocaine dependence: an open label trial.* Revista Brasileira de Psiquiatria, 2008. **30**: p. 132-135.
56. Kampman, K.M., et al., *A pilot trial of topiramate for the treatment of cocaine dependence.* Drug Alcohol Depend, 2004. **75**(3): p. 233-40.
57. Johnson, B.A., et al., *Topiramate for the treatment of cocaine addiction: a randomized clinical trial.* JAMA Psychiatry, 2013. **70**(12): p. 1338-46.
58. Schiffer, W.K., D. Marsteller, and S.L. Dewey, *Sub-chronic low dose γ-vinyl GABA (vigabatrin) inhibits cocaine-induced increases in nucleus accumbens dopamine.* Psychopharmacology, 2003. **168**(3): p. 339-343.
59. Brodie, J.D., E. Figueroa, and S.L. Dewey, *Treating cocaine addiction: from preclinical to clinical trial experience with gamma-vinyl GABA.* Synapse, 2003. **50**(3): p. 261-5.
60. Burmeister, J.J., et al., *Differential Roles of 5-HT Receptor Subtypes in Cue and Cocaine Reinstatement of Cocaine-Seeking Behavior in Rats.* Neuropsychopharmacology, 2003. **29**(4): p. 660-668.
61. Fox, B.S., et al., *Efficacy of a therapeutic cocaine vaccine in rodent models.* Nat Med, 1996. **2**(10): p. 1129-32.
62. Kosten, T.R., et al., *Vaccine for cocaine dependence: a randomized double-blind placebo-controlled efficacy trial.* Drug Alcohol Depend, 2014. **140**: p. 42-7.
63. Mets, B., et al., *A catalytic antibody against cocaine prevents cocaine's reinforcing and toxic effects in rats.* Proc Natl Acad Sci U S A, 1998. **95**(17): p. 10176-81.

64. Baird, <*Baird_2000_J Pharmacol Exp Ther-natural and artificial nz against cocaine.pdf*>. J Pharmacol Exp, 2000.
65. Briscoe, R.J., et al., *A catalytic antibody against cocaine attenuates cocaine's cardiovascular effects in mice: a dose and time course analysis.* Int Immunopharmacol, 2001. **1**(6): p. 1189-98.
66. Landry, D.W., et al., *Antibody-catalyzed degradation of cocaine.* Science, 1993. **259**(5103): p. 1899-901.
67. Stewart, D.J., et al., *Hydrolysis of cocaine in human plasma by cholinesterase.* Life Sci, 1977. **20**(9): p. 1557-63.
68. Lockridge, O., et al., *Naturally Occurring Genetic Variants of Human Acetylcholinesterase and Butyrylcholinesterase and Their Potential Impact on the Risk of Toxicity from Cholinesterase Inhibitors.* Chem Res Toxicol, 2016. **29**(9): p. 1381-92.
69. Mack, A. and A. Robitzki, *The key role of butyrylcholinesterase during neurogenesis and neural disorders: an antisense-5'butyrylcholinesterase-DNA study.* Prog Neurobiol, 2000. **60**(6): p. 607-28.
70. Ballard, C.G., *Advances in the treatment of Alzheimer's disease: benefits of dual cholinesterase inhibition.* Eur Neurol, 2002. **47**(1): p. 64-70.
71. Bresler, M.M., et al., *Gene cloning and nucleotide sequencing and properties of a cocaine esterase from Rhodococcus sp. strain MB1.* Appl Environ Microbiol, 2000. **66**(3): p. 904-8.
72. Larsen, N.A., et al., *Crystal structure of a bacterial cocaine esterase.* Nat Struct Biol, 2002. **9**(1): p. 17-21.
73. Narasimhan, D., J.H. Woods, and R.K. Sunahara, *Bacterial cocaine esterase: a protein-based therapy for cocaine overdose and addiction.* Future Med Chem, 2012. **4**(2): p. 137-50.
74. Brazzolotto, X., et al., *Human butyrylcholinesterase produced in insect cells: huprine-based affinity purification and crystal structure.* Febs j, 2012. **279**(16): p. 2905-16.
75. Huang, Y.J., et al., *Recombinant human butyrylcholinesterase from milk of transgenic animals to protect against organophosphate poisoning.* Proc Natl Acad Sci U S A, 2007. **104**(34): p. 13603-8.
76. Gao, D., et al., *Thermostable variants of cocaine esterase for long-time protection against cocaine toxicity.* Mol Pharmacol, 2009. **75**(2): p. 318-23.
77. Cooper, Z.D., et al., *Rapid and robust protection against cocaine-induced lethality in rats by the bacterial cocaine esterase.* Mol Pharmacol, 2006. **70**(6): p. 1885-91.
78. Narasimhan, D., et al., *Structural analysis of thermostabilizing mutations of cocaine esterase.* Protein Eng Des Sel, 2010. **23**(7): p. 537-47.
79. Collins, G.T., et al., *Repeated administration of a mutant cocaine esterase: effects on plasma cocaine levels, cocaine-induced cardiovascular activity, and immune responses in rhesus monkeys.* J Pharmacol Exp Ther, 2012. **342**(1): p. 205-13.
80. Park, J.B., et al., *PEGylation of bacterial cocaine esterase for protection against protease digestion and immunogenicity.* J Control Release, 2010. **142**(2): p. 174-9.

81. Brim, R.L., et al., *A thermally stable form of bacterial cocaine esterase: a potential therapeutic agent for treatment of cocaine abuse.* Mol Pharmacol, 2010. **77**(4): p. 593-600.
82. Desai, R.I., et al., *Identification of a dopamine transporter ligand that blocks the stimulant effects of cocaine.* J Neurosci, 2005. **25**(8): p. 1889-93.
83. Carroll, F.I., et al., *Cocaine and 3 beta-(4'-substituted phenyl)tropane-2 beta-carboxylic acid ester and amide analogues. New high-affinity and selective compounds for the dopamine transporter.* J Med Chem, 1995. **38**(2): p. 379-88.

Chapter 2

Strategic Targeting Of Poly(ethylene glycol) To Cocaine Esterase For Development Into A Protein-based Amelioration Of Cocaine Addiction

Introduction

Cocaine addiction remains prevalent in today's society. According to current statistics, around 1.6 million people in the United States fit the criteria of a cocaine addict[1]. To compound this problem, one in one hundred teenagers fit the classification of a cocaine addict. According to the Monitoring the Future Study, conducted in 2014, almost 30,000 students in the 8^{th} grade reported using some form of cocaine in the last month, with the number increasing to over 58,000 for 12^{th} grade students [2]. More urgently, there was a 42% increase in the number of cocaine related deaths between 2001 and 2014. Approaches to treat cocaine addiction have been developed over the last several decades; however, none have proven successful as seen through the prevalence of addiction. Cocaine antagonists at two of its major sites of action, the dopamine transporter and the voltage-dependent Na^{+}-channel, unfortunately displayed similar efficacy as cocaine and both blocked the channel and the transporter[3, 4]. Anti-cocaine antibodies (catalytic and non-catalytic) and vaccines have represented attractive avenues to reverse cocaine's bioavailability *in vivo* but

unfortunately proved to be surmountable by higher doses of cocaine [5]. Alternatively, we and others have taken a protein-based enzymatic approach to modify the pharmacokinetics of cocaine and accelerate its metabolism to inactive metabolites benzoic acid and ecgonine methyl ester (Reviewed in [6]). *In vivo* studies in rodents with CocE suggested that it could protect against cocaine-induced cardiovascular, respiratory and CNS effects, and even lethality [7-9]. Despite the effectiveness of WT-CocE the enzyme is thermolabile with a $t_{1/2}$ ~15 min at 37C, limiting its full potential as a therapeutic [8].

To circumvent the thermostability issues we first incorporated a protein structure-based approach to identify regions of thermolability and successfully generated a thermostable mutant (known as RQ-CocE) that retained its endogenous enzymatic activity at 37°C in assay buffer [8].The thermostable form not only protects against cocaine-induced cardiovascular and respiratory effects that lead to lethality but can diminishes self-administration of cocaine in both primate and rodent models [9-11]. In addition, RQ-CocE is capable of rescuing rodents pre-administered with otherwise toxic doses of cocaine suggesting that the enzyme has therapeutic potential for cocaine overdose. CocE was also tested for its capacity to restore cardiovascular function following cocaine-administration in rhesus monkeys [12]. More recent positron emission tomography studies using labeled cocaine suggest that systemically administered CocE can accelerate the removal of cocaine from the CNS [13].

More significantly, CocE has been tested in humans for its capacity to accelerate cocaine removal supporting CocE's potential as an antidote for

cocaine overdose/toxicity [14]. In these extremely encouraging Phase II clinical trials RQ-CocE accelerated the reduction of systemic cocaine levels nearly 10,000-fold faster than vehicle. We look forward to seeing RQ-CocE advance to Phase III trials.

We also determined that CocE forms a symmetrical dimer and determined that dimer disruption leads to protein aggregation and enzyme inactivation. Using x-ray crystallography we delineated the dimeric nature of the enzyme and the dimer interface. Through the strategic incorporation of cysteine residues on the amino terminus on each protomer, the major participant of the dimer interface, we engineered two disulfide bridges spanning the interface. The crosslinked dimer (known as CC-CocE) exhibited superior thermal stability in *in vitro* assays ($t_{1/2}$~12 hours at 37°C) [15]. Through combining both RQ-CocE and CC-CocE mutants, we constructed the most thermostable CocE mutant to date, CCRQ-CocE, which retains full *in vitro* enzymatic activity for over 40 days after incubation at 37°C in buffered saline [15].

More recently we demonstrated that CCRQ-CocE potently abrogates cocaine self-administration, a model cocaine addiction and drug seeking behavior in rats, supporting its potential as a treatment for cocaine [12]. Suppression of self-administration along with behavioral therapy could represent a major breakthrough in treatment of cocaine addiction.

Our initial studies in rodents with CCRQ-CocE found that its in vivo activity disappears in less than 24 hours. Modification of CocE with branched polyethylene conjugates of maleimide (PEGylation) extended this $t_{1/2}$ to greater

than 48hrs in both rat and mouse models [15]. In this current study we have ascertained the location of the surface cysteine residues that are PEGylated and, with the aid of high-resolution structural models of CocE, hypothesize that current PEGylation strategies cover only a portion of the enzyme. Incomplete PEG coverage would have less than optimal 'stealth' properties and be more susceptible to immune surveillance and/or proteolysis. In this chapter, we describe the use of structural information on CocE to guide the strategic placement and number of PEG moieties on CocE and its enhanced effect on $t_{1/2}$ in rodents.

Early studies with CCRQ-CocE suggested that the enzyme's *in vivo* activity disappears within 24 hours. To extend the *in vivo* residency time we incorporated a stealth approach to elude immune surveillance or proteolysis, utilizing covalent modification of CocE with polyethylene glycol (PEG) polymers. PEGylation of RQ CocE does not inhibit the enzymatic activity and protects against cocaine toxicity as effectively as un-PEGylated CocE [16]. Due to the relative instability of RQ-CocE, we then pursued PEGylation of CCRQ-CocE since this is the most stable form of CocE to date. Our initial study found that PEG:CCRQ-CocE protects rodents against a lethal dose of cocaine for up to 48 hours [15]. In this current study we assess whether PEGylation of CocE could be enhanced and whether the enhancement yields an extended *in vivo* residency time. The key questions that we aim to answer in the current study are: 1) Where is CocE being PEGylated?, 2) Does adding more PEG molecules per monomer of CocE prolong *in vivo* activity? and 3) How does the size and shape

of PEG effect the protection of CocE *in vivo*? We utilize site-directed mutagenesis to map the PEGylation and combine analysis of the enzyme's crystal structure to guide the placement of additional PEG moieties of varying complexities.

Methods

Generation of CocE point-mutants: Oligonucleotides (IDT, San Diego, CA) were designed based on the crystal structure of CCRQ-CocE [15] and used in a modified Quickchange™ protocol (Stratagene, La Jolla, CA) to replace a specific codons in the CocE nucleotide sequence (Oligo sequences listed in Table 1 of the Supplemental data section). We utilized bacterial expression vectors (pET23) containing the currently most thermostable mutant of CocE, CCRQ-CocE, as a template for the mutagenesis studies [15]. The expressed protein has a Hisx6 tag at the amino-terminus to facilitate protein purification. Sequences for all mutant plasmids were confirmed by DNA sequencing.

Production of CocE: BL21 *E. coli* cells expressing recombinant forms of CocE were grown in Terrific Broth media at 37°C to an OD_{600} of 0.8. Protein expression was induced by adding isopropyl-b-thiogalactopyranoside (IPTG) to a final concentration of 1 mM. Expression was carried out at 18°C for 12-15 hours. At the end of induction, the cells were pelleted by centrifugation (5000 x g), resuspended in 50 mM Tris-HCl, pH 7.4 at 4C, 135 mM NaCl and 5 mM KCl (1 X

TBS), supplemented with protease inhibitors (PIs) (3 mg/mL each of leupeptin and lima bean or soybean trypsin inhibitor). Cells were lysed using a French press (Thermo Scientific) and particulate fractions were removed by ultracentrifugation and the supernatant, containing CCRQ-CocE mutants were captured using Talon™ metal chelation affinity chromatography (Clontech Laboratories, Inc.) and eluted with 1XTBS containing PIs and 100 mM imidazole. Fractions containing CCRQ-CocE mutants were subjected to oxidation using 100 μM $CuCl_2$ (4°C overnight) to covalently link the CocE dimer. The oxidized protein was further purified using anion-exchange chromatography (Q-Sepharose) fast performance liquid chromatography column (GE Healthcare). CCRQ-CocE mutants was eluted with a 150–450 mM NaCl linear gradient in buffers containing 50 mM Tris-HCl, pH 8.0. The peak fractions were pooled and concentrated to 5 mg/ml using Centricon™-30 concentrators (Millipore), and then snap frozen in liquid nitrogen and stored at -80°C.

PEGylation of CCRQ-CocE mutants: CCRQ-CocE mutants were dialyzed into 1X TBS, pH 6.5 (at 4C), prior to PEGylation. 5K, 10K, 15K and 20K-branched polyethylene glycols (PEGs) were purchased from JenKem Inc. (JenKem Technology USA, Plano, TX). PEG was added to the protein solution at 5:1 molar excess and the reaction proceeded for 4 hr at room temperature. The PEG:CocE was purified on a Q-Sepharose Fast Flow column and eluted with a linear gradient of NaCl between 150-450 mM. The fractions from the first elution peak were pooled and concentrated to 10 mg / ml prior to use.

SDS-PAGE analysis of PEG:CocE: CocE mutants were resolved by SDS-PAGE under reducing and non-reducing conditions (where noted) on a 6 % acrylamide gel and detected by coomassie blue staining.

Activity assay of PEG:CCRQ-CocE mutants: Purified, PEGylated CCRQ-CocE mutants were analyzed using an UV absorbance-based cocaine hydrolysis assay as described previously [12]. Here, cocaine (Mallinckrodt, Hazelwood, MO) is added a 96-well UV-permeable plate (Costar; Corning Life Sciences, Lowell, MA) at 200, 100, 50, 25, 10, 5, 1 and 0.5 μM concentrations. The reaction is initiated by the addition of CocE (65 ng/ml, or 32.5 ng/ml final) at a 1:1 dilution in the plate. The velocity of the reaction was measured every 10s for 20 minutes by a SpectraMax Plus 384 UV plate reader (Molecular Devices, Sunnyvale, CA) using OFTmax Pro software (version 3.1.2). The absorbance readings were converted to change in concentration of product using using Beer's law. The specific activity of the enzyme was plotted using Prism software (GraphPad Software Inc., San Diego, CA) and kinetics of the reaction (k_{cat} and K_m) generated.

In vivo analysis of PEG:CCRQ-CocE: Male wildtype NIH Swiss mice (Harlan Inc., Indianapolis, IN) (25-32g) were housed under the guidelines of National Institutes of Health according to the *Guide for the Care and Use of Laboratory Animals* (Institute of Laboratory Animal Resources, 1996). Mice were housed

five mice per cage and allowed ad libitum access to food and water, and they were maintained on a 12-h light/dark cycle. The University Committee on the Use and Care of Animals (UCUCA) at the University of Michigan approved all experimental protocols. In each survival study, mice were given PEG:CCRQ-CocE at 32 mg / kg body mass via tail vein injection. Cocaine (Mallinkrodt) was dissolved in 1X PBS, pH7.4 and passed through a sterile syringe prior to intra peritoneal administration into mice. Purified preparations of CocE were administered 30 min prior to challenge with cocaine (180 mg/kg i.p. cocaine injection). Animals were re-challenged with cocaine every 24 hours following the administration of the CocE enzyme.

Results

Cocaine esterase, CocE, is an alpha-beta hydrolase that effective metabolizes cocaine into inactive metabolites ecgonine methylester and benzoic acid. We have previously demonstrated the effectiveness of CocE to reduce the dangerous cardiovascular and neurological effects of administered cocaine [17, 18]. Indeed, administration of CocE not only rescues rodents from lethal doses of cocaine (toxicity) but it can also effectively suppress many models of cocaine self-administration [15, 17, 19, 20]. Here we extend our investigation on the effectiveness of PEGylation, a technique effectively used to prolong the *in vivo* half-lives of many biologics and drugs [21], to prolong the *in vivo* half-life of CocE. Short and long-chain PEG polymers, as well as large, branched versions

covalently incorporated onto proteins serve as a stealthy means to evade the immune surveillance system, as well as in some cases stabilizing the protein itself [22, 23]. The latter characteristic is likely the result of protection against protease accessibility that would normally lead to degradation. Likewise, we have previously reported on the capacity of PEGylation to prolong CocEs *in vivo* activity up to 48 hrs, representing more than a two-fold improvement over the non-PEGylated form [15].

While these studies were valuable we sought to increase the stealth-like effects of PEGylation of CocE using a more systematic approach. By first assessing which native cysteine residue(s) incorporate maleimide-conjugated PEGs we proceeded to utilize available structural information to engineer mutant forms of CocE to increase the PEG:CocE stoichiometry and thereby enhance the surface area of protection by PEG polymers. More complete coverage should provide better stealth properties for the enzyme and result in longer *in vivo* lifetime.

Site of PEG attachment and activity of PEG:CCRQ-CocE*:* We have previously described the use of maleimide-coupled PEGs to PEGylate CocE. We prefer maleimide labeling over amine-coupling since there are only 4 cysteine residues (Cys^{107}, Cys^{429}, Cys^{477} and Cys^{551}) in total per CocE protomer, as opposed to amine-coupling to a possible nine lysine residues. Moreover, CocE, exists stably as a dimer, and has yet to be isolated as a monomer. As we and others have demonstrated disulfide-mediated cross-linking and stabilization of

the dimer has been shown to significantly thermally stabilize the enzyme suggesting that the monomeric form is unstable [15], [24]. We therefore prefer not to risk interfering with the dimer interface with the placement of PEG polymers.

In order to elucidate where PEG is attaching to CocE, we first generated a CocE mutant where all four cysteine residues were mutated to serine (CCRQ-CocE-D^{4}C) and then sequentially restored the cysteines one residue at a time using the CCRQ-CocE backbone. While all mutants express, purify and display wild-type catalytic activity, only the mutant containing Cys^{551} efficiently accommodates a 40kDa branched PEG, as indicated by the large shift in the migration time through the SDS-PAGE gel (Figure 1). The gel shift was larger than expected for the addition of a 40 kDa PEG polymer however its aberrant retention time likely exacerbated by the charge to mass ratio of PEG and its poor capacity to bind SDS. Mutants C^{107}S, C^{429}S, and C^{477}S do not appear to couple to PEG similar to CCRQ-CocE-D^{4}C. Through the process of elimination we determined that only Cys^{551} is PEGylated in CCRQ-CocE, and likely in all of our previous PEGylation studies.

The CCRQ-CocE (551) was PEGylated and resolved by anion exchange chromatography (Q sepharose) into 2 major and 2 minor peaks (see Supplemental data Figure S1, upper panel). SDS-PAGE analysis of the peaks under non-reducing conditions reveals that the two major peaks (peak 2 and 3 in Figure S1) displayed considerable gel shifts compared to the unPEGylated peak 4. We surmise that the peak 3 contains only one PEG polymer per CocE dimer

whereas peak 2 contains two (*ie.* 1 PEG per CocE monomer). Fractions contained in peak 2 were used for all subsequent experiments. Peak 1 displayed no enzymatic activity (data not shown) that we suspect is simply dead protein.

The purified PEG:CCRQ-CocE (C^{551}) was subjected to our standard cocaine hydrolysis assay using non-PEGylated CCRQ-CocE as a control. The results are plotted in Figure 2 and indicate indistinguishable effects on PEGylation on the catalytic properties of CCRQ-CocE (V_{max} ~2012 +/- 57 moles of cocaine per minute and K_M of ~13.8 +/-1.1 μM) and PEG-CCRQ-CocE (V_{max} ~1982 +/- 54 per minute and K_m of ~13.0 +/-1.01 μM).

Single-site PEGylation at position 551 offered protection from cocaine-induced lethality for 48 hrs relative to unPEGylated versions, which provided less than 12 hours of protection against cocaine-induced lethality (see Figure 2.5), in good agreement with previous studies [15].

Incorporation of additional PEGs - Strategic attachment of PEG to CocE:

Once we established Cys^{551} as the primary cysteine that accommodated the maleimide-PEG in wt-CocE (or CCRQ-CocE), our intent was to incorporate additional cysteine residues to accept PEG polymers in order to further extend the *in vivo* duration of the enzyme's activity. Our residue selection was based on maximizing the possible solvent accessible surface area of CocE that PEG moieties could 'protect' but still allow accessibility of the PEG polymers to the substrate cysteine residue. Figure 2.3A depicts the x-ray crystal structure of the CocE dimer highlighting the enzymes three distinct domains: Domain 1 (yellow,

aa 1-144, aa 241-354), Domain 2 (blue, aa 145-240), and Domain 3 (green, aa 354-574). The figure also highlights regions on the surface of the enzyme that are likely protected by PEGylation of Cys^{551} alone, indicated by the transparent sphere (in panel A). We selected nine candidate surface residues on the CocE dimer that are within the large surface area that are not likely protected by PEGylation of Cys^{551}. The candidate residues, modelled in red spheres in panels B (side view) and C (top view) were individually mutated to cysteines, expressed and purified and tested for enzymatic activity (summarized in Table 2.1). Those mutant enzymes that expressed well and exhibited full esterase activity were then PEGylated and subjected to *in vitro* (enzyme activity assays) and *in vivo* survival assay in mice using the cocaine-induced lethality model.

As indicated in Table 1 the best performing mutants with 2 PEG molecules attached per monomer were $A^{92}C$ and $A^{330}C$. The loss of protection against cocaine-induced lethality suggests that the second PEGylation site at residue 330 provided no additional protection over the single PEGylation (Figures 2.4 and 2.5A). In contrast, incorporating an additional PEG moiety at residue 92 provided greater than 72 hours of protection against cocaine-induced lethality, an additional 24 hours of protection upon addition of another PEG moiety.

Since PEGylated CCRQ-CocE $A^{92}C$ performed best in the survival assay, this construct was used as the template for generating CocE mutants containing one additional PEG molecule per monomer (three total). Here we attempt to utilize the crystal structure to guide the placement of a third PEG moiety, a process largely based on regional instability (*ie.* high anisotropy or high B- or

temperature-factor) and on their solvent accessibility. Figure 2.4 illustrates the structure of the CocE dimer rendered to highlight the regional instability. This rendering illustrates the anisotropic regions as a function of B-factor and is indicated by the thickness of the polypeptide chain and also by the color-coding, or heat map (red has the highest B-factor whereas blue has the lowest). Candidate residues were selected on regions of the enzyme that displayed high B-factors, with the assumption that unstructured regions might be more sensitive to proteolysis in the peripheral circulatory system. In addition, these regions may likely incorporate a PEG moiety more efficiently without perturbing the structure and hence enzyme activity. Indeed, incorporation of a third PEG moiety on most of the candidate residues did not appear to affect enzyme activity (Table 2.2). Unfortunately, with the exception of CCRQ-CocE $A^{92}C/S^{179}C$, all other triple mutants appeared to provide less protection against cocaine-induced lethality than CCRQ-CocE $A^{92}C$ (Figure2.5B). Moreover, the addition of a third PEG moiety per monomer of CocE (CCRQ-CocE $A^{92}C/S^{179}C$) did not appear to provide substantial additional protection over the PEGylated CCRQ-CocE $A^{92}C$ form of the enzyme (Figures 2.5B and 2.7).

Analysis of PEG polymer length*:* We previously demonstrated that branched 40 kDa PEG polymer covalently labelled RQ-CocE [16] and CCRQ-CocE [15] prolonged *in vivo* half-life. In this current study we compared the 40 kDa branched PEG polymer with linear 5, 10, and 20 kDa PEG molecules (Figure 2.6) using CCRQ-CocE $A^{92}C/S^{179}C$ as a substrate. Longer PEG polymers appear to

provide better protection with the branched 40 kDa PEG polymer providing the most effective protection against cocaine-induced lethality. While 10 and 20 kDa PEGs could maintain *in vivo* enzyme activity and provide protection against cocaine-induced lethality for 24 and 48 hrs, respectively, the branched 40 kDa PEG polymer could protect for greater than 72 hrs. Unfortunately we were unable to test branched PEG at less than 40 kDa nor linear 40 kDa PEG as they are not available from commercial sources.

Discussion

Since we were not able to provide dramatic enhancements in *in vivo* protection through adding more than 2-3 PEG per monomer versions of CocE, we speculate that we have achieved the maximum protection from this approach. Similar observations were recently reported in another thermostable form of CocE [24]. Analysis of the structure of the CocE dimer suggests that attachment of three PEGs to each monomer will cover most of the surface of the dimer (Figure 2.7 B). Specifically, one PEG molecule was placed on each of the three domains of CocE: $A^{92}C$ in Domain I, $S^{179}C$ in Domain II, and Cys^{551} in Domain III. The three residues are located on only one face of each monomer however since the dimer is arranged with 2-fold symmetry, the enzyme is protected.

The observation that position $S^{179}C$ offered the stronger protection in our 3 PEG per monomer group is intriguing. Our earlier studies on developing a thermostable form of CocE, [25], found that Domain 2 of this protein (residues

145-240) has the highest flexibility that could lead to thermal instability. Thus, generating $L^{169}K$ or $T^{172}R$ coupled with $G^{173}Q$ gave rise to the most thermostable mutant at that time. It would follow that adding a large, flexible molecule such as a PEG polymer to this domain might perturb the structure enough to inactivate that protein through reversing the stability gained with the double mutation (RQ). Such was not the case as the $S^{179}C$ in the RQ background was fully active protein and offered the best *in vivo* protection, suggesting that the large but flexible PEG moiety did not perturb the structure of this helix-loop-helix.

Figure 2.7 also illustrates that one region of the CocE dimer, located on the 'back-side' of the Domain 3 is relatively unprotected. Analysis of mutants illustrated in Figure 2.4B suggests that placing PEG moieties on positions 384 and 436 should provide a more extensive coverage of the dimer. Unfortunately, the $G^{384}C$ mutant displayed poor enzymatic activity and was not tested for PEGylation or any subsequent in vivo experimentation. Similarly, the $T^{436}C$ mutant, despite displaying wild-type enzymatic activity prior to PEGylation, appears less effective at protecting against cocaine-induced lethality even at early time points, suggesting that PEGylation of residue 436 was deleterious.

The application of cocaine esterase as a therapeutic to accelerate the metabolism of systemic cocaine has shown significant clinical potential. Indeed, the use of thermal stable mutants of this enzyme has progressed past Phase II clinical trials as a therapeutic, or rather antidote, against cocaine-induced toxicity. The protein half-live *in vivo* and *in vitro* is approximately 4-5 hrs [8], certainly long enough to allow for acute administration to lower systemic cocaine levels well

below toxic levels. While we are thrilled that this enzyme is showing strong clinical potential to save cocaine overdose victims, our long-term goal with this project is to develop a protein-based therapy that can be applied to cocaine addiction, a procedure that would require good patient compliance or the use of therapeutics with long *in vivo* half-lives [14]. We have previously demonstrated that CocE administration in rats trained on cocaine can curb their craving for the drug in a dose dependent manner [19, 20]. These studies also suggest that CocE will be a more realistic therapeutic if it has a *longer in vivo* activity. In this current study we utilized a structure-based strategy to engineer a form CocE that efficiently accommodates the stealth-like properties of PEG polymers, in order to evade systems of immune surveillance and proteolysis and to extend the *in vivo* half-life. Our ability to provide more than 72 hours of protection against cocaine-induced lethality following a single administration of our best version of PEG:CocE, suggests that PEGylated CocE may be display strong potential to abrogate cocaine self-administration and thus a viable treatment for cocaine addiction.

Mutant	Expression	Activity
$A^{92}C$	good	+++
$S^{99}C$	poor	-
$E^{103}C$	poor	-
$G^{324}C$	good	+
$T^{326}C$	poor	-
$A^{330}C$	good	+++
$D^{355}C$	good	-
$A^{357}C$	good	*

Table 2.1: CocE residues selected for Cysteine replacement (2PEG per monomer) Residues mutated to Cysteine for positioning additional PEGs around the CocE protein. CCRQ CocE was used as the backbone for the 2 PEG per monomer mutants. Expression and activity levels are denoted next to each mutant. Only fully active, good expressing mutants were examined *in vivo*.

+++ = *Full activity*
+ = *Low activity*
- = *No activity*
* = *Aggregates during oxidation*

Mutant	Expression	Activity
$S^{179}C$	good	+++
$D^{180}C$	good	+++
$A^{181}C$	good	+++
$Q^{191}C$	poor	-
$G^{201}C$	good	+++
$L^{353}C$	poor	-
$G^{384}C$	good	+
$T^{436}C$	good	+++
$G^{517}C$	poor	-

Table 2.2. CocE residues selected for Cysteine replacement (3 PEG per monomer) Residues mutated to Cysteine for positioning additional PEGs around the CocE protein using $A^{92}C$ (CCRQ-CocE) as a template to yield 3 PEGs per monomer. Expression and activity levels are denoted next to mutant. Only fully active, good expressing mutants were examined in vivo.

+++ = *Full activity*
+ = *Low activity*
- = *No activity*
* = *Aggregates during oxidation*

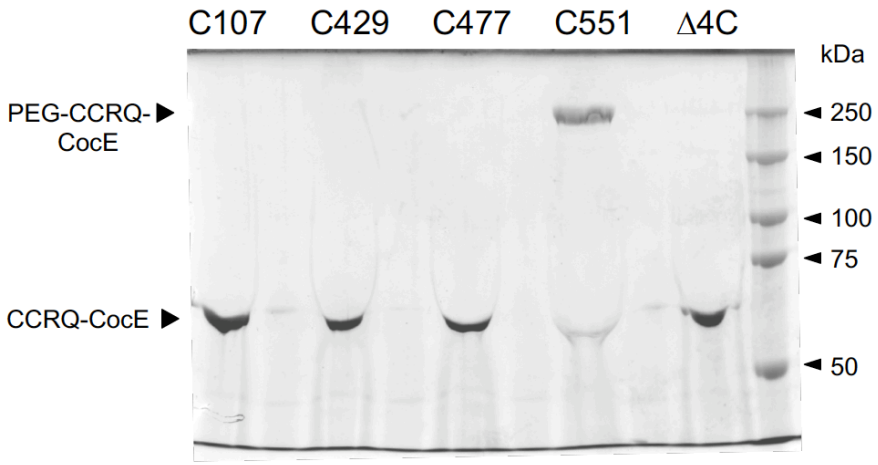

Figure 2.1: PEGylation of CocE at Cys551. CocE was systematically mutated, replacing three of four endogenous cysteine residues with serine, to interrogate which residue(s) incorporates a PEG polymer. As a control, all four cysteine residues were mutated to serine to confirm that the PEGylation is cysteine-mediated (lane Δ4C). Incubation with a 40kDa branched maleimide-coupled PEG, only CocE with a cysteine at position 551 shows a gel shift in size due to the presence of covalently attached PEG. Note that the free PEG is aberrantly migrating at approximately 70kDa and thus affecting the migration of the unPEGylated CocE through the SDS-PAGE gel.

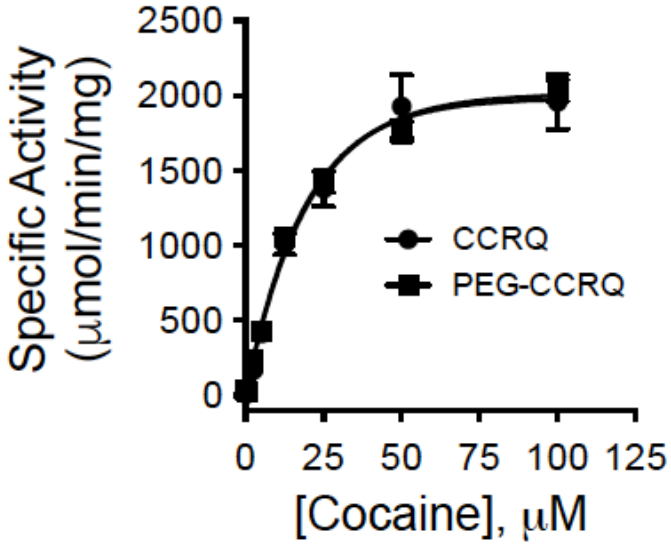

Figure 2.2: CocE retains activity after PEGylation. An *in vitro* characterization of the enzymatic activity assay was performed comparing CCRQ-CocE to the PEGylated enzyme (PEG:CCRQ-CocE). Illustrated are the velocities of CCRQ-CocE converting cocaine into inactive metabolites ecgonine methyl ester and benzoic acid. Kinetic constants of the PEGylated enzyme (V_{max} ~1982 +/- 54 moles of cocaine per minute and K_m of ~13.0 +/-1.01 μM) are indistinguishable from unPEGylated CCRQ-CocE (V_{max} ~2012+/- 57 moles of cocaine per minute and K_m of ~13.8 +/-1.1 μM).

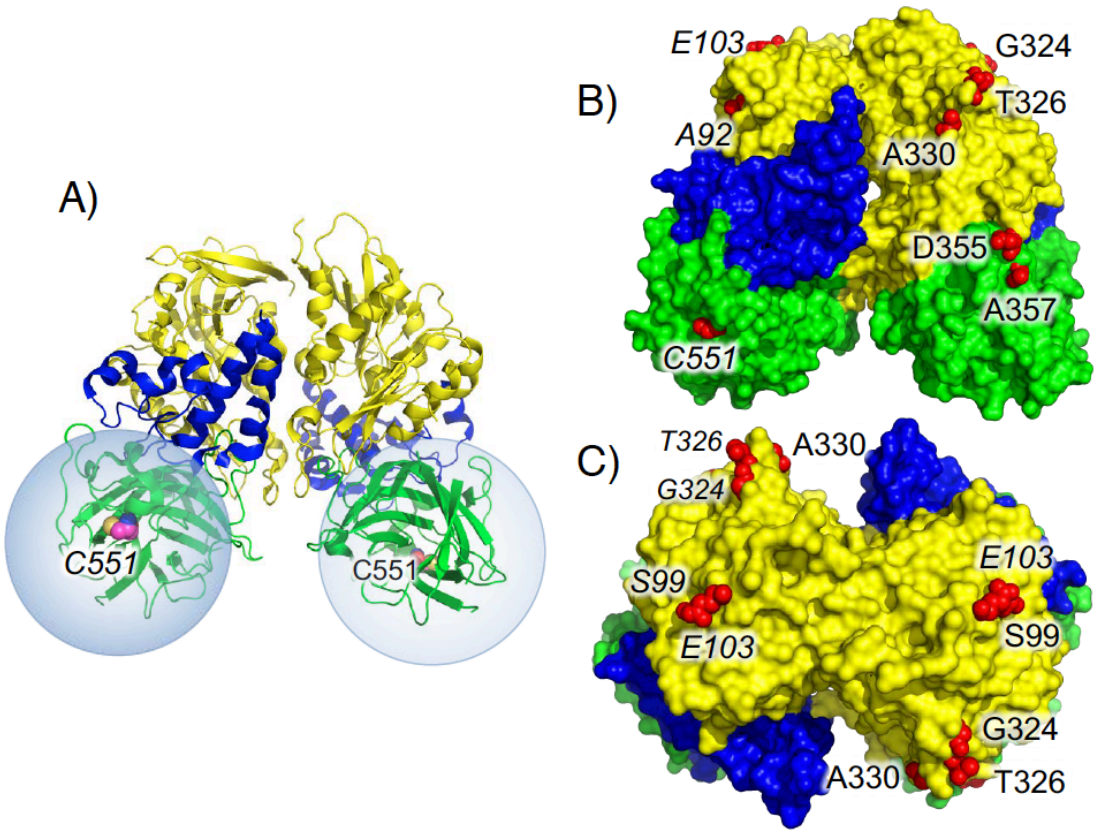

Figure 2.3: Position of endogenous and mutated cysteine residues on CocE. The three domains of CocE are shown in yellow (I), blue (II) and green (III). ***A)*** Ribbon structure of the stabilized CCRQ-CocE dimer identifying Cys551 from each protomer as the preferred PEGylated residues. Highlighted is the hypothetical surface area protected by the 40 kDa branched PEG polymer if attached to Cys551. ***B)*** and ***C)*** Illustrated is the surface representation of the CCRQ-CocE stabilized dimer identifying candidate residues (A^{92}, E^{103}, G^{324}, T^{326}, T^{330}, D^{355}, A^{357} and C^{551}) for our first round of PEG addition selected for their solvent facing R-groups and surface area coverage. The candidate residues, rendered as red spheres, were individually replaced by cysteine and subjected to PEGylation. (B, side view; C, top view). The coordinates for CocE stabilized dimer (PDB: 3PUH, [15]) was rendered using Pymol (The PyMOL Molecular Graphics System, Schrödinger, LLC).

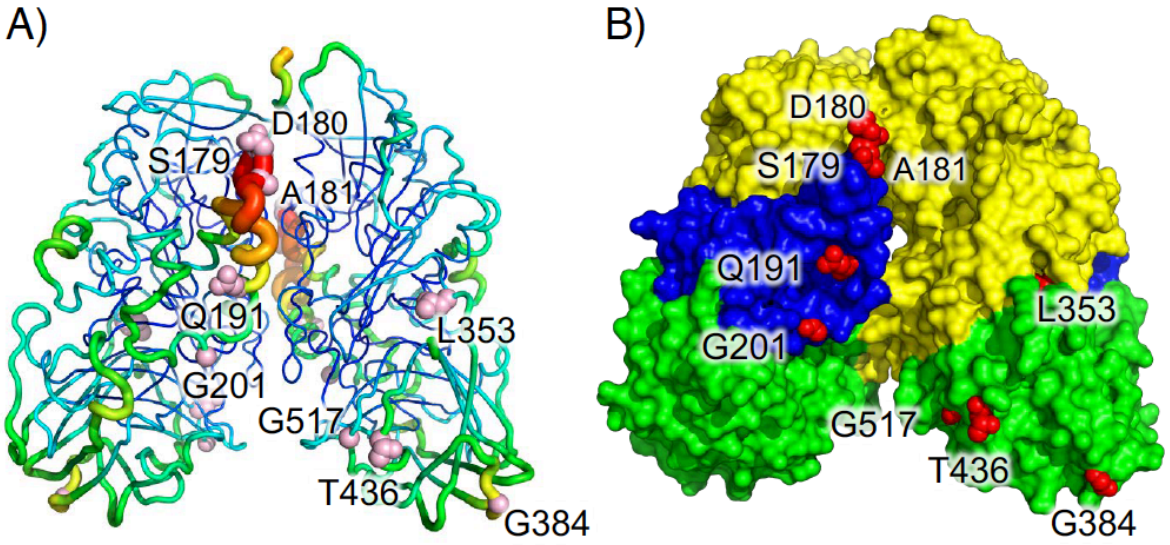

Figure 2.4: Enhancing the surface area protection by PEGylation. Using the CCRQ-CocE-A^{92}C/C^{551} as a template we identified additional residues on CocE that may offer further *in vivo* protection by PEGylation. ***A)*** illustrated is the structure of CCRQ-CocE rendered as 'putty' to indicate regions of higher disorder, based on their temperature factors, or B factors. Also indicated are candidate residues rendered as pink spheres individually subjected to mutagenesis to cysteines as substrates for PEGylation. ***B)*** Candidate residues for this second round of mutagenesis that provides a third PEGylation site on CocE (S^{179}C, D^{180}C, A^{181}C, Q^{191}C, G^{201}C, L^{353}C, G^{384}C, T^{436}C and G^{517}C and rendered as red spheres) are mapped on the surface representation of the stabilized CCRQ-CocE dimer, using the A^{92}C/C^{551} as a template.

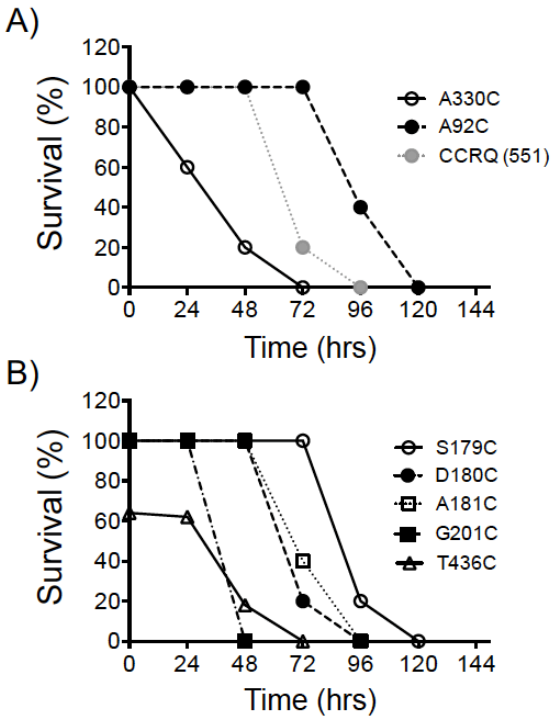

Figure 2.5: ***In vivo*** **protection against cocaine-induced lethality by PEGylated CocE.** Purified preparations of CCRQ-CocE selected for PEGylation (ie, for 1, 2 and 3 PEG per monomer of CocE) and tested for their capacity to protect against cocaine-induced lethality, using the rodent model. ***A)*** Illustrated are the survival curves of PEGylated versions of CCRQ-CocE(C^{551}) (1 PEG per monomer, gray dotted line), CCRQ-CocE-$A^{92}C$(C^{551}) (2 PEG per monomer, black circles and broken line) and CCRQ-CocE-$A^{330}C$(C^{551}) (2 PEG per monomer, open circles) representing the first round of mutagenesis (ie, 1 and 2 PEGs per monomer of CocE). ***B)*** The effect of incorporating a third PEG per monomer of CCRQ-CocE on survival following cocaine administration (using CCRQ-CocE-$A^{92}C$(C^{551}) as a template). Illustrated are the protective effects of CocE following the additional $S^{179}C$ (open circles), $D^{180}C$ (closed circles), $A^{181}C$ (open squares), $G^{201}C$ (closed squares), and $T^{436}C$ (open triangles) put in the CCRQ-CocE-$A^{92}C$(C^{551}) background. Preparations of the mutant enzymes were administered to mice at 32 mg/kg dose (i.v., tail vein) 30 minutes prior to challenge with cocaine (180 mg/kg i.p. cocaine injection). Animals were subsequently re-challenged with cocaine every 24 hours following the initial administration of the CocE enzyme. All studies were done with 5 mice in each cohort (n = 5). All experimental protocols were approved by The University Committee on the Use and Care of Animals (UCUCA) at the University of Michigan.

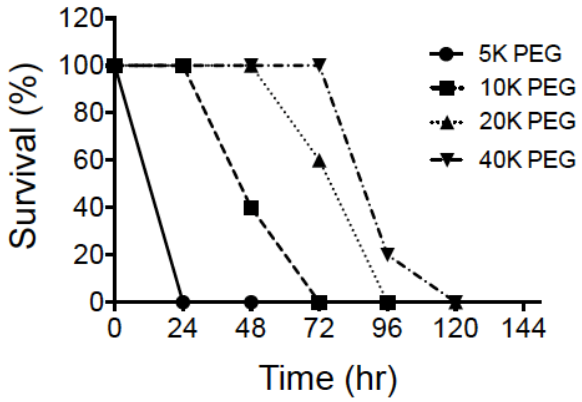

Figure 2.6: *In vivo* protection against cocaine-induced lethality by PEGylated CocE: effect of PEG complexity. CCRQ-CocE-A^{92}C/S^{179}C(C^{551}) was modified by PEG moieties of varying complexity and size polymers (5KDa, circles; 10KDa, squares; 20 KDa, triangles; and branched 40KDa PEG, inverted triangles). PEGylated enzymes were administered to mice at 32 mg/kg dose (i.v., tail vein) 30 minutes prior to challenge with cocaine (180 mg/kg i.p. cocaine injection). Animals were subsequently re-challenged with cocaine every 24 hours following the initial administration of the CocE enzyme. All studies were done with 5 mice in each cohort (n = 5). All experimental protocols were approved by The University Committee on the Use and Care of Animals (UCUCA) at the University of Michigan.

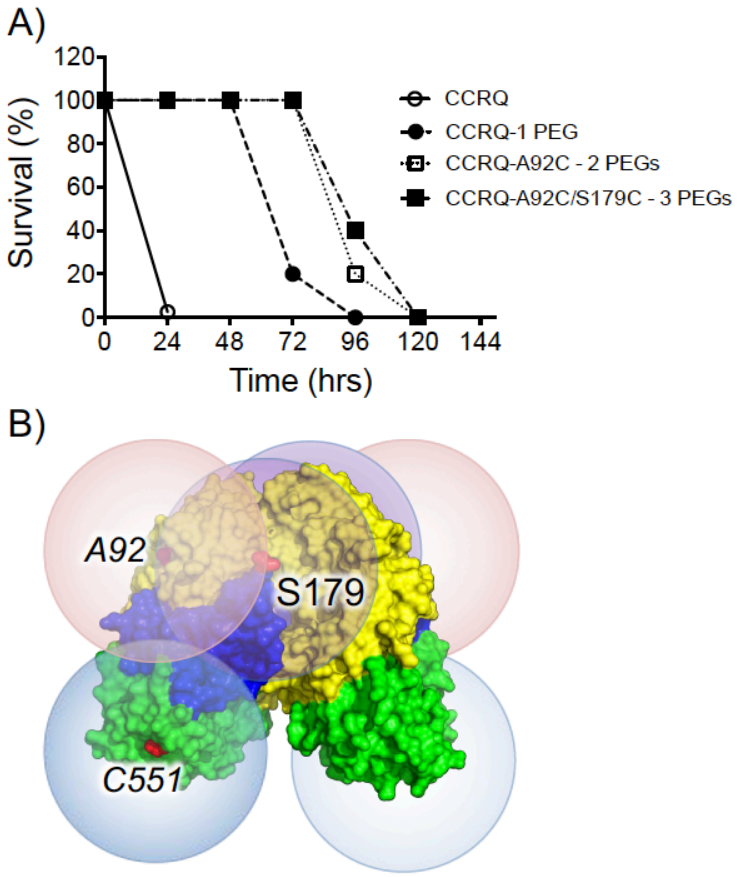

Figure 2.7: Enhancing the *in vivo* life-time of Cocaine Esterase through extending the protective coverage of the enzymes surface area offered by PEGylation. A) Summary of the in vivo effects of incorporating 1 (C^{551}, solid circles), 2 ($A^{92}C/C^{551}$, open squares), or 3 ($A^{92}C/S^{179}C/C^{551}$, closed squares) PEG moieties per monomer of CocE as a protection against cocaine-induced lethality, compared to unPEGylated CCRQ-CocE (open circles). B) Hypothetical protective coverage of the surface area of the CocE dimer through strategically placed PEG moieties provided by modification of residue 92 (transparent red sphere), 179 (transparent purple sphere) and 551 (transparent blue sphere). Residues are rendered as solid red spheres.

References:

1. NIDA. *Cocaine*. 2011; Available from: https://www.drugabuse.gov/drugs-abuse/cocaine.
2. Johnston, L.O.M., Patrick. Miech, Richard. Bachman, Jerald. Schulenberg, John., *Monitoring the Future: National Survey Results on Drug Use.* 2016.
3. Desai, R.I., et al., *Identification of a dopamine transporter ligand that blocks the stimulant effects of cocaine.* J Neurosci, 2005. **25**(8): p. 1889-93.
4. Shorter, D. and T.R. Kosten, *Novel pharmacotherapeutic treatments for cocaine addiction.* BMC Med, 2011. **9**: p. 119.
5. Orson, F.M., et al., *The future potential for cocaine vaccines.* Expert Opin Biol Ther, 2014. **14**(9): p. 1271-83.
6. Narasimhan, D., J.H. Woods, and R.K. Sunahara, *Bacterial cocaine esterase: a protein-based therapy for cocaine overdose and addiction.* Future Med Chem, 2012. **4**(2): p. 137-50.
7. Wood, S.K., et al., *Prevention and reversal by cocaine esterase of cocaine-induced cardiovascular effects in rats.* Drug Alcohol Depend, 2009. **106**(2-3): p. 219-29.
8. Gao, D., et al., *Thermostable variants of cocaine esterase for long-time protection against cocaine toxicity.* Mol Pharmacol, 2009. **75**(2): p. 318-23.
9. Brim, R.L., et al., *A thermally stable form of bacterial cocaine esterase: a potential therapeutic agent for treatment of cocaine abuse.* Mol Pharmacol. **77**(4): p. 593-600.
10. Brim, R.L., et al., *A thermally stable form of bacterial cocaine esterase: a potential therapeutic agent for treatment of cocaine abuse.* Mol Pharmacol, 2010. **77**(4): p. 593-600.
11. Narasimhan, D., et al., *Structural analysis of thermostabilizing mutations of cocaine esterase.* Protein Eng Des Sel, 2010. **23**(7): p. 537-47.
12. Collins, G.T., et al., *Repeated administration of a mutant cocaine esterase: effects on plasma cocaine levels, cocaine-induced cardiovascular activity, and immune responses in rhesus monkeys.* J Pharmacol Exp Ther, 2012. **342**(1): p. 205-13.
13. Howell, L.L., et al., *A thermostable bacterial cocaine esterase rapidly eliminates cocaine from brain in nonhuman primates.* Transl Psychiatry, 2014. **4**: p. e407.
14. Nasser, A.F., et al., *A randomized, double-blind, placebo-controlled trial of RBP-8000 in cocaine abusers: pharmacokinetic profile of rbp-8000 and cocaine and effects of RBP-8000 on cocaine-induced physiological effects.* J Addict Dis, 2014. **33**(4): p. 289-302.
15. Narasimhan, D., et al., *Subunit stabilization and polyethylene glycolation of cocaine esterase improves in vivo residence time.* Mol Pharmacol, 2011. **80**(6): p. 1056-65.

16. Park, J.B., et al., *PEGylation of bacterial cocaine esterase for protection against protease digestion and immunogenicity.* J Control Release, 2010. **142**(2): p. 174-9.
17. Collins, G.T., et al., *Amelioration of the cardiovascular effects of cocaine in rhesus monkeys by a long-acting mutant form of cocaine esterase.* Neuropsychopharmacology, 2011. **36**(5): p. 1047-59.
18. Collins, G.T., et al., *Effects of a long-acting mutant bacterial cocaine esterase on acute cocaine toxicity in rats.* Drug Alcohol Depend, 2011. **118**(2-3): p. 158-65.
19. Collins, G.T., et al., *Cocaine esterase prevents cocaine-induced toxicity and the ongoing intravenous self-administration of cocaine in rats.* J Pharmacol Exp Ther, 2009. **331**(2): p. 445-55.
20. Collins, G.T., et al., *Long-lasting effects of a PEGylated mutant cocaine esterase (CocE) on the reinforcing and discriminative stimulus effects of cocaine in rats.* Neuropsychopharmacology, 2012. **37**(5): p. 1092-103.
21. Kontermann, R.E., *Half-life extended biotherapeutics.* Expert Opin Biol Ther, 2016. **16**(7): p. 903-15.
22. Abuchowski, A., et al., *Effect of covalent attachment of polyethylene glycol on immunogenicity and circulating life of bovine liver catalase.* J Biol Chem, 1977. **252**(11): p. 3582-6.
23. Abuchowski, A., et al., *Alteration of immunological properties of bovine serum albumin by covalent attachment of polyethylene glycol.* J Biol Chem, 1977. **252**(11): p. 3578-81.
24. Fang, L., et al., *Rational design, preparation, and characterization of a therapeutic enzyme mutant with improved stability and function for cocaine detoxification.* ACS Chem Biol, 2014. **9**(8): p. 1764-72.
25. Brim, R.L., et al., *The ability of bacterial cocaine esterase to hydrolyze cocaine metabolites and their simultaneous quantification using high-performance liquid chromatography-tandem mass spectrometry.* Mol Pharmacol, 2011. **80**(6): p. 1119-27.

Chapter 3

Crystallographic Study of a Cocaine Analog bound to Cocaine Esterase and Inhibition of Cocaine Esterase

Introduction

We have been developing cocaine esterase (CocE) as a protein-based therapeutic to treat cocaine toxicity and addiction. One of the early mutant forms of CocE is currently being evaluated in Phase III clinical trials after having successfully completed the Phase II trial[1]. The results from this trial demonstrated the efficacy with which CocE can metabolize cocaine from circulation in humans. Our group, in collaboration with Dr. Leonard Howell (Emory University) recently conducted a positron emission tomography (PET) imaging study cocaine clearance in living rhesus monkey[2]. The imaging studies looking at brain found clearance rates of cocaine similar to the human studies whereby almost no detectable cocaine was found fifteen minutes after cocaine administration when challenged with a PEGylated form of CocE. The ability of CocE to rapidly remove cocaine from peripheral circulation as well as the central nervous system (CNS) has promoted this protein to the forefront of potential drugs to treat cocaine toxicity. We have also previously shown the potential for cocaine to recondition rodents away from cocaine seeking behavior[4]. Though CocE has exhibited the capacity for treating both immediate cocaine toxicity and

models of long-term addiction, using it as a prophylactic to treat cocaine addiction in humans will require an improvement in the catalytic properties to enhance its efficacy by also aid in drug formulation efforts.

CocE's efficiency can be demonstrated through a ratio of its rate of catalysis (k_{cat}) to the binding of substrate (Michaelis constant - K_M) and is coupled to the rate of product release. Improving the efficiency of an enzyme results from increasing the maximal velocity (V_{max}) and/or decreasing the K_M[5]. An increase in V_{max} reflects an improved chemistry of hydrolysis in the active site. Increasing the proton transfer rate between active site residues or increasing the rate of the nucleophilic attack on the substrate could potentially contribute toward improving the chemistry. Due to the catalysis of a substrate into a product in an enzyme, the binding rate of substrate to the enzyme is not the only parameter measured. Both the substrate binding (on rate –or- K_{on}) and release (off rate –or- K_{off}) reflect the substrate binding affinity and is related as the Michaelis constant (K_M), the concentration of substrate at which the enzyme has reached fifty percent of its maximal velocity. Therefore, a decreased K_M arises from better substrate binding [6].

The first crystallographic study of CocE contained a non-covalently bound benzoic acid molecule modeled in the active site (PDB: 1JU4) [7]. The researchers were able to identify critical residues that were responsible for interacting with the partial product based on their coordination and proximity to benzoic acid. Interestingly, in this study the authors report in that the benzoate appeared as a contaminant in their enzyme preparation and was not added

exogenously during enzyme purification nor during crystallogenesis. Note that the purification steps reported in the Larsen *et al* study were not rigorous and only entailed serial affinity chromatography steps. Several aromatic residues surrounding the phenyl ring of benzoic acid, likely accounting for its high affinity, achieved the coordination, largely through Van der Waals interactions. These data suggest that the strong coordination of this enzymatic product, benzoic acid, contributes to its slow off-rate and therefore to its role as the rate-limiting step in catalysis. In order to improve CocE's efficiency, we reasoned that a structural analysis of CocE's active site could yield information by revealing residues that interact with cocaine and thus contribute to the K_{on} portion of CocE's K_M value. We wanted to build on this information gained from the partial product containing structure by generating a new structure of CocE with the intact cocaine substrate bound in the active site.

Trapping a molecule of substrate bound to an enzyme in crystallographic studies is extremely difficult without the use of catalytically impaired forms of the protein. Alternatively, non-cleavable substrate analogs (inhibitors) could be co-crystallized, or soaked in the crystals, to approximate the nature of the substrate binding site. In order to obtain such a model of substrate bound to the enzyme, we decided on two approaches: 1) use a catalytically inactive mutant enzyme co-crystallized with cocaine; or, 2) use a non-hydrolysable analog of cocaine trapped in a complex with the enzyme. Of the three residues in CocE that form the catalytic triad (Ser^{117}, Asp^{259} and His^{287}) we first targeted the Asp^{259} and replaced it with an Asn residue. While we were able to isolate, crystallize and

even determine structures of the soaks, no success was gained in obtaining structures bound to non-hydrolyzed cocaine. As it turns out we were, however, able to obtain a structure of an acyl-enzyme intermediate of the enzyme. While this extremely interesting structure is informative regarding catalysis and is the subject of the following chapter, it does not reveal anything regarding the contributions of the tropane ring of cocaine to binding affinity and thus the K_M. We thus sought to test whether non-hydrolyzable substrate analogs of cocaine (i.e. – non-ester containing molecules) that could be trapped in the binding site. Using this latter approach we were fortunate to obtain a data set and delineate a high-resolution structure of CocE bound to a tropane-containing cocaine analogue. As these two approaches yielded significantly different results that may be applied to either understanding catalysis, k_{cat} (acyl-enzyme intermediate) or understanding substrate binding, K_M (non-hydrolyzable cocaine analog-bound CocE), each approach has been divided into separate chapters.

Studying an enzyme's mechanism of action on its endogenous substrate has proven difficult due to their inherent activity. One approach to elevating this problem comes from using a substrate analog that is structurally similar to the endogenous substrate but lacks the ability to be converted to a product by the enzyme[8, 9]. Structural studies with kinases give multiple examples of this approach. Due to the transfer of the γ-phosphate from ATP to the awaiting serine, threonine, or tyrosine residue, studying the positioning of both ATP and protein target in the kinase active site becomes problematic. Using a non-hydrolyzeable ATP analog, AMP-PNP - that contains an imido linkage between

the β- and γ-phosphates, protein crystals can be generated with both ATP and a target protein bound to the kinase[9, 10]. Information gathered from these studies aid in determining the residues that come in contact with either substrate prior to enzymatic turnover or product after turnover.

In order to investigate the physiological effect of cocaine, several cocaine analogs have been developed that are capable of blocking reuptake at monoamine transporters, with each analog having a unique and distinct structural makeup compared to cocaine [11-13]. Since several of these analogs do not contain a internal ester bond between the phenyl and tropane ring portions, we reasoned that these molecules could be used in our crystallographic studies in lieu of the actual substrate, cocaine.

We were able to procure two non-hydrolyzable cocaine analogs: RTI-150 and WIN 35,065-2 (see Figure 3.1). The RTI-150 compound was originally synthesized to study the capacity of phenyltropane molecules to binding to dopamine transporters. This molecule showed five times the potency at DAT versus cocaine [11, 14] while WIN 35,065-2 displayed several times higher potency than cocaine at DAT, but a lower affinity at SERT compared to cocaine [12, 15].

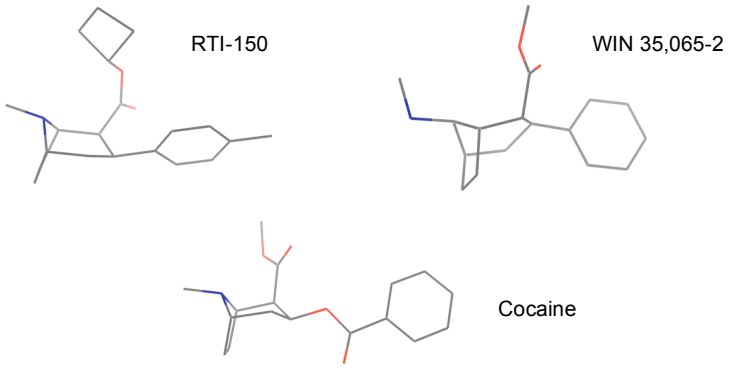

Figure 3.1: Structures of non-hydrolyzable cocaine analogs RTI-150 and WIN 35,065-2. RTI-150 and WIN 35,065-2 shown above structure of cocaine. Both molecules lack the ester bond connecting the phenyl and tropane rings, rendering them unsuitable substrates of CocE.

Our crystallographic analysis of the cocaine analog-CocE complexes yielded results with electron densities corresponding to either RTI-150 and WIN 35,065-2 in an overlapping position; however, the ligand density was distinctly removed from the enzyme's active site, based on the benzoic acid structure, as well as our new acyl-enzyme intermediate structure, Because this site does not overlap with our projected substrate-binding site, we reasoned that if these analogs could be acceptable cocaine surrogate molecules, they might be able to inhibit the enzyme in some fashion. In other words, if they bind to the active site, they could function as a competitive inhibitor. Alternatively, if they bind at another site, yet still influence enzyme kinetics, then they could be an inhibitor of some other classification.

Testing these two compounds for their potential to inhibit CocE immediately presented a problem due to our convention for testing activity of the enzyme. We have relied on an absorbance-based assay that measures the decrease of cocaine absorption. Since both of the inhibitors used in this study

absorb at 240 nm as well, we were unable to use the same assay for determining inhibition of CocE with RTI-150 or WIN 35,065-2.

In an attempt to find a more suitable substrate for testing the activity of cocaine esterase, we found a compound that could be used in fluorescence and absorbance based assays that contained an ester bond. Resorufin acetate (RA) is a tricyclic compound that shows a shift in fluorescence and absorbance after cleavage of its ester bond. We have been able to utilize this compound in our CocE activity assays in order to analyze the inhibition of benzoic acid (product of cocaine hydrolysis), and the inhibitors RTI-150 and WIN 35,065-2. With the development of a new activity assay for CocE, using resorufin acetate as a substrate, the inhibition of CocE with either inhibitor can be monitored without the interference of the inhibitors on the readout of the assay.

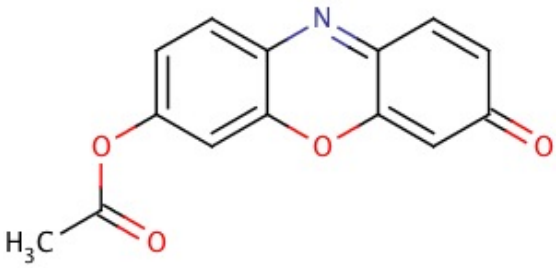

Figure 3.2: Structure of Resorufin Acetate
Resorufin Acetate, 7-acetoxy-3H-phenoxazin-2-one, is a tricyclic molecule with a methylester group that induces a shift in absorbance and fluorescence emission when hydrolyzed[3]. PubChem CID: 3080579

Methods

Generation of CocE: The mutants of CocE were generated using a variation on the Quick-Change method for site directed mutagenesis mentioned previously [16]. Oligonucleotides directed towards $A^{51}E$: 5' -GAC GTG TTC **GAA** TGG TCG ACG - 3'; $A^{51}N$: 5' - GAC GTG TTC **AAC** TGG TCG ACG - 3'; $Q^{55}E$: 5' - TGG TCG ACG **GAA** TCG ACA AAC - 3'; $L^{169}E$: 5' - TGG TCA GCT **GAA** ATA GGT CGC - 3'; $I^{170}K$: 5' - TCA GCT CTC **AAA** GGT CGC CAG - 3'; $I^{170}Q$: 5' - TCA GCT CTC **CAG** GGT CGC CAG - 3'; $I^{170}R$: 5' - TCA GCT CTC **CGT** GGT CGC CAG - 3' were ordered from Integrated DNA Technology (La Jolla, CA) The thermostable mutant of cocaine esterase with the longest acting *in vivo* activity was used in the RA analysis (92-CocE). The gene encoding CocE was expressed from pET-22b (+) plasmid in BL21 (DE3) (Novagen) bacterial cells. Cells were grown to OD_{600} = 0.6 AU, temperature shifted to 18°C, and protein expression was initiated with the addition of 1mM Isopropyl β-D-1-thiogalactopyranoside (IPTG) (Genesee Scientific). Expression continued for 16 hours, and cells were pelleted and stored at -80°C until purification. The cell pellet was resuspended in 1X Tris-buffered saline (TBS) and broken with two passes through a French Press. (ThermoScientific) Bacterial lysate was clarified by centrifugation at 25,000 x *g* and loaded onto a Ni^{2+}NTA column equilibrated with 1 x TBS at pH 7.4. The protein was eluted using 1 x TBS with 150 mM imidazole. Protein dimers were covalently cross-linked by incubating with 50 μM $CuCl_2$ at 4°C overnight. The entire reaction was loaded onto a Q-sepharose

column equilibrated with 50 mM Tris, pH 8.0. CocE protein was eluted off with a gradient of NaCl in buffer B. Peak fractions were analyzed with 10 % SDS-PAGE, then pooled and concentrated to 10 mg/ml with Amicon concentrators (Millipore) and stored at -80°C.

Generation of Crystal Structures: CocE crystals were grown by hanging drop vapor diffusion in 24-well VDX trays (Hampton Research). One microliter of protein (either inactive D259N or H287A, or RQ-CocE with WIN and RTI compounds) and well solution (18% PEG (average size = 3550 kDa), 25 mM MES pH 6.5, 1 M NaCl) were mixed on siliconized glass coverslips (Hampton Research) and placed over 1 ml of well solution. Trays were incubated at 12°C and crystal growth was observed after 2-3 days. Crystals were scooped and placed in cryoprotectant (well solution supplemented with 20 % glycerol) alone or with saturating solution of either WIN 35,065-2 or RTI-150 and allowed to incubate at room temperature for 5 minutes. Crystals were mounted on proper sized loops (0.2 – 0.4 μm – Hampton Research) and flash frozen in liquid nitrogen. X-ray diffraction data were collected at the Advanced Photon Source (Beamline 21-ID-D). Data were integrated and scaled using HKL2000[17]. Molecular replacement by Phaser was run using 3IDA structure of KQ-CocE as the search model. Successive rounds of refinement were performed using Phenix software [18] and manual density fitting using Coot [19].

Cocaine esterase activity assays: Cocaine assay: Purified PEG:CocE was analyzed using our standard absorbance-based cocaine assay, described previously. (Brim, 2011) Here, cocaine (Mallinckridt, Hazelwood, MO) is added a

96-well UV-permeable plate (Costar; Corning Life Sciences, Lowell, MA) at 200, 100, 50, 25, 10, 5, 1 and 0.5 μM concentrations. The reaction is initiated by the addition of PEG:CocE (65 ng/ml) at a 1:1 dilution in the plate. The velocity of the reaction was measured every 10s for 20 minutes by a SpectraMax Plus 384 UV plate reader (Molecular Devices, Sunnyvale, CA) using SOFTmax Pro software (version 3.1.2). The absorbance readings were converted to change in concentration of product using using Beer's law. The specific activity of the enzyme was plotted using Prism software (GraphPad Software Inc., San Diego, CA) and kinetics of the reaction (k_{cat} and K_m) generated.

Resorufin Acetate Assay: Assays with resorufin acetate were conducted in the same manner as the cocaine based assays with the exception of a difference in concentration of substrate. RA was diluted to 400, 200, 100, 50, 25, 10, 5, 2.5 μM in PBS. The assays were performed at 37°C for 1 hour, while the increase of absorbance at 570 nm is recorded at 2-minute intervals.

Inhibition assays with WIN and RTI: WIN 35,065-2 and RTI-150 were dissolved in dH_20 to a final concentration of 10 mM. The resorufin acetate assay was used to measure the inhibition potential of both compounds. The assays were performed by adding inhibitor to the reaction at several concentrations: 1000, 333, 33, and 10 μM.

Dixon and Cornish-Bowden analyses: Data from the kinetic analysis of the inhibition studies were plotted as either the reciprocal of the velocity (1/v - Dixon plot) or the concentration of substrate over velocity (s/v – Cornish-Bowden plot) using Prism software (Graph Pad Software Inc., San Diego, CA).

Drugs: RTI-150 and WIN 35,065-2 were kindly provided by Dr. F. Ivy Carroll (Research Triangle Institute, North Carolina)

Results

Structure of inhibitors: Both inhibitors have a nitrogen-containing tropane ring and a phenyl group as part of their molecular makeup. RTI-150 ($C_{20}H_{27}NO_2$) ((-)-2β-carbocyclobutoxy-3β-(4-methylphenyl)tropane) (PubChem CID – 9972881) also has a cyclobutane group off of its sole ester bond. In this molecule, the phenyl ring contains a methyl group at the *para* position of the tropane ring. WIN 35,065-2, ($C_{16}H_{21}NO_2$) ((-)-2β-Carbomethoxy-3β-pheyltropane) (also known as troparil – PubChem CID – 170832) has a methylester and a phenol group coming off of the tropane ring at positions 2 and 3, respectively.

Crystallographic analysis of CocE bound to RTI-150 or WIN 35,065-2: Using hanging drop vapor diffusion of CocE crystallization media containing RTI-150 we were successful in obtaining crystals large enough to diffract greater than 1.8Å (Figure 3.3). Although similar co-crystallization attempts were unsuccessful with WIN 35,065-2, crystal soaks with saturating concentrations of the cocaine analog did yield diffracting crystals.

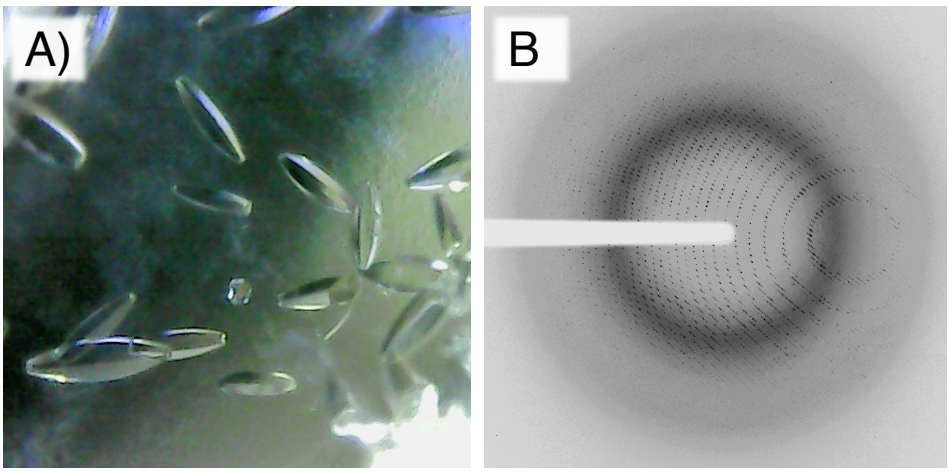

Figure 3.3: Crystals and x-ray diffraction of RTI-150-CocE Complex. A) Crystals grown in 18% PEG3550, 25 mM MES pH 6.5, 1 M NaCl in 1 mM RTI-150 at a protein concentration of 10 mg/ml under vapor diffusion at 12C. B) Diffraction pattern of an RTI-150-CocE Complex crystal was collected at LS-CAT at APS in Argonne National Laboratories.

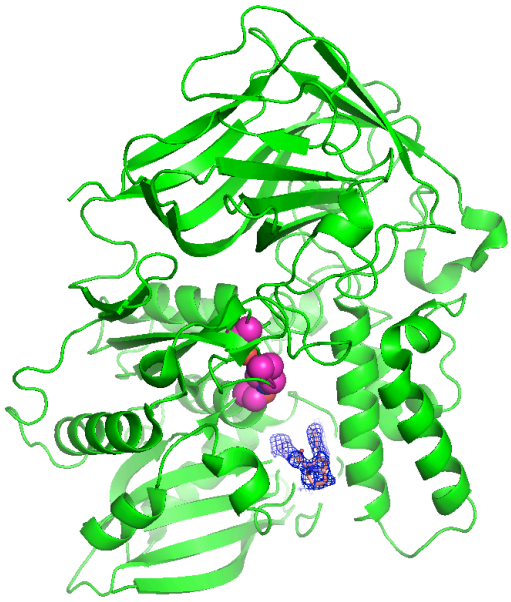

Figure 3.4A: Structure of RTI-150-bound CocE. Highlighted is the electron density (blue mesh). The active site, defined by the catalytic residues, Ser^{117}, Asp^{259} and His^{287}, are highlighted in magenta spheres.

Data sets for both structures were generated at a resolution limit of 1.8 Å.

Both data sets contained two monomers per asymmetric unit as seen in previous

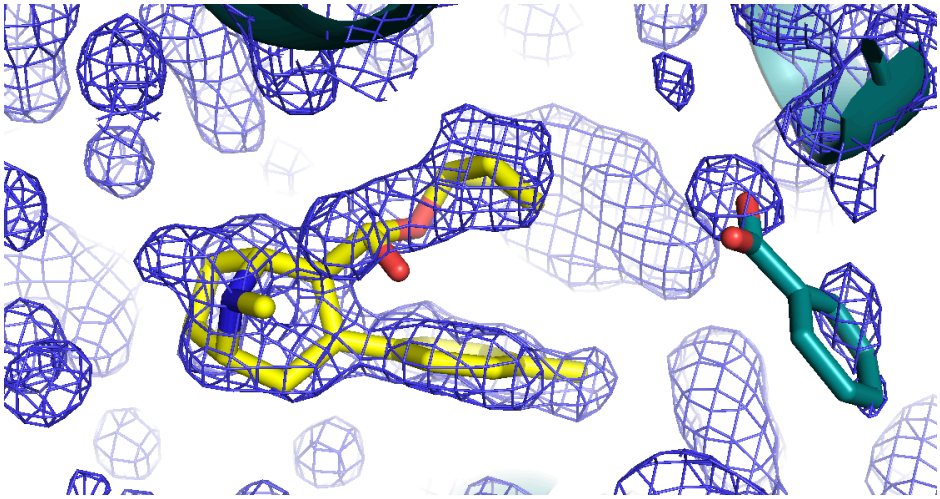

Figure 3.4B: Electron density in the RTI-150-CocE crystals Density found at a site distal from the putative active site based on the benzoic acid-bound CocE structure (PDB: 1JU4). RTI-150 is (rendered in yellow) and benzoic acid (sage) are illustrated. Note that the electron density indicates the presence of the cocaine analog binding site on CocE where its phenyl ring is at least 8Å away from the location of benzoic acid binding site.

CocE structures generated under similar conditions. Table 3.1 contains all refinement statistics.

Composite omit maps of the RTI-150-bound CocE density with respect to unliganded CocE reveals a strong density located between the Domain I and II but at a site 8Å away from the active site, based on the structure benzoic acid-bound CocE (PDB: 1JU4) (Figure 3.4 A and B).

The co-crystallization of RTI and soaking in of WIN yielded similar results. Electron densities that correspond to the shape of each molecule were found positioned between helices of Domain I and II, but distant from the active. This position, however, does not correspond to where we believe cocaine sits in the

active site, and also, this position would put the substrate too far from the active site residues for chemistry of hydrolysis to occur.

The nitrogen of the tropane ring is closest to the exterior solvent exposed face of the protein, and the more hydrophobic methylbenzene and cyclobutane ring portions of RTI-150 point inward towards the active site pocket with more hydrophobic residues. (Figure3.6)

As illustrated in Figure 3.4 electron density compatible with models of both RTI-150 (Figure 3.5A) and WIN 35,065-2 (Figure 3.5B) and suggest a similar binding site for the cocaine analogs and likely for cocaine itself. Though we collected datasets on CocE complexes that show density corresponding to the structures of either WIN 35,065-2 or RTI-150, the RTI density was much more complete, therefore the remainder of the analyses will be restricted to the RTI-150-bound CocE complex structure (see Figure 3.6).

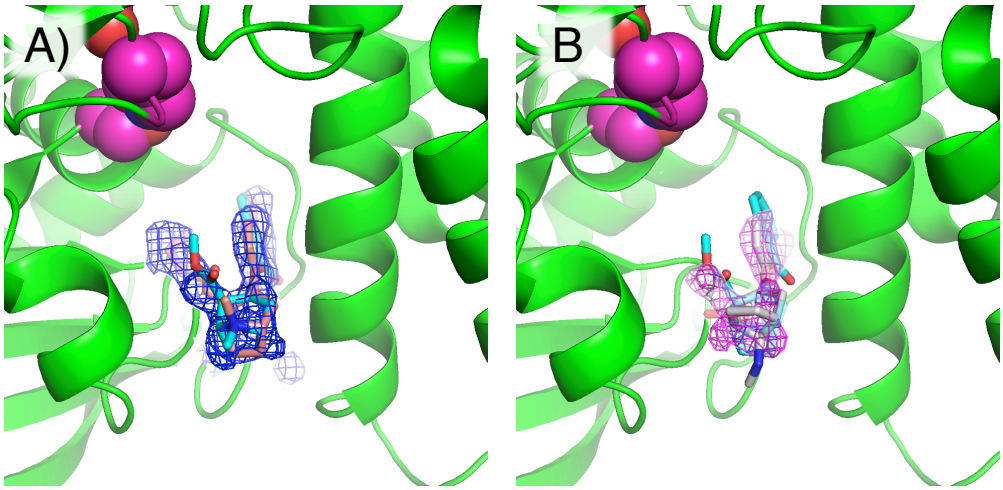

Figure 3.5: **Structure of the non-hydrolyzable cocaine analogues bound to CocE.** Illustrated is cocE and the members of the catalytic triad (magenta spheres). A) CocE bound to RTI-150 (fleshtone) and corresponding electron density (blue mesh). Superimposed is the cocaine modeled onto the tropane ring. B) CocE bound to WIN 35,065-2 (grey) and corresponding electron density (magenta mesh). Superimposed is the cocaine modeled on the tropane ring. Electron density was set at a 2 σ cutoff.

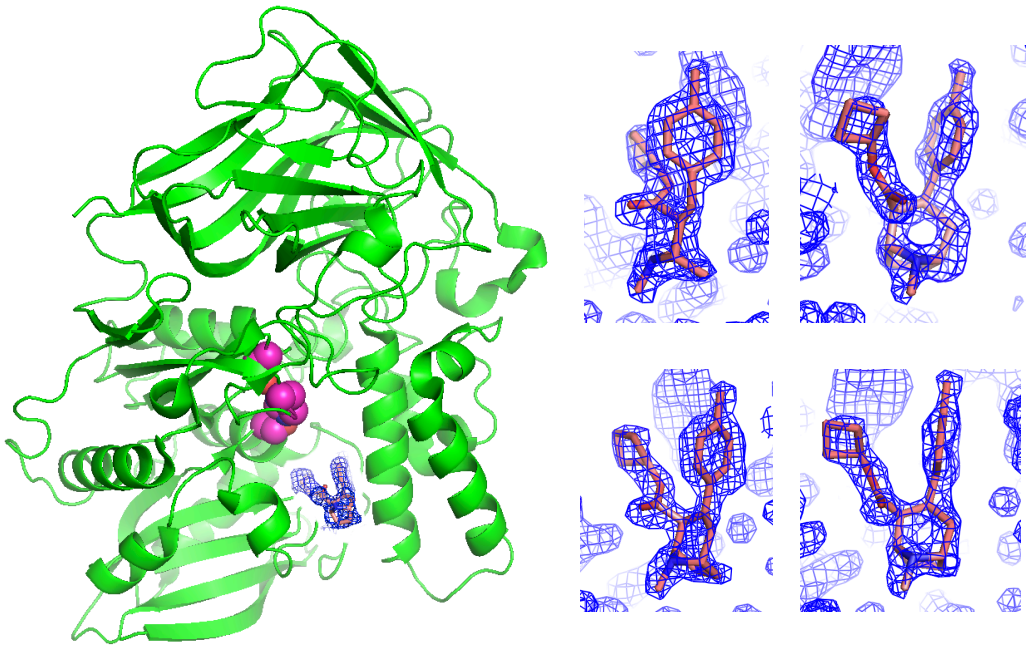

Figure 3.6: Electron density of RTI-150-containing CocE structures. The position of this novel site is distal from the active site (magenta spheres). Right panels display four different views of the RTI-150 model overlayed into the electron density (blue mesh).

The binding site for cocaine suggested by the structures of the cocaine analogues away for the site of hydrolysis is unanticipated. One interpretation may be that the relatively hydrophobic cocaine analogs merely took advantage of a hydrophobic surface on CocE at a site that is catalytically unrelated to the active site for cocaine itself. The notion is that cocaine, owing to its slightly different structure (ie. presence of an ester linkage) would bind preferably to the catalytic site implied by the benzoic acid-bound CocE structure. Alternatively, this novel site may actually represent legitimate docking site through which cocaine passes through on its way to the catalytic site. In this model the

substrate cocaine may initially dock at this entrance to the CocE active site, prior to hydrolysis, where it may be desolvated in order to enter the enzyme's active site. To test whether this site is relevant to cocaine binding and hydrolysis and not merely a binding site that is specific to the non-hydrolyzable cocaine analogs, we generated a series of site-directed mutagenesis studies and assessed their capacity to influence the K_M of cocaine.

Looking at the potential molecular interactions between the RTI-150 structure and residues in CocE, we identified several residues within van der Waals and hydrogen bonding distances from RTI-150 in our model. The residues in closest proximity to the RTI-150 are Tyr^{44}, Ala^{51}, Gln^{55}, Leu^{169}, and Ile^{170} (see Figure 3.7).

Tyr^{44} is one of two residues (also Tyr^{118}) that form the oxyanion hole, and is shown to be crucial for enzyme functioning as mutagenesis to Phe yields a catalytically dead enzyme [7]. Both Ala^{51} and Gln^{55} extend off of the A1 helix of DOM1. The methyl group off Ala^{51} resides approximately 5 Å away from the methyl attached to the nitrogen atom of the tropane ring of RTI-150. The methyl group of Ala^{51} also resides ~3.8 Å away from the carbonyl carbon of cyclobutane ester of the tropane ring of RTI-150. Like Ala^{51}, the sidechain of Gln^{55} is positioned ~5 Å from the cyclobutane ring of RTI-150 in our model. On the opposite face of the cocaine analog the sidechains of both Leu^{169} and Ile^{170} sit close enough to the methyl phenyl group of RTI-150 to form extensive van der Waals contacts (Figure 3.7).

Putative docking site residues

Ala^{51} and Gln^{55}: The crystal structure of the RTI-150 CocE complex suggested that residues at positions 51 and 55 may influence binding of cocaine substrate to the active site. Interestingly these residues were also identified in an computational study of CocE using molecular dynamic simulations suggesting a possible interaction with the tropane ring of cocaine[20]. They further predicted that mutating these residues to glutamate might enhance the interaction between the residue and substrate by forming additional attraction between the nitrogen bridge of the tropane ring and the acidic residue's R group.

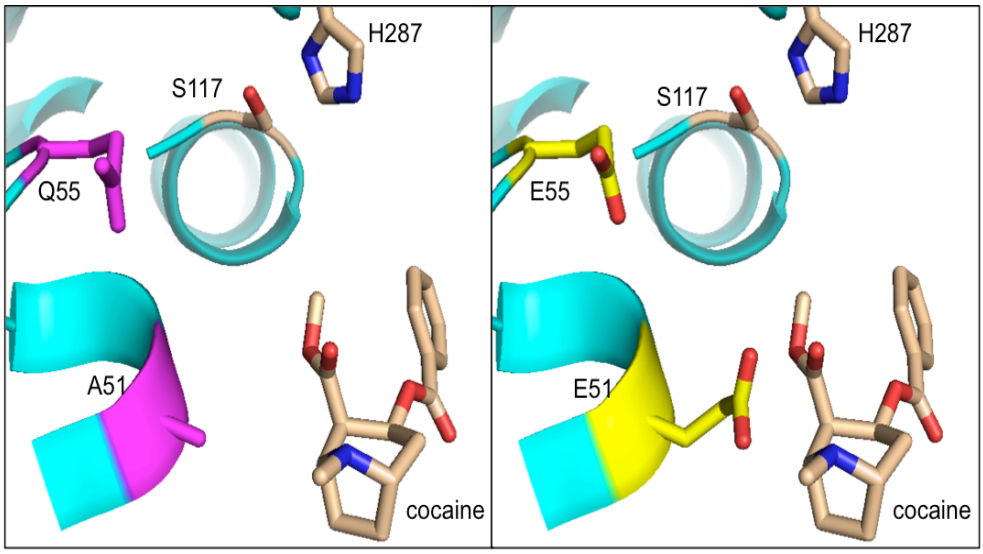

Figure 3.7: CocE residues 51 and 55 that may contribute to cocaine binding. Left panel illustrates the native CocE residue Ala^{51} and Gln^{55} . Right panel displays the hypothetical positions of the sidechain of Ala^{51}Glu and Gln^{55}Glu.

Table 3.2: Kinetic values of CocE mutants – $A^{51}E$, $A^{51}N$, and $Q^{55}E$

Mutants	K_M (μM)	V_{max} (min^{-1})	Catalytic Efficiency ($\mu M^{-1} \bullet min^{-1}$)
$Ala^{51}Glu$	5.5 +/- 0.8	920+/- 41	168
$Ala^{51}Asn$	15.3 +/- 3.0	2200 +/- 118	143
$Gln^{55}Glu$	4.1 +/- 0.7	750 +/- 30	184

As summarized in Table 3.2, analysis of these residues by site-directed mutagenesis and substitution to glutamate significantly improves the K_M of the enzyme with a mild decrease in the maximal velocity. Substitution of either residue to glutamate improves the K_M by approximately 5-fold over WT-CocE or CCRQ, the thermostable for of CocE. The fact that the $Ala^{51}Glu$ displays such a dramatic effect on the K_M of cocaine not only validates the model predicted by Huang *et al* [20], but also strongly supports that the putative cocaine docking site predicted from our RTI-150-CocE structure. In this model the sidechain of $Ala^{51}Glu$ would interact directly with the bridging nitrogen of cocaine and enhance its binding.

The dramatic observed improvement in the K_M and most likely the improved affinity at the docking site may actually negatively affect the K_{cat} of the enzyme. In this manner the maximal velocity of the $Ala^{51}Glu$ mutant may negatively affect the V_{max} through slowing the transition from the docking site to the active site. This rationale is supported by kinetic analysis of the $Ala^{51}Asn$ mutation. The improved cocaine binding results from an interaction with the oxygen of the carboxamide of asparagine and the bridging nitrogen on the tropane ring. Since there is not a fully formed hydrogen bond through the carboxylate side chain (i.e. of Glu) and the bridging nitrogen, the substrate's

transition may be less impeded to the active site and display a WT-like maximal velocity.

Leu^{169}: Residue 169 lies in the middle of helix 2 of DOM2 and faces towards the active site cleft (See Figure 3.8). We have previously identified a thermostable mutant of CocE, Leu^{169}Lys that together with Gly^{173}Gln displayed the highest reported velocity of any mutant of CocE, and it also remained active for almost 3 days at 37°C in buffer [21]. Based on crystallographic evidence we reasoned that the ζ-nitrogen can hydrogen bond with the hydroxyl of Tyr^{44}, and provide added structural stability to CocE. Why this mutant was able to perform chemistry almost three times faster than other CocE mutants was unclear at the time. In order to evaluate the potential of this basic residue substitution, we investigated placing an acidic residue with the hypothesis that it would have an opposite effect.

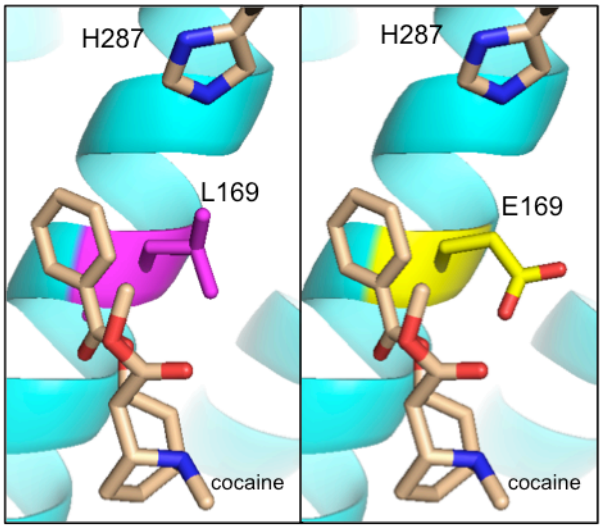

Figure 3.8: Leu^{169} may contribute to the docking site of cocaine. Illustrated is the native Leu^{169} (Left panel) and the Leu^{169}Glu (right panel) with respect to the putative cocaine docking site.

Table 3.3: Kinetic values of CocE mutant – Leu^{169}Glu

Mutant	K_M (μM)	V_{max} (min^{-1})	Catalytic Efficiency (μM^{-1}•min^{-1})
Leu^{169}Glu	17 $^{+/-}$ 3.0	2600 $^{+/-}$ 160	157

The goal of this mutation was to disrupt the potential van der Waals contacts between the sidechain of Leu^{169} and the benzoyl moiety of cocaine (See Figure 3.8). However, as illustrated in Table 3.3 there was not a dramatic effect on the overall kinetics of cocaine hydrolysis by Leu^{169}Glu mutant of CocE and if anything there was a slight improvement in K_M with no change in the enzymes V_{max}. This improvement to K_M may be analogous to the effect of Ala^{51}Glu on its interaction with the tropane ring but its modest effect may be due to the large hypothetical distance between the bridging nitrogen on the tropane ring of cocaine and oxylate group of Leu^{169}Glu.

Ile^{170}: Residue 170 lies in the middle of helix 2 of DOM2 and faces towards the active site cleft (see Figure 3.9). The δ-carbon atom of this residue could potentially interact with the tropane ring or the methyl group off the nitrogen atom of the tropane ring.

As indicated in Table 3.3 substitution of Ile^{170} to either Lys, Gln or Arg yields similar but high K_M values that are outside of the detectable limit (ie. beyond our maximal concentration of substrate). We intentionally chose residues with bulkier R-groups to mimic that of isoleucine, but selected charged residues hoping to influence the kinetics in one of two ways. First, lysine and

arginine were selected in hopes that their positive charge might repel the tropane ring in the ecgonine methylester partial product in a way that would increase overall velocity. The large basic residues may also repel the tropane ring of the substrate

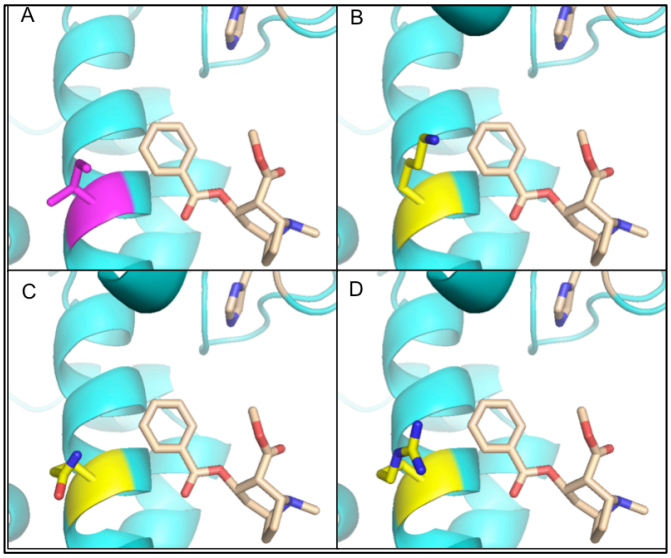

Figure 3.9: The contributions of Ile^{170} to substrate binding to CocE. A) native CocE residue Ile^{170} with cocaine modelled in its putative docking site. The hypothetical positions of sidechains of mutants Ile^{170}Lys (panel B), Ile^{170}Gln (panel C) and Ile^{170}Arg (panel D).

Table 3.4: Kinetic values of CocE mutants – Ile^{170}Lys, Ile^{170}Gln, and Ile^{170}Arg

Mutation	K_M (μM)	V_{max} (min^{-1})	Catalytic Efficiency ($\mu M^{-1} \bullet min^{-1}$)
Ile^{170}Lys	>100	1900 +/- 190	NC
Ile^{170}Gln	>100	1800 +/- 490	NC
Ile^{170}Arg	>100	1700 +/- 150	NC

cocaine and increase the K_M. Second, glutamine was selected to complement the above strategy with basic residues but by having a substrate facing oxygen atom that could potentially attract the nitrogen atom in the tropane ring, via hydrogen bonding. Improving the interaction prior to hydrolysis in a manner that may improve the K_M. Here the results indicated the dramatic loss K_M to over 100

μM in all three mutants such that the overall catalytic efficiency was not calculated. They data do suggest however that the maximal velocity of each mutant is unimpaired.

Taken together these results strongly support the location of putative cocaine docking site model by demonstrating a loss of substrate's capacity to bind to CocE upon mutagenesis of residues that coordinate RTI-150 binding. By placing a large, charged or uncharged residue in place of the hydrophobic isoleucine, the K_M increased several fold. The fact that each mutant enzyme retained high activity suggests that the mutations do not interfere with the chemistry of cocaine hydrolysis by CocE and strongly support the notion that the site identified by the RTI-150-CocE crystal structure is a bona fide binding site for cocaine, perhaps serving as a docking site.

Catalysis using the resorufin acetate fluorescence assay: The crystallographic data with the cocaine analogs suggests that they may bind preferentially to a site distinct from the active site; however, mutagenesis of residues surrounding this site appeared to dramatically affect cocaine hydrolysis. These data suggest that the analogs may inhibit cocaine esterase even through binding to this docking site. To measure this inhibition, we developed a new absorbance-based assay using following resorufin acetate (RA) hydrolysis. Resorufin absorbs at 570 nm after hydrolysis of the ester-bonded acetate. The ability to measure absorbance at 570 nm has significant advantages over our standard absorbance-based cocaine assay since both benzoic acid and the

analogues contain phenyl rings that absorbs in the UV spectra. Hydrolysis was measured as an increase of absorbance at 570 nm.

The assay was conducted using dilutions of RA listed in the materials and methods section. The most thermal stable form of CocE (CCRQ-A92C) was used as the test protein in these assays. Several assay times were tested ranging from 20 minutes (similar to the cocaine based assay) out to 6 hours. We found that a one-hour assay was adequate to assay CocE's hydrolysis of this substrate and within the linear progress curve. The kinetics of RA hydrolysis were determined to be a K_M of 67μM and a V_{max} of 850 min^{-1}. (Figure 3.10)

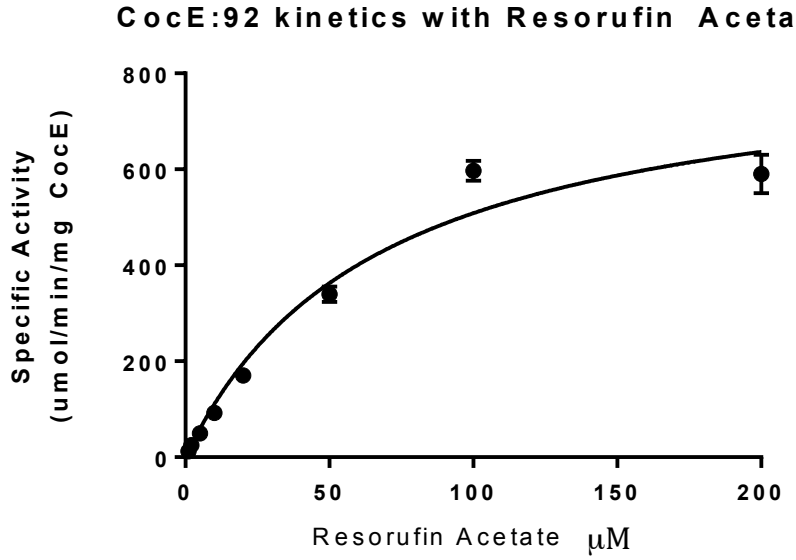

Figure 3.10: Resorufin Acetate assay. CocE at concentration of 100 ng/ml was found to hydrolyze resorufin with a K_M~67 μM and a V_{max}~ 850 min^{-1}.

Inhibition of resorufin acetate hydrolysis by Benzoic acid*:* By taking advantage of the spectral properties of resorufin acetate during hydrolysis we tested the capacity benzene containing molecules (eg. RTI-150, benzoic acid) to inhibit its hydrolysis by CocE. We surveyed four different concentrations of

benzoic acid were tested – 1000 μM, 500 μM, 333 μM, and 33 μM. These concentrations were selected because they encompassed the entire range of RA substrate concentrations in the assay. The Michaelis-Menton plot of benzoic acid inhibition of RA hydrolysis displays a concentration-dependent inhibition. The inhibition also decreased the V_{max} of the reaction while simultaneously increasing the K_M. (Figure 3.11)

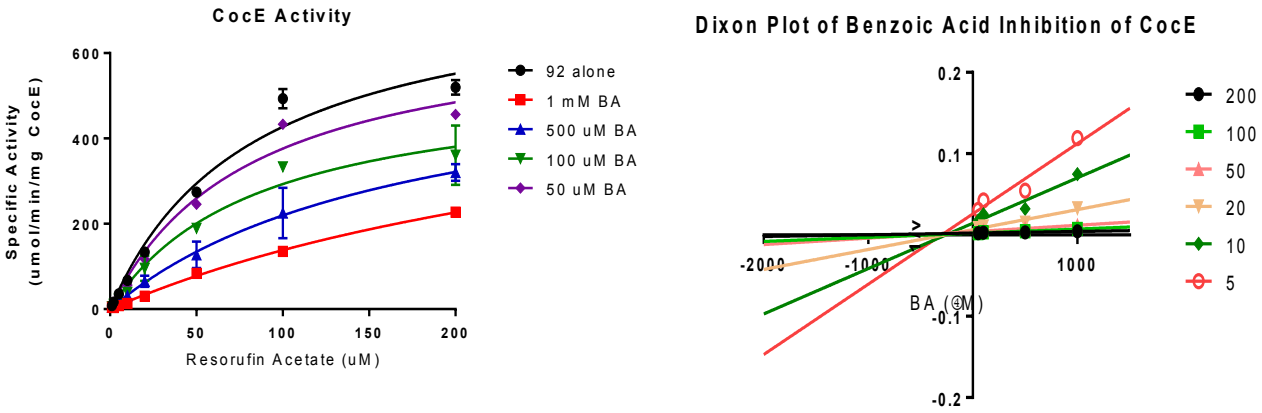

Figure 3.11: Inhibition of CocE hydrolysis of RA by benzoic acid. Left panel shows the Michaelis-Menton plot of concentration dependent decrease of V_{max} and increase of K_m by benzoic acid. Right side displays the Dixon plot of the same inhibition assay. By plotting the reciprocal of the velocity (1/v) of each concentration of RA, the plot shows benzoic acid to be a noncompetitive inhibitor.

With these kinetic parameters, a reciprocal plot of the velocity was performed to generate a Dixon analysis [22] to determine the type of inhibition by benzoic acid (Figure 3.11 right panel). Examining the point of intersection on the x-axis of each line representing substrate concentration, the benzoic acid has an apparent K_i value of ~355 μM. (Figure 3.9) The Dixon analysis also shows that

benzoic acid fits the pattern of a noncompetitive inhibitor, consistent with a product-type of inhibition.

***Inhibition of resorufin acetate hydrolysis with RTI-150*:** We next assessed the capacity of RTI-150 to inhibit resorufin acetate hydrolysis by CocE. We tested four concentrations of RTI-150 (1000 μM, 500 μM, 333 μM, and 33 μM) to inhibit resorufin acetate hydrolysis by CocE. The assay was set up in the same manner, using the same assay parameters with the same substrate/inhibitor concentrations. (Figure 3.12).

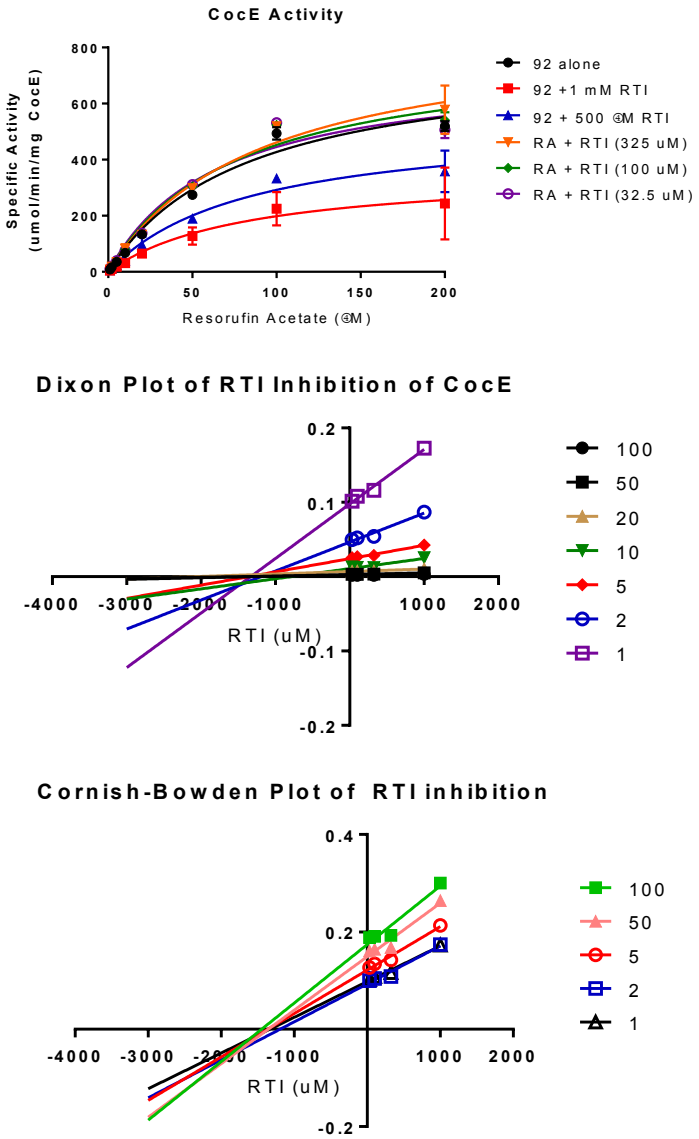

Figure 3.12: Inhibition of CocE hydrolysis of RA by RTI-150. Top panel shows MM kinetics of RA assay with RTI-150's concentration dependent inhibition. Middle panel is the Dixon plot of same inhibition assay. Due to the intersection of each plotted line being below the x-axis, method of inhibition is unclear. Bottom panel shows the Cornish-Bowden analysis showing noncompetitive inhibition.

After plotting the inhibition data, the results of the Dixon analysis were unclear (Figure 3.12 middle panel) but did indicate that the K_i of RTI ≈ 1340μM. The regression lines for each concentration of substrate all intersected below the x-axis, suggesting a mixed, competitive and non-concompetitive inhibitors,

according to the closest interpretation of traditional Dixon analysis. Cornish-Bowden analysis (Figure 2.12, lower panel) of the same assay data, which normally can differentiate more stringently between competitive and mixed inhibitors also revealed a mixed mode of inhibition [23]. The statistics of the inhibition studies support the goodness of fit for our data, but as mentioned earlier, this substrate is not ideal due to the solubility issues.

Discussion

The inhibition of CocE-mediated hydrolysis resorufin acetate by RTI-150 has lent some support to the crystal structures solved in this study. The results suggest that RTI-150 can inhibit hydrolysis in either a noncompetitive or a mixed type of inhibition, consistent with the notion that RTI-150 may bind to multiple sites (Figure 3.12). It is tempting to speculate that RTI-150 may bind to the docking site of CocE, as indicated by the crystal structure, and non-competitively inhibit access to the catalytic site. Alternatively, RTI-150 binding to the docking site may allosterically alter the enzymes capacity to hydrolyze the substrate through altering the enzymes k_{cat}. The mixed mode of inhibition indicated by the resorufin acetate hydrolysis data suggests that RTI-150 may also inhibit in a competitive manner directly at the active site.

Regardless of the mode of inhibition, the resorufin acetate hydrolysis data do support the existence of an additional site for the cocaine analog and together with the mutagenesis data suggest that this site could also be occupied/utilized by cocaine.

We understand that the results need to be viewed through two potential limitations. First, the solubility of RA in water was an initial challenge that took several approaches before finally settling on the current assay. Looking at the kinetics, however, we believe that this assay is reflective of the actual kinetic values of RA when hydrolyzed by CocE. (Figure 3.10) Secondly, the inhibition assay was performed with RTI-150 inhibiting RA hydrolysis and not measuring the inhibition of cocaine hydrolysis directly. We do not know exactly where RA binds to CocE during hydrolysis, but we have shown that it is a substrate for this enzyme.

The position of RTI-150 in our CocE structure was a surprising result. The intent was to generate a surrogate model of cocaine binding to the active site by using a non-hydrolysable cocaine analog (either RTI-150 or WIN 35, 065-2) together with a fully active CocE mutant (RQ-CocE). Since the structure solved generated from the WIN 35, 065-2-containing crystals show incomplete electron density, it was not fully refined nor was it used as a model to test residues that could potentially interact with cocaine. The fact remains, however, that this molecule does bind to the same region of CocE as RTI -150 giving support to the existence of a cocaine docking site. We then needed to elucidate whether or not this is a bona fide binding site for cocaine substrate.

Based on the crystallographic results, we initially hypothesized that RTI-150 bound to an initial binding site where cocaine is positioned prior to moving into the active site for hydrolysis (see Figure 3.13). We further reasoned that this site might be used to desolvate the substrate prior to moving into the active site.

We have noticed that the CocE active site contains a rather sizeable hydrophobic presence, primarily composed of aromatic residues. The salt form of cocaine is readily dissolved in water presumably due to the nitrogen on the tropane ring and two esters elsewhere on the molecule that act as 5 distinct sites of hydrogen bond acceptors[24]. In order to fit properly into the active site, prior to hydrolysis, the molecule may need to shed bound waters for proper positioning between the catalytic triad. We reasoned that this process might be initiated by binding at the site where RTI-150 was located in the crystal structure.

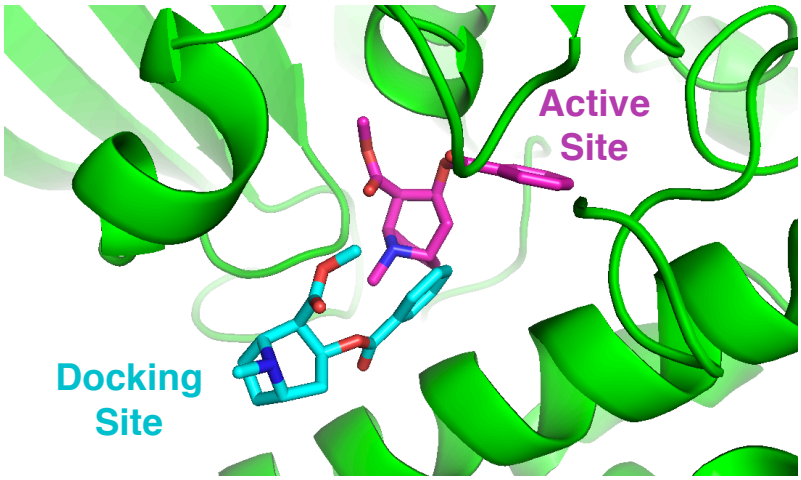

Figure 3.13: Two putative substrate binding sites on CocE. Illustrated is a model of the substrate cocaine bound to the active site (magenta) based on the structure of CocE bound to benzoic acid (PDB: 1JU4) or the docking site (cyan) based on the RTI-150 crystal structure.

In order to test the legitimacy of this docking site to cocaine hydrolysis, we utilized site-directed mutagenesis to test whether residues proximal to RTI-150, Tyr^{44}, Ala^{51}, Gln^{55}, Leu^{169}, and Ile^{170} all sit in close enough to the tropane analog to potentially influence cocaine binding. Tyr^{44} has been previously shown to be part of the two-component oxyanion hole, and mutation of this residue to phenylalanine was found to have deleterious effects on CocE's activity[25].

Since its presence is deemed crucial to enzyme activity, it will not be mutated in the future study.

Ala^{51}, Gln^{55}, Leu^{169}, and Ile^{170} were all found in close enough proximity to interact with the RTI molecule and will be explored for potential to influence enzymatic efficiency. A previously reported study of cocaine binding to the active site of CocE (based on the benzoic acid-CocE complex structure) using molecular dynamic simulation suggested that both Ala^{51} and Gln^{55} could interact with the bridging nitrogen of the tropane ring of cocaine and influence its binding [26]. This proposed interaction was predicted to enhance the K_M of cocaine despite the large distance of Ala^{51}, in particular, to the bridging nitrogen of cocaine in the active site (see Figure 3.14). The researchers postulated that a mutation to glutamate at either of these positions should improve the K_M of cocaine binding and our biochemical data confirmed this.

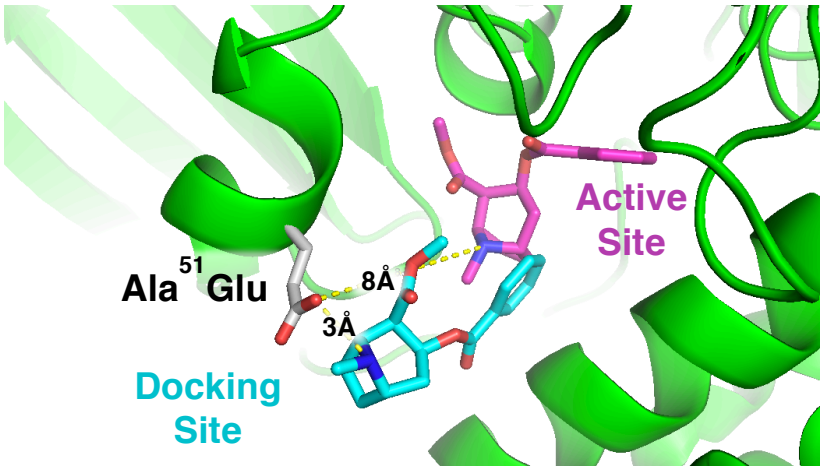

Figure 3.14: Potential interaction of Ala^{51}Glu with the bridging nitrogen on cocaine in the docking vs active sites. Illustrated is a model of the substrate cocaine bound to the active site (magenta) based on the structure of CocE bound to benzoic acid (PDB: 1JU4) or the docking site (cyan) based on the RTI-150 crystal structure and mapped on to the Ala^{51}Glu mutant. Rotomer selection the Ala^{51}Glu sidechain was based on minimizing clashes with substrate. Distances between the oxalate and bridging nitrogens of cocaine in the docking site or active site are indicated in Ångstroms.

We have recently generated similar results through an MD simulation in collaboration with Alisha Caliman, in the McCammon lab (UCSD), where cocaine was docked into the CocE structure (PDB: 3IDA). Here we found that cocaine would move within 3 Å of both residues, with the tropane ring in particular moving closest to both residues. The simulation also showed a hydrophobic interaction between the benzoic acid and Phe^{261} (Unpublished data – Figure 3.15).

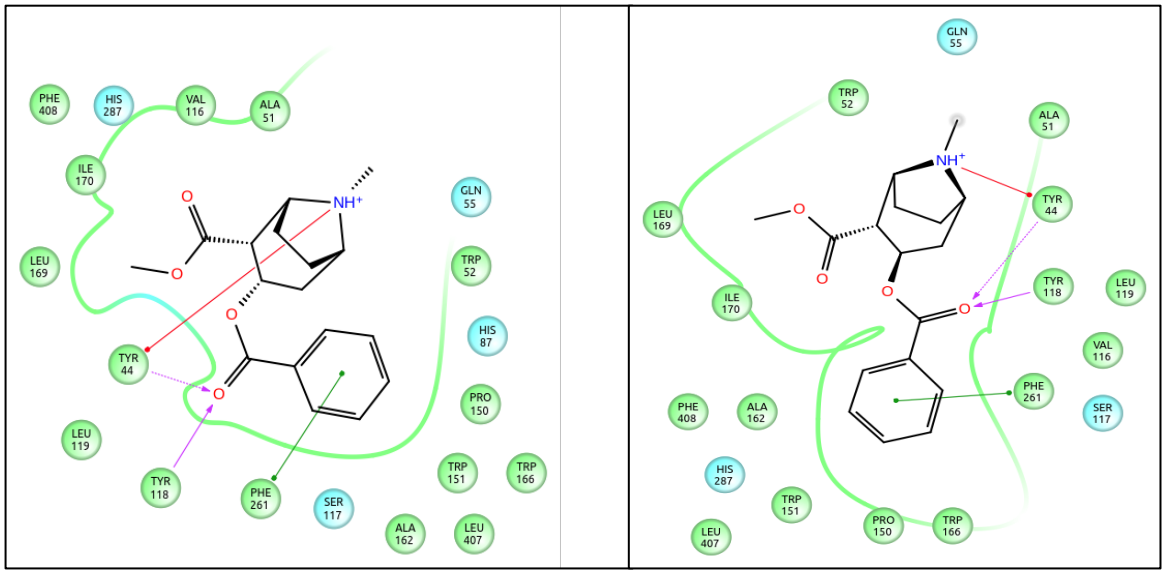

Figure 3.15: Results of Molecular Dynamic simulation done with CocE (PDB: 31DA) and cocaine. Both panels show the interactions between Phe^{261} and benzoic acid portion of cocaine and between Tyr^{118} and unbounded oxygen of benzoic acid. Ala^{51} and Gln^{55} reside in close proximity to tropane ring of cocaine.

We began this study hoping to find specific residues that could improve the overall efficiency of CocE with the original assumption that interrogating the residues nearest the active site, based on the benzoic acid-bound CocE structure, might reveal critical residues for catalysis and/or substrate binding.

The identification of a novel binding site for cocaine, using a non-hydrolyzable cocaine analog in crystallographic studies is striking. The structure of the RTI-150-CocE complex thus reveals a significantly different potential avenue to improve the binding kinetics of cocaine through unraveling a novel cocaine docking site. In particular two residues near the docking site, Ala^{51} and Gln^{55}, when mutated to glutamates, yielded significant improvements in the substrate affinity, as indicated by their dramatically lower K_M. The importance of these residues will be further explored in Chapter 5 of this thesis where the specific residues that improve kinetics are tested. Taking these data together we feel extremely enthusiastic that we may indeed be able to improve the catalytic constants for cocaine hydrolysis by CocE and that these may translate into engineering an effective treatment for cocaine abuse and intoxication.

	RTI-150	WIN 35,065-2
X-ray Source	APS LS-CAT 21-ID-D	APS LS-CAT 21-ID-D
Wavelength (Å)	1.02	1.02
Resolution range (Å)	44.2 - 1.8 (1.85 - 1.78)	37.8 - 1.8 (1.85 - 1.78)
Space group	P 21 21 21	P 21 21 21
Unit cell	64 98.763 197.502 90 90 90	67.8 100.7 213 90 90 90
Total reflections	768718	601283
Unique reflections	118557 (10657)	136517 (12019)
Completeness (%)	99.04 (90.43)	98.4 (88)
Mean I/sigma(I)	12.6	8.54
Wilson B-factor	15.8	17.9
R-merge	0.112	0.102
R-meas	0.143	0.125
CC1/2	0.955	0.935
CC*	0.988	0.983
R-work	0.2298 (0.2564)	0.177 (0.268)
R-free	0.2663 (0.2903)	0.206 (0.308)
Number of non-hydrogen atoms	8740	10251
macromolecules	8740	8737
ligands	*	*
water	0	1514
Protein residues	1142	1141
RMS(bonds)	0.007	0.007
RMS(angles)	1.09	1.1
Ramachandran favored (%)	96	96
Ramachandran allowed (%)	2.8	2.8
Ramachandran outliers (%)	1.3	1.2
Clashscore	1.45	1.92
Average B-factor	17.9	26.2
macromolecules	17.9	24.9
ligands	*	*
solvent	*	33.7

Table 3.1: Statistics of crystal structures produced with RTI-150 and WIN 35,065-2.
* = final ligand values will be added after refinement with ligand.

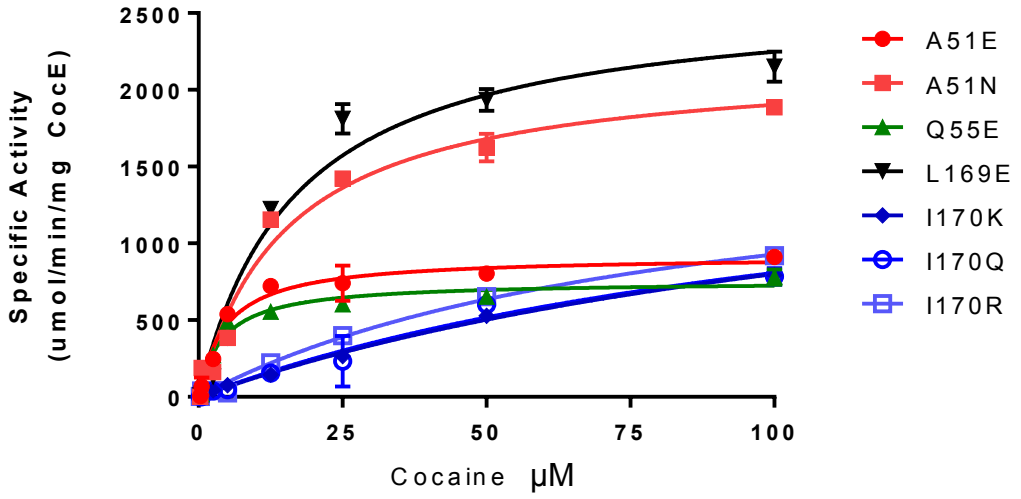

	A51E	A51N	Q55E	L169E	I170K	I170Q	I170R
V_{max}	920 +/- 40	2200 +/-120	750 +/-30	2600 +/-170	1900 +/-200	1800 +/-500	1700 +/-150
K_M	5.5 +/- 0.8	15 +/-3	4.1 +/- 0.7	17 +/- 3	140 +/-20	130 +/-50	180 +/-13

Figure 3.16: Kinetics of binding site mutants Mutations at residues 51, 55, 169, and 170 The kinetics of each mutation discussed in this chapter are shown with their respective Michaelis-Menton plots.

References

1. Nasser, A.F., et al., *A randomized, double-blind, placebo-controlled trial of RBP-8000 in cocaine abusers: pharmacokinetic profile of rbp-8000 and cocaine and effects of RBP-8000 on cocaine-induced physiological effects.* J Addict Dis, 2014. **33**(4): p. 289-302.
2. Howell, L.L., et al., *A thermostable bacterial cocaine esterase rapidly eliminates cocaine from brain in nonhuman primates.* Transl Psychiatry, 2014. **4**: p. e407.
3. Information, N.C.f.B.; Available from: https://pubchem.ncbi.nlm.nih.gov/compound/3080579
4. Collins, G.T., et al., *Cocaine esterase prevents cocaine-induced toxicity and the ongoing intravenous self-administration of cocaine in rats.* J Pharmacol Exp Ther, 2009. **331**(2): p. 445-55.
5. Bisswanger, H., *Enzyme Kinetics: Section 2.1–2.5*, in *Enzyme Kinetics*. 2008, Wiley-VCH Verlag GmbH & Co. KGaA. p. 59-124.
6. Bisswanger, H., *Enzyme Kinetics: Section 2.6–2.12*, in *Enzyme Kinetics*. 2008, Wiley-VCH Verlag GmbH & Co. KGaA. p. 124-193.
7. Larsen, N.A., et al., *Crystal structure of a bacterial cocaine esterase.* Nat Struct Biol, 2002. **9**(1): p. 17-21.
8. Vassylyev, D.G., et al., *Structural basis for substrate loading in bacterial RNA polymerase.* Nature, 2007. **448**(7150): p. 163-8.
9. Dixon-Clarke, S.E., et al., *Structures of the CDK12/CycK complex with AMP-PNP reveal a flexible C-terminal kinase extension important for ATP binding.* Sci Rep, 2015. **5**: p. 17122.
10. Chimnaronk, S., et al., *The crystal structure of JNK from Drosophila melanogaster reveals an evolutionarily conserved topology with that of mammalian JNK proteins.* BMC Struct Biol, 2015. **15**: p. 17.
11. Kimmel, H.L., F. Ivy Carroll, and M.J. Kuhar, *Locomotor stimulant effects of novel phenyltropanes in the mouse.* Drug & Alcohol Dependence, 2001. **65**(1): p. 25-36.
12. Carroll, F.I., et al., *Cocaine and 3 beta-(4'-substituted phenyl)tropane-2 beta-carboxylic acid ester and amide analogues. New high-affinity and selective compounds for the dopamine transporter.* J Med Chem, 1995. **38**(2): p. 379-88.
13. Scheffel, U., J.W. Boja, and M.J. Kuhar, *Cocaine receptors: in vivo labeling with 3H-(-)cocaine, 3H-WIN 35,065-2, and 3H-WIN 35,428.* Synapse, 1989. **4**(4): p. 390-2.
14. Kimmel, H.L., et al., *Faster onset and dopamine transporter selectivity predict stimulant and reinforcing effects of cocaine analogs in squirrel monkeys.* Pharmacol Biochem Behav, 2007. **86**(1): p. 45-54.

15. Runyon, S.P. and F.I. Carroll, *Dopamine transporter ligands: recent developments and therapeutic potential.* Curr Top Med Chem, 2006. **6**(17): p. 1825-43.
16. Narasimhan, D., et al., *Structural analysis of thermostabilizing mutations of cocaine esterase.* Protein Eng Des Sel, 2010. **23**(7): p. 537-47.
17. Otwinowski, Z., W. Minor, and et al., *Processing of X-ray diffraction data collected in oscillation mode.* Methods Enzymol, 1997. **276**: p. 307-26.
18. Adams, P.D., et al., *PHENIX: a comprehensive Python-based system for macromolecular structure solution.* Acta Crystallogr D Biol Crystallogr, 2010. **66**(Pt 2): p. 213-21.
19. Emsley, P., et al., *Features and development of Coot.* Acta Crystallogr D Biol Crystallogr, 2010. **66**(Pt 4): p. 486-501.
20. Huang, X., D. Gao, and C.G. Zhan, *Computational design of a thermostable mutant of cocaine esterase via molecular dynamics simulations.* Org Biomol Chem, 2011. **9**(11): p. 4138-43.
21. Brim, R.L., et al., *A thermally stable form of bacterial cocaine esterase: a potential therapeutic agent for treatment of cocaine abuse.* Mol Pharmacol, 2010. **77**(4): p. 593-600.
22. Dixon, M., *The determination of enzyme inhibitor constants.* Biochemical Journal, 1953. **55**(1): p. 170-171.
23. Cornish-Bowden, A., *A simple graphical method for determining the inhibition constants of mixed, uncompetitive and non-competitive inhibitors (Short Communication).* Biochemical Journal, 1974. **137**(1): p. 143-144.
24. ; Available from: https://pubchem.ncbi.nlm.nih.gov/compound/446220.
25. Turner, J.M., et al., *Biochemical Characterization and Structural Analysis of a Highly Proficient Cocaine Esterase.* Biochemistry, 2002. **41**(41): p. 12297-12307.
26. Fang, L., et al., *Rational design, preparation, and characterization of a therapeutic enzyme mutant with improved stability and function for cocaine detoxification.* ACS Chem Biol, 2014. **9**(8): p. 1764-72.

Chapter 4

Crystallographic Study Of Cocaine Esterase's Catalytic Triad

Introduction

Enzymes perform most naturally occurring reactions by lowering the activation energy required to form a product from a substrate. The active site of an enzyme houses the residues that conduct this chemistry. One well-defined set of residues that make up the active site of hydrolases such as acetylcholinesterase, proteases and cocaine esterase, is the catalytic triad of aspartic acid, histidine, and serine. This particular set of residues has evolved in enzymes that act on a diverse set of macromolecules, such as proteins, and small molecules, like alkaloid compounds[1].

The three residues that form the catalytic triad need to be in close enough proximity in order to transfer a proton from one R-group to another (Figure 4.1). The enzymatic mechanism includes abstraction of a proton from histidine by the neighboring aspartic acid. This initial proton abstraction includes polarization of histidine such that it allows the imidazole R-group of histidine to form a temporary bond with the proton of the hydroxyl of the serine side chain. By abstracting the proton away from serine, the oxygen of serine's hydroxyl group becomes a good nucleophile. The serine can now target a carbonyl carbon of the substrate for nucleophilic attack. Covalent attachment of the serine to the substrate becomes

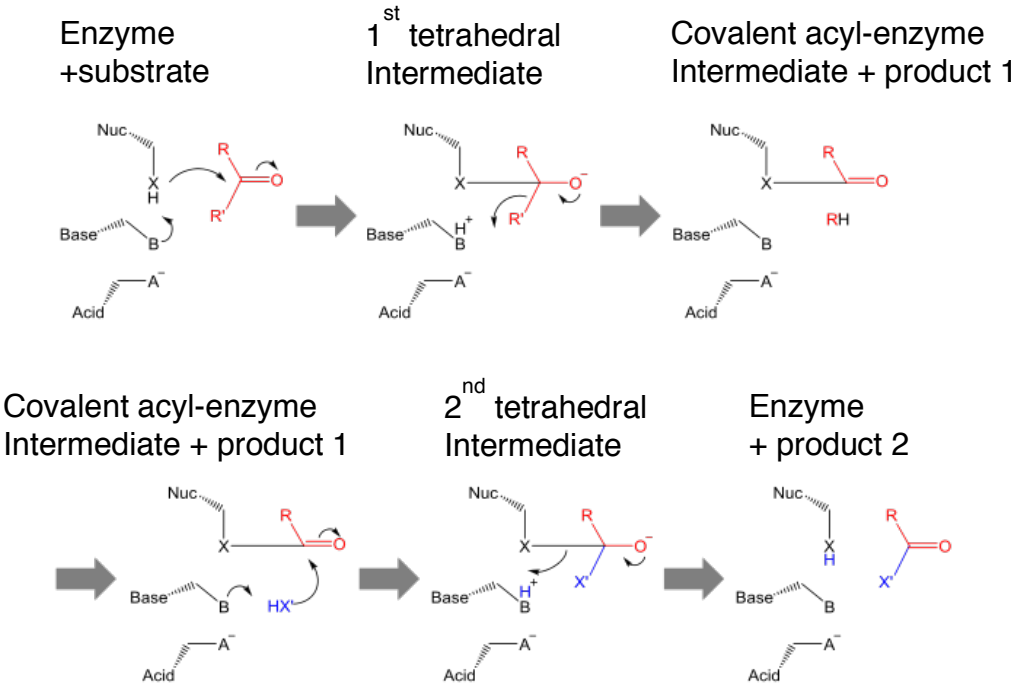

Figure 4.1: Enzymatic activity of a catalytic triad. Adapted from Wikipedia (https://en.wikipedia.org/wiki/Catalytic_triad) by Thomas Shadfee 2014.

the first tetrahedral intermediate formed between enzyme and substrate. This intermediate is resolved by abstraction of the proton from histidine, and the subsequent release of the first partial product follows. At this point, the histidine is able to abstract another proton from a molecule coordinated in the active site (H_2O in the case of hydrolases) and stabilize the nucleophile for attack on the carbon bound to the acyl-enzyme intermediate attached to the serine. After this second nucleophilic attack a second tetrahedral intermediate is formed and typically stabilized by an oxyanion hole on the enzyme. This intermediate is subsequently resolved by flow of electrons from the oxygen on carbonyl carbon of the second partial product back on to said carbon, reforming the double bond.

The attachment of serine to this carbon is destabilized and the serine abstracts the proton on histidine allowing for partial product release[1].

Cocaine esterase performs the same reaction mechanism on cocaine through its catalytic triad consisting of Asp^{259}, His^{287} and Ser^{117}. Mutations of any of these residues renders the enzyme inactive[2]. Though we know which residues are responsible for the hydrolytic activity of CocE, we have not established a clear role for the residues surrounding the active site nor have we studied the movement of active site residues during hydrolysis. The later phenomenon is also an important aspect of enzyme function[3]. More specifically, researchers were able to follow the movement of the active site histidine of an α/β-hydrolase during hydrolysis as the enzyme move from an "open" to "closed" conformation. Here the open conformation of the protein exists when substrate is not bound to the enzyme, and upon substrate binding the enzyme adopts a closed conformation that accompanies a shift in the position of the active site histidine, presumably allowing the hydrolysis reaction to follow.

Having a structure for each step in the enzymatic pathway would provide a more thorough description of the residues that coordinate substrate and product and the position of each member in the catalytic triad during hydrolysis of cocaine. Fortunately, a couple structures of CocE trapped in intermediate and product-bound states have been reported and are available. The original crystal structure of CocE captured a partial product trapped in the active site, modelled as benzoic acid[4]. The structure reveals a hydroxyl group of benzoic acid that is

coordinated by interactions with Trp^{166} and Tyr^{44} and by the amide in the backbone of Ser^{117}(PDB: 1JU4 - Figure 4.2 A). This structure also offered the first information on the orientation of the catalytic triad. Interestingly, the active site serine is positioned away from the partial product. They also found a water coordinated precisely between active site Ser^{117}, His^{287}, and Asp^{259}. By soaking the CocE crystals in phenyl boronic acid, the group produced a structure of a tetrahedral intermediate bound to Ser^{117} (PDB: 1JU3 - Figure 4.2 B). This structure reveals a 120° rotation of the Ser^{117} sidechain away from the position where it was found the benzoic acid-bound structure. During covalent attachment of the tetrahedral intermediate, the serine presumable undergoes a rotation of about 110-120° into position where the bound phenyl boronic acid can occupy a space near where the benzoic acid was shown to occupy. The catalytic triad histidine revolves ~57° away from the product, but the nitrogen of its imidazole ring still coordinates with one hydroxyl of the phenyl boronic acid. The other hydroxyl of boronic acid is positioned approximately where the hydroxyl of the benzoic acid was, coordinated by Trp^{166}, Tyr^{44}, and the backbone amide of Ser^{117}.

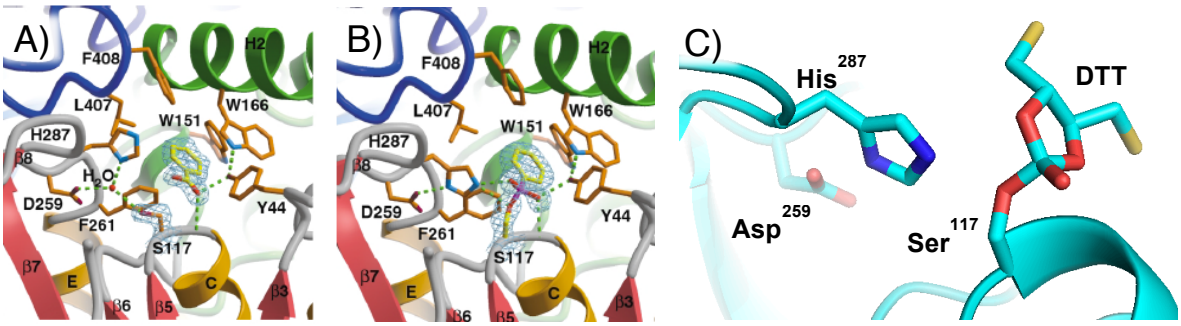

Figure 4.2: Structures of the active site of CocE in a complex with products or acyl intermediates. A) Structure CocE bound to benzoic acid (PDB:1JU4), B) Structure of CocE bound covalently to phenyl boronic acid (PDB:1JU3) and C) CocE bound as and adduct to DTT (PDB: 3I2K, Brim *et al* 2009). A) and B) were taken from Larsen *et al* 2002.

During a crystallographic analysis of CocE generated in our lab, we were able to produce another covalently bound molecule with similar but distinct aspects to the phenyl boronic acid-bound intermediate structure[5]. This structure reveals a DTT adduct bound to Ser^{117} (PDB: 3I2K – Figure 4.2 C). DTT was included in the protein purification procedures and during crystallogenesis in order to prevent non-specific disulfide bonding or oxidation of the cysteine residues on CocE.

In both structures, the serine residue adopts a similar position as found in 1JU3, projecting away from other active site residues. The dioxolane ring structure of DTT sits in the similar plane as the phenyl boronic acid.

These structures demonstrate the importance of several residues that could interact with products. Other than the residues mentioned above, structures PDB:1JU3 and PDB:1JU4 show that Phe^{261}, Leu^{407} and Phe^{408} all coordinate the ring structure of benzoic acid through hydrophobic interactions. Comparison of these structures with apo-CocE structures also reveal the movement of active site residues during the enzymatic reaction. While these

structures provide evidence of how CocE's residues interact with product, we still need to analyze how the intact substrate binds prior to hydrolysis.

To that end, we set out to gather structural information for how cocaine binds to CocE using x-ray crystallography. To address this question we take two approaches to trap components in the active site of CocE: 1) an enzyme bound to a non-hydrolysable tropane analog of cocaine; or, 2) an inactive enzyme with cocaine bound in the active site. Chapter 3 of this thesis described the results of the first approach through delineating a high-resolution structure of CocE structure bound to non-hydrolyzable cocaine analog RTI-150. The structure identified a novel docking site quite distal from the active site (>8Å away), as define by the benzoic acid and phenyl borate-bound structures. More interestingly, analysis of this site by mutagenesis suggests that this novel site is important for cocaine binding and hydrolysis. This chapter (Chapter 4) describes the crystal structure of an inactive mutant of CocE co-crystalized with cocaine, or unexpectedly metabolites thereof.

As stated previously, we realize that the high enzymatic activity of CocE would prohibit us from merely soaking cocaine into a crystal of CocE, even when it is trapped in a crystal. Therefore, we designed point mutants at each of the residues in the catalytic triad in the active site, and sequentially generated mutants $Ser^{117}Ala$, $Asp^{259}Asn$, and $His^{287}Ala$. Using these inactive mutants, we hoped to arrive at a structure of cocaine bound in CocE's active site. With such a structure in hand we could determine which residues interact with the substrate, and use this information to help us understand the substrate-binding portion of

the CocE's K_M value[6]. Here, models of CocE bound to substrate or product could be analyzed through interrogating interacting residues by mutagenesis and their enzymology. The models could be validated or altered depending on the enzymatic behavior the new mutations, and any mutations that show an improvement to CocE kinetics could be employed towards our long-term goal of developing a catalytically more efficient enzyme.

Methods

Generation of CocE: The enzymatically dead mutants of CocE were generated using a variation on the Quick-Change method for site-directed mutagenesis mentioned previously [5]. Oligonucleotide primers for Ser^{117}Ala, Asp^{259}Asn and His^{287}Ala were synthesized by Integrated DNA Technology (La Jolla, CA) with sequences: Ser^{117}Al= 5'- TTC GCG TTG CCT ACT TGG GTG –3'; Asp^{259}Asn = 5'- GGG TGG TAC AAC GGG TTC GTC G-'3; and His^{287}Ala = 5'-CCT TGG AGT GCC AGC AAC CTC-3'. For the active site mutations, oligonucleotide primers for Y^{118}A: 5' - C GGC GTT TCG **GCG** TTG GGT GTG - 3'; Y^{118}F: 5' - C GGC GTT TCG **TTT** TTG GGT GTG - 3'; M^{141}A: 5' - GCG CCG TCC **GCC** GCG TCG GCG - 3'; and S^{288}T: 5' -TGG AGT CAC **ACC** AAC CTC AC - 3' were ordered from Integrated DNA Technology and used in a PCR with the CC-CocE gene as template for the reaction.

Following site-directed mutagenesis the gene encoding CocE was expressed from pET-22b (+) plasmid in BL21 (DE3) (Novagen) bacterial cells. Cells were grown to OD_{600} = 0.6 AU, temperature-shifted to 18°C, and protein

expression was initiated with the addition of 1mM Isopropyl β-D-1-thiogalactopyranoside (IPTG) (Genesee Scientific). Expression continued for 16 hours, and cells were pelleted and stored at -80°C until purification. The cell pellet was resuspended in 1X Tris-buffered saline (TBS) in the presence of protease inhibitors limabean trypsin inhibitor and leupeptin and broken with two passes through a French Press. (ThermoScientific) Bacterial lysate was clarified by centrifugation at 25,000 x *g* and loaded onto a Ni^{2+}NTA column equilibrated with 1 x TBS at pH 7.4. The protein was eluted using 1 x TBS with 150 mM imidazole. Protein dimers were covalently cross-linked by incubating with 50 μM $CuCl_2$ at 4°C overnight. The entire reaction was loaded onto a Q-sepharose column equilibrated with 50 mM Tris, pH 8.0 and eluted with linear NaCl gradient. Peak fractions were analyzed with SDS-PAGE, pooled and concentrated to 10 mg/ml with Amicon concentrators (Millipore) and stored at -80°C.

Generation of Crystal Structures: CocE crystals were grown by hanging drop vapor diffusion in 24-well VDX trays (Hampton Research). One microliter of protein (either inactive Asp^{259}Asn or His^{287}Ala, or RQ-CocE with saturating concentrations of cocaine) and well solution (PEG/MES/NaCl) were mixed on siliconized glass coverslips (Hampton Research) and placed over 1 ml of well solution. Trays were incubated at 12°C and crystal growth was observed after 2-3 days. Crystals were harvested and placed in cryoprotectant (well solution supplemented with 20 % glycerol) and flash-frozen in liquid or alternatively crystals were soaked in cryoprotectant containing saturating solution of either

cocaine allowed to incubate at room temperature for 5 minutes. Crystals were mounted on proper sized loops (0.2 – 0.4 μm – Hampton Research) and flash frozen in liquid nitrogen. X-ray diffraction data were collected at the Advanced Photon Source. Data were integrated and scaled using HKL2000[7]. Molecular replacement using Phaser was run using PDB:3IDA as the search model. Successive rounds of refinement were performed using Phoenix software [8] and manual fitted using Coot [9].

Cocaine esterase activity assays: Cocaine assay: Purified PEG:CocE was analyzed using our standard absorbance-based cocaine assay, described previously[10]. Here, cocaine (Mallinckridt, Hazelwood, MO) is added a 96-well UV-permeable plate (Costar; Corning Life Sciences, Lowell, MA) at 200, 100, 50, 25, 10, 5, 1 and 0.5 μM concentrations. The reaction is initiated by the addition of PEG:CocE (65 ng/ml) at a 1:1 dilution in the plate. The velocity of the reaction was measured every 10s for 20 minutes by a SpectraMax Plus 384 UV plate reader (Molecular Devices, Sunnyvale, CA) using SOFTmax Pro software (version 3.1.2). The absorbance readings were converted to change in concentration of product using using Beer's law. The specific activity of the enzyme was plotted using Prism software (GraphPad Software Inc., San Diego, CA) and kinetics of the reaction (k_{cat} and K_m) generated.

Results

Crystal structure from inactive CocE cocrystallized with cocaine: After expression and purification of the $Ser^{117}Ala$, $Asp^{259}Asn$ and $His^{287}Ala$ CocE mutants, an enzymatic assay was performed using cocaine as the substrate and confirmed that no measureable activity based on the absorbance assay could be detected (data not shown).

While no crystals were obtained with the $Ser^{117}Ala$ mutant in co-crystallization attempts, nor were any satisfactory diffraction data sets collected on the $Ser^{117}Ala$ crystals soaks, we were able to generate good data sets with the crystals of $Asp^{259}Asn$ and $His^{287}Ala$ CocE. The resolution limit of $Asp^{259}Asn$ was 1.8 Å, and the limit for $His^{287}Ala$ was 2.6 Å. The data contained two monomers per asymmetric unit as seen in previous CocE structures generated under similar conditions. The refinement statistics are detailed in Table 4.1.

The model generated from these data showed a distinct electron density around Ser^{117} in the active site (Figure 4.3) that resembles the density found for benzoic acid-bound structure (PDB:1JU4) rather than the much larger substrate cocaine. It thus appears, based on the electron density that we have trapped a molecule of benzoic acid in the active site, puzzling since the enzyme is a confirmed catalytically inactive mutant. Careful comparative analysis of this novel structure with PDB:1JU4 reveals subtle but distinctly structural different in the position of the benzyl ring (tilt angle), the residues that compose the catalytic

triad, and the presence of a strong density consistent with a deprotonate water, (OH^-) near Ser^{117}. Similar to the benzoic acid-CocE structure Phe^{261}, Leu^{407}, and Phe^{408} all sit within 5 Å of the phenyl ring of the product. These residues have become important in our next study attempting to generate a more efficient CocE enzyme. (Chapter 5 of this thesis)

The most obvious difference between the two structures is the continuous electron density found between the benzoic acid and the Ser^{117} side chain the rotomeric angle of the serine and the proximity of the benzoic acid to the Ca carbon of Ser^{117} (See Figure 4.3). These features are consistent with a covalent intermediate of benzoyl moiety bound to Ser^{117}.

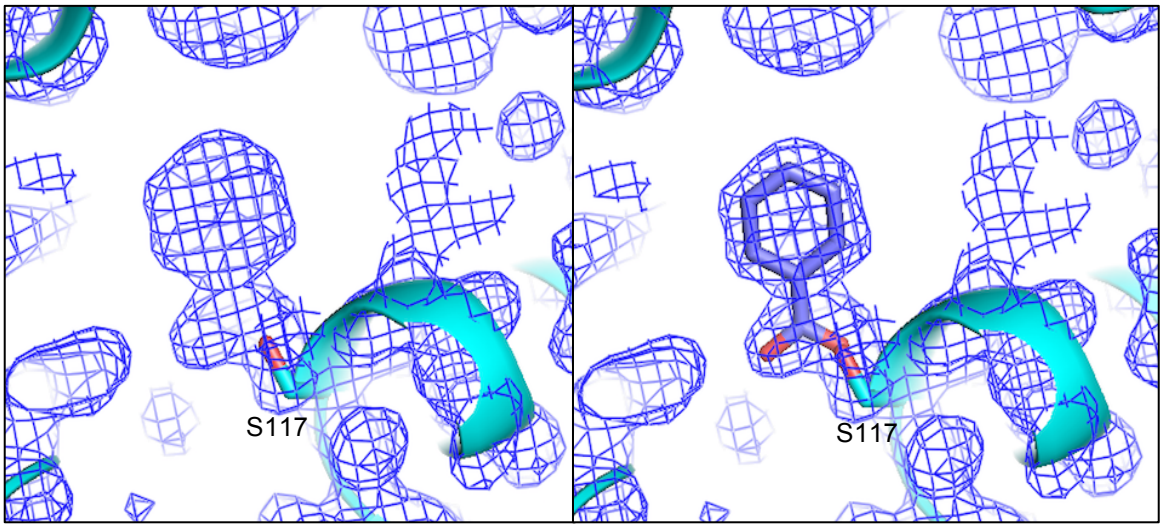

Figure 4.3: Covalent intermediate attached to Ser^{117} Electron density present after co-crystallizing Asp^{259}Asn with cocaine. Purple mesh represents composite omit map generated at 1.8 Å shown at 3 σ. Right panel contains representative structure of benzoic acid positioned within the density for visualizing results.

Looking at the active site residues, we see the most dramatic shift in His^{287} (Figure 4.4). Analysis of these structures reveal that His^{287} is within hydrogen bonding distance to Asp^{259} in the transition state intermediate modelled

from phenylborate-bound CocE structure (PDB:1JU3). However, following hydrolysis to product benzoic acid the side chain of His^{287} appears to lose it's hydrogen binding to Asp^{259} and rotates away(PDB:1JU4). His^{287} in our structure, which contains the covalent acyl-enzyme intermediate, resembles more of the benzoic acid structure, and rotating toward the neighboring Ser^{288}. Accompanying this rotation away from Asp^{259} is 180° flip of the imidazole ring where the N-1 (*pros* – *π*) nitrogen appears closer to Ser^{288} and more importantly the N-2 (*tele* – *τ)* nitrogen is close to the oxyanion of the benzoyl moiety.

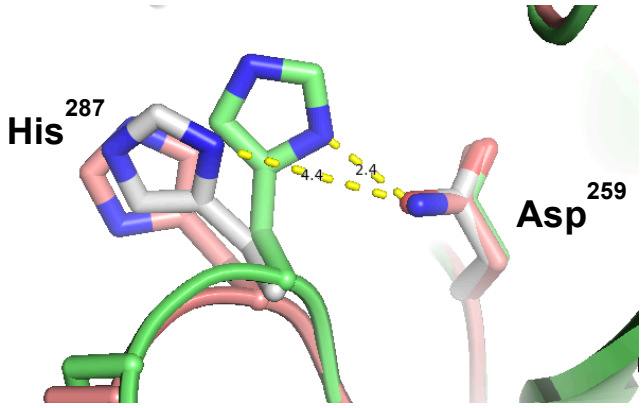

Figure 4.4: Rotation of His^{287} during catalysis. Illustrated is the position of His^{287} bound to phenylboronic acid (green, PDB:1JU3), benzoic acid (grey, PDB:1JU4), or as an acyl-enzyme intermediate (fleshtone). Indicated is the distance (Å) between the imidazole ring of His^{287} and the oxalate of Asp^{287}.

To further investigate the position of active site residues, several residues were selected for mutation. Two residues directly downstream of active site residues were chosen, Tyr^{118} and Ser^{288}, based on the movement of Ser^{117} and His^{287}, respectively. Also, methionine at position 141 was chosen due to its orientation above the active site, showing potential to influence both substrate and catalytic triad.

Analysis of CocE active site mutants

Table 4.2 Catalytic constants of substitutions of Tyr^{118}

Mutant	K_M (μM)	V_{max} (min^{-1})	Catalytic Efficiency (μM^{-1}•min^{-1})
Tyr^{118}Ala	>400	6500*	NC
Tyr^{118}Phe	42 +/- 13	370 +/- 50	8.7
* note that this value is insignificant since the Km> concentrations of cocaine used in the assay			

***Tyr^{118}*:** Tyr^{118} sits at the N-terminus of alpha helix C in domain I. This residue is not close enough to substrate to interact with the molecule, but its proximity next to the active site serine (Ser^{117}) and could influence the hydrolysis of cocaine by CocE. As stated above, CocE belongs to the α/βhydrolase superfamily of proteins, and as such, contains a slight variation of the GXSXG motif surrounding

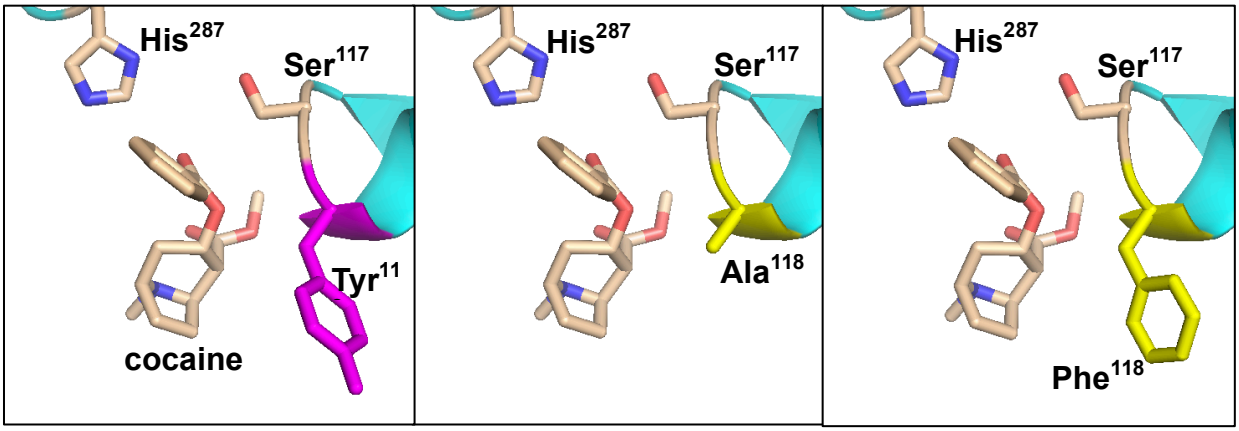

Figure 4.5: CocE residue Tyr^{118}. The left panel shows the native residue Tyr^{118} positioned near the active site and possibly interacting with the tropane ring. The middle panel displays mutant Tyr^{118}Ala whereas the right panel contains position of Tyr^{118}Phe according to its minimal energy constraints.

the active site serine. In CocE, the sequence around Ser^{117} reads GVSYLG, having an extra residue (leucine) preceding Gly^{120}.

Both mutations generated at position 118 produced enzymes that were virtually inactive. The Tyr^{118}Phe mutant retained some activity with a K_M that is almost twice that of our control CocE kinetics, but the V_{max} of this mutant dropped to only 370 min^{-1}. By retaining the aromatic group of tyrosine with the phenylalanine mutation, the enzyme could retain the overall structure at this position but apparently lost its ability to hydrolyze substrate in an appreciable manner.

The Tyr^{118}Ala mutant showed almost no capacity to hydrolyze cocaine due to it's undeterminable Km. We interpret the removal of the aromatic ring as removing a major component of the interaction with the tropane ring of cocaine and thus removing a major interaction surface resulting in dramatic decreases in substrate binding affinity. As a result of the deficit in substrate binding affinity to the point where the conditions of our absorbance assay could not accurately determine the Vmax, nor overall catalytic efficiency (NC).

Met^{141}: Met^{141} sits at the C-terminus of the β6 strand, in a loop region that connects DOM1 and DOM2. Since it is positioned within 4 Å of two active site residues, Ser^{117} and Asp^{259}, so it has potential to influence the orientation of these two residues during enzymatic activity. This residue was also chosen due to its position in proximity to an active site water modeled in to the density map in 1JU3 and our maps with the RTI compound. Our reasoning was that by increasing the hydrophobicity of this pocket, excluding water, the D^{259} would

become more acidic and increase proton transfer to S^{117}, and therefore increase overall velocity of the enzyme.

Mutation from methionine to alanine was a first step in exploring the hydrophobic effect at this position. Though alanine does not have the overall density of methionine, we reasoned that an alanine would provide a more structured hydrophobic presence and potentially hold help exclude waters. The results suggest that decreasing the size of the residue has only hindered the ability of cocaine to bind, increasing the overall K_M, and also disrupting chemistry in the active site, decrease in V_{max}. Mutating to a larger hydrophobic residue (isoleucine or phenylalanine) will provide a larger hydrophobic density that might support our initial positing of how the hydrophobic effect can increase active site proton transfer through exclusion of water.

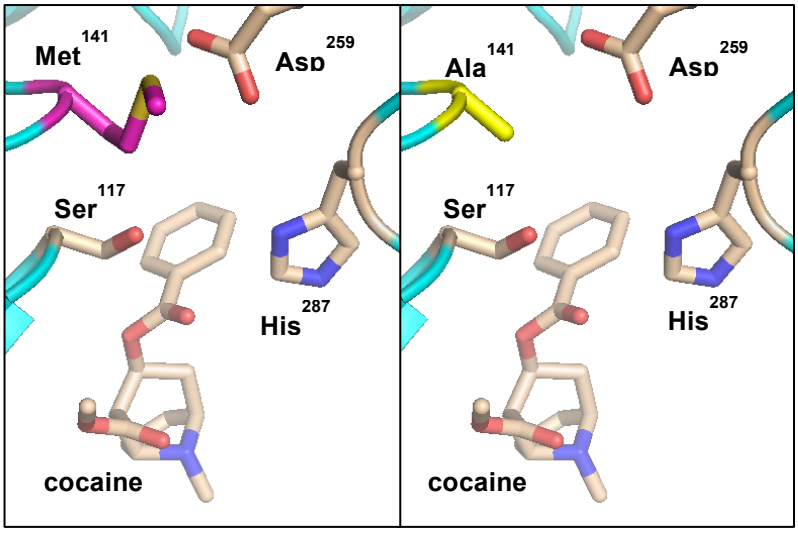

Figure 4.6: CocE residue 141 Left panel shows residue Met^{141} in proximity to the catalytic triad. Right panel shows hypothetical positioning of Ala^{141}

Table 4.3: Kinetics of CocE mutant – $M^{141}A$

Mutant	K_M (μM)	V_{max} (min^{-1})	Catalytic Efficiency ($\mu M^{-1} \bullet min^{-1}$)
M141A	110 +/- 30	580 +/- 98	5.4

$Ser^{288}Thr$: The long loop region connecting the β8 and β8a strands of DOM1 contains Ser^{288} (Figure 4.7) We believe that the R-group of this residue sits in close enough proximity to His^{287} for it to influence the positioning of the imidazole group and therefore the overall chemistry. We chose threonine as the residue to replace serine so that the hydroxyl presence is preserved, but the increased size of the R-group may provide crowding to bring the His closer to the ester bond being hydrolyzed, and expedite resolution of the tetrahedral intermediate.

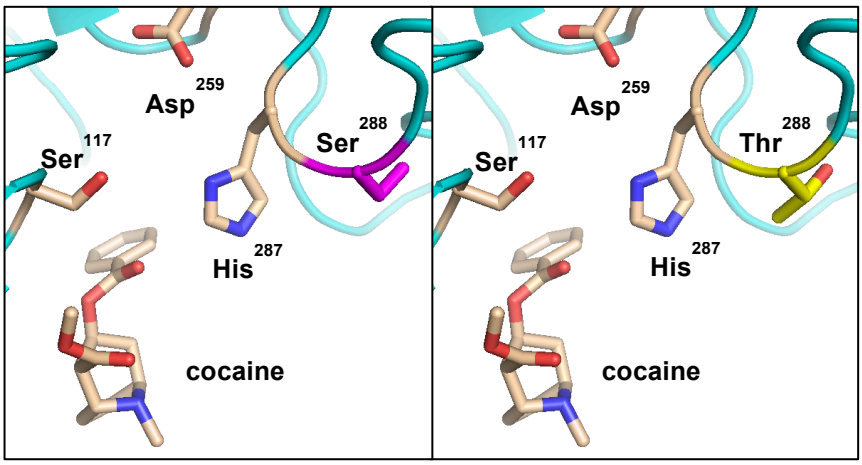

Figure 4.7 CocE residue 288 Left panel shows position of Ser^{288} next to His^{287} of catalytic triad. Right pane shows positioning of Thr^{288} mutation.

Table 4.4: Kinetics of CocE mutant – $Ser^{288}Thr$

Mutant	K_M (μM)	V_{max} (min^{-1})	Catalytic Efficiency ($\mu M^{-1} \bullet min^{-1}$)
$Ser^{288}Thr$	31 $^{+/-}$ 9.0	4800 $^{+/-}$ 54	154

This mutant showed some of the best kinetic improvement of all mutants tested. The velocity increased almost two-fold, and the change in K_M although only slightly elevated is better than some of our most thermostable mutants. The overall catalytic efficiency, therefore is improved almost 50% above our highest activity mutant (KQ-CocE). We hypothesize that this increase in V_{max} is due to a more optimized positioning of His, as stated above and will be elaborate in chapter 5, but further analysis will require structural information.

Discussion

Finding the benzoic acid covalently attached to Ser^{117} in the $Asp^{259}Asn$, rather than the substrate cocaine bound to this catalytically inactive enzyme, was an unexpected result. The intention was to obtain the structure of CocE bound to cocaine using a catalytically inactive mutant. Removing the acidic residue (Asp^{259}) from the catalytic triad should disrupt the orientation of the histidine residue, and presumably not allow the initial nucleophilic attack of the Ser^{117} on the substrates ester carbonyl carbon due to the imidazole group of His^{287} not abstracting the proton from Ser^{117}. The role of Asp^{259} is normally to help stabilize the base (His^{287}) in its protonated form until it can donate the proton to the 1st product (Figure 4.1). Though the mutants showed no activity when assayed, the $Asp^{259}Asn$ mutant still possessed enough energy to promote a “half-turnover” style chemistry that allowed the first tetrahedral intermediate to form and then be resolved, thus releasing one mole of ecgonine methylester per mole of enzyme.

Interestingly, a strong electron density is found in the acyl-enzyme intermediate structure located just above the ether linkage on Ser^{117} (Figure 4.8). This strong density is too large to be a cation and extremely well ordered. It is also located at the same position of as one of the hydroxyls of phenyl boronic acid bound to CocE as a tetrahedral intermediate. We therefore surmise that the density may represent a hydroxyl (OH^-) poised for nucleophilic attack of the carbonyl of the benzoyl moiety of acyl-enzyme intermediate. It is not clear how the OH^- is stabilized since the proton-accepting capacity of His^{287} was compromised the $Asp^{259}Asn$ mutation. A likely explanation is the presence of Tyr^{44} positioned directly above the active site and pointing directly at the putative OH^-. Note that a $Tyr^{44}Phe$ is catalytically inactive [4].

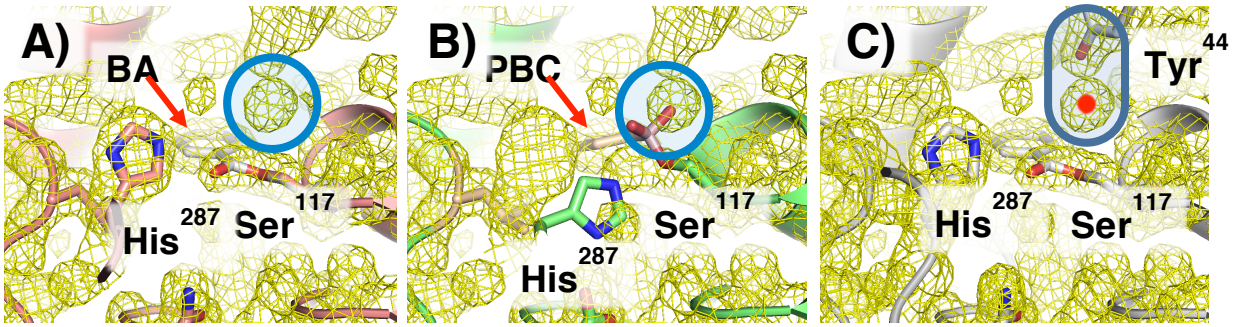

Figure 4.8 Trapping the attacking OH^- in the Acyl-enzyme intermediate structure. A) a strong electron density (circled in blue) was located above the Ser^{117}-benzoyl ester. B) the strong density superimposes on the OH^- of phenyl borate-CocE in the tetrahedral intermediate structure (PDB: 1JU3). C) the attacking OH-maybe be stabilized by Tyr^{44}, located directly above.

The reaction mechanism for resolving the second tetrahedral intermediate involves activation of a water molecule by proton abstraction by histidine. Upon

activation, the water can perform a nucleophilic attack on the carbon covalently attached to Ser^{117}. His^{287} is capable performing the proton abstraction after it is coordinated by an active site aspartic acid (Asp^{259}). In our structure, the reaction appears to have halted after the release of the first product, EME, and the enzyme is attenuated in the covalent acyl-enzyme intermediate step (Figure 4.8). It therefore appears that the His^{287} coordination by Asp^{259} is only necessary for resolving the second covalent intermediate.

We hypothesize that this model is supported by our covalent intermediate structure in terms of how the His^{287} residue is positioned away from the active site. As described above, the active site histidine resides similar to that found in the tetrahedral intermediate structure in 1JU3. Since this histidine is shifted away from the active site, the proton abstraction from the active site water could be attenuated and therefore final resolution of the second tetrahedral intermediate prohibited.

The position His^{287} in the RTI-150 containing structure provided another half step in generating a model of CocE's mechanism of hydrolysis. Considering each structure covered so far, the imidazole ring of His^{287} resides in one of two positions: 1) with the π-nitrogen of imidazole facing the active site, or 2) with the same nitrogen facing away from the active site. The residue will shift approximately 3 Å in the same plane towards or away from the active site, but the aforementioned rotation is the greatest movement seen in this residue. His^{287} of the RTI-150 structure is the only result showing the ring portion out of plane, perpendicular to the histidine of all other CocE structures. Though we can

only speculate towards a reason, we know that this structure is not a completely ligand-free, or apo, structure. While there is no substrate or product in the active site, there is a putative substrate bound to the enzyme. The perturbation of this substrate binding may be shifting the histidine towards the active position, where it is ready for proton abstraction from the serine residue that will initiate chemistry of hydrolysis.

In this study, several mutants were generated to investigate repositioning the active site residues. The Michaelis-Menton plot of enzyme assays is summarized in Figure 4.10. Both mutations to Tyr^{188} altered CocE activity by either completely disrupting cocaine binding (Tyr^{118}Ala) or by reducing chemistry to a V_{max} almost a full order of magnitude lower compared to a fully active enzyme (Tyr^{118}Ala). Presumably, taking away the van der Waals contacts of the phenyl ring in the alanine substitution opens the active site up so that substrate can't bind with an appreciable affinity. Note that the high V_{max} value in this mutant is therefore a projected value with little significance since the Km estimates are beyond the limits of the assay. Alternatively, by removing the hydroxyl of tyrosine, leaving the phenylalanine, the substrate is able to bind (demonstrated by slightly perturbed K_M of 40 μM) and chemistry occurs albeit at a much-reduced rate.

The Met^{141}Ala mutation was viewed as a "whole system" perturbation due to how the R-group of methionine sits across the active site, and shows potential to influence positioning of active site residues and substrate alike. The results of this mutation demonstrate exactly that. By removing the bulky R-group, the K_M

reduced by over 4-fold and the V_{max} lost an order of magnitude in value. Thought we cannot explain the results through the effect on substrate or active site coordination, by affecting all aspects of the kinetics, this mutation shows the importance of this residue. Future studies could focus on using different residues to see if a more optimal mutation exists.

Perhaps the most interesting mutation is the $Ser^{288}Thr$ substitution as it provides improvement to only the velocity. Looking at the structures, by placing a bulkier residue in place of serine, *eg.* a methyl group of a threonine residue, but keeping the hydroxyl presence, we may have positioned the His^{287} in the position closest to the active site residues as demonstrated from the various structures in Figure 4.4. A more thorough discussion of this mechanism is discussed in the following chapter (Chapter 5).

This new acyl-enzyme intermediate structure has now allowed us to generate a more complete snapshot of the enzymatic reaction of cocaine hydrolysis by CocE. The structural data along with site-directed mutagenesis studies have helped to delineate the contributions of many of the residues surrounding the catalytic sites. Below is a pictorial summary of the structural information now available to our laboratory presented in sequentially ordered fashion to reflect the reaction coordinate of cocaine metabolism by cocaine esterase (Figure 4.9).

Since we are trying to generate a more efficient CocE enzyme, we hypothesize that this new structure could significantly help in our enzyme engineering efforts. Three residues look to be in close enough proximity to have

hydrophobic interactions with the phenyl ring of benzoic acid. Phe^{261} and Phe^{408} along with Leu^{407} all have potential to interact with the benzoic acid product. While interpreting the results of the Larsen *et al* study, we reasoned that they found benzoic acid trapped in the active site due to the failure of the enzyme to release this final partial product. Our structure shows which residues may be interacting with the benzoic acid as well as provides the pivotal information to help us understand the catalytic mechanism. We hope to use these data as well as the spectacular new date in Chapter 5 which describes the existence of an additional binding site, a docking site, for the substrate cocaine. The identification of mutants described here and mutants described and characterized in Chapter 5, which were all based on novel crystallographic data on CocE, will provide multiple templates for engineering enzymes with improved catalytic constants and improved overall catalytic efficiency.

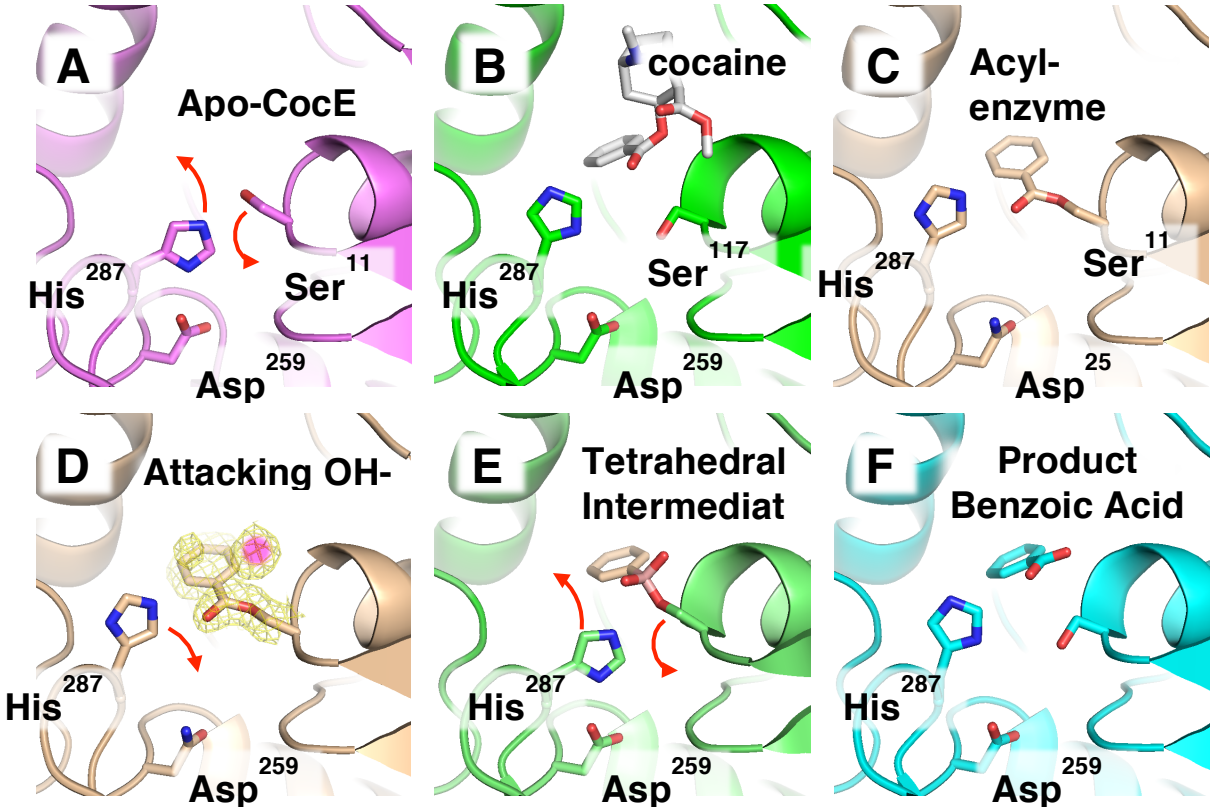

Figure 4.9 Structural representation of chemistry of cocaine hydrolysis by cocaine esterase. A) The catalytic triad located in the active site of CocE. B) Both His^{287} and Ser^{117} have to move their side chains (red arrows) to accommodate the binding of cocaine, based on the benzoic acid-bound form of CocE (PDB:1JU4). C) Acyl His^{287} may be able to perform limited proton donor activity to allow for the nucleophilic attack of the Ser^{117} side chain on the carboxyl ester of cocaine. The result is the formation of an acyl-enzyme intermediate. D) Tyr^{44} (not shown) helps to deprotonate H_20creating a nucleophile (OH-) poised to attach the carbonyl of the Ser^{117}-benzyol intermediate. D) rotation of the imidazole ring of His^{287} toward a more productive interaction with Asp^{259}, to aid in stabilizing the protonated state of His^{287}. E) The tetrahedral intermediate, modeled here based on the phenyl boronic acid structure (PDB: 1JU3) contains a OH- on the ester-CocE linkage at the precise location of the position of the OH- in D). F) Nucleophilic attack of the Ser^{117} by the OH- releases the product benzoic acid(PDB:1JU4). As a result both the Ser^{117} side chain and His^{287} imidazole ring adopt the apo-CocE position.

	D259N Covelent Intermediate
X-ray Source	APS LS-CAT 21-ID-D
Wavelength (Å)	1.02
Resolution range (Å)	47.1 – 1.8 (1.86 - 1.8)
Space group	P 21 21 21
Unit cell	63.8 98.5 197 90 90 90
Total reflections	757167
Unique reflections	116242 (11274)
Completeness (%)	99.7 (97.8)
Mean I/sigma(I)	18.1
Wilson B-factor	18.3
R-merge	0.081
R-meas	0.101
CC1/2	0.955
CC*	0.988
R-work	0.164 (0.23)
R-free	0.187 (0.27)
Number of non-hydrogen atoms	9893
macromolecules	8771
ligands	37
water	1085
Protein residues	1147
RMS(bonds)	0.007
RMS(angles)	1.09
Ramachandran favored (%)	96
Ramachandran allowed (%)	2.6
Ramachandran outliers (%)	0.26
Clashscore	2.83
Average B-factor	23.1
macromolecules	22
ligands	41.6
solvent	30.9

Table 4.1: Statistics of crystal structures produced with $D^{259}N$ containing a covalent intermediate bound to Ser^{117}.

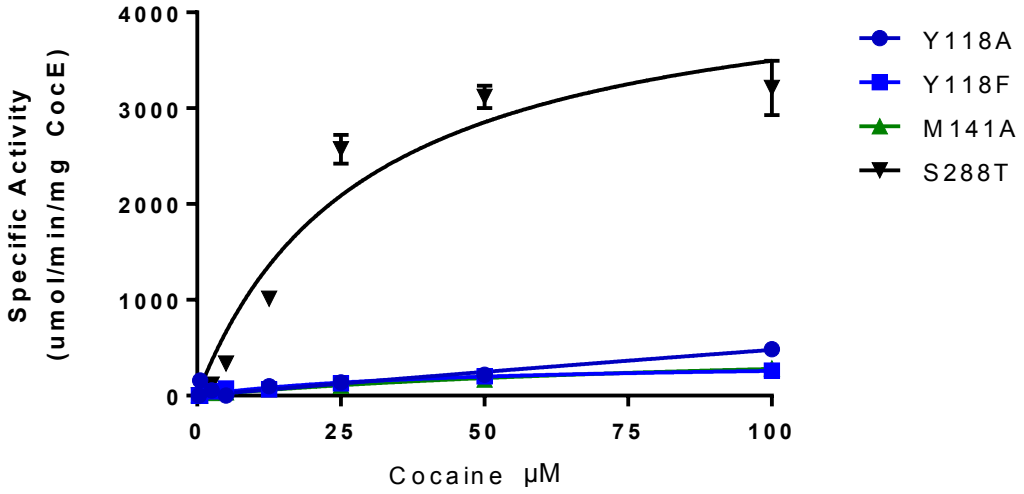

	Y118A	Y118F	M141A	S288T
V_{max} (min^{-1})	6500*	370 +/- 50	580 +/- 98	4800 +/- 54
K_M (µM)	1300*	42 +/- 13	110 +/- 30	31 +/- 9

Figure 4.10 Kinetics of CocE mutants Single mutations to CocE generated in CC background. All mutations were tested in standard cocaine based assay. Analysis of individual data points covered in respective sections in text.

References

1. Voet, D., Voet, J.G., & Prat, C.W., *Principles of Biochemistry*, in *Principles of Biochemistry*, J.W. Sons, Editor. 2010, John Wiley & Sons: Singapore.
2. Turner, J.M., et al., *Biochemical Characterization and Structural Analysis of a Highly Proficient Cocaine Esterase.* Biochemistry, 2002. **41**(41): p. 12297-12307.
3. Sun, Y., et al., *Molecular basis of the general base catalysis of an alpha/beta-hydrolase catalytic triad.* J Biol Chem, 2014. **289**(22): p. 15867-79.
4. Larsen, N.A., et al., *Crystal structure of a bacterial cocaine esterase.* Nat Struct Biol, 2002. **9**(1): p. 17-21.
5. Narasimhan, D., et al., *Structural analysis of thermostabilizing mutations of cocaine esterase.* Protein Eng Des Sel, 2010. **23**(7): p. 537-47.
6. Huang, X., D. Gao, and C.G. Zhan, *Computational design of a thermostable mutant of cocaine esterase via molecular dynamics simulations.* Org Biomol Chem, 2011. **9**(11): p. 4138-43.
7. Otwinowski, Z., W. Minor, and et al., *Processing of X-ray diffraction data collected in oscillation mode.* Methods Enzymol, 1997. **276**: p. 307-26.
8. Adams, P.D., et al., *PHENIX: a comprehensive Python-based system for macromolecular structure solution.* Acta Crystallogr D Biol Crystallogr, 2010. **66**(Pt 2): p. 213-21.
9. Emsley, P., et al., *Features and development of Coot.* Acta Crystallogr D Biol Crystallogr, 2010. **66**(Pt 4): p. 486-501.
10. Brim, R.L., et al., *A thermally stable form of bacterial cocaine esterase: a potential therapeutic agent for treatment of cocaine abuse.* Mol Pharmacol, 2010. **77**(4): p. 593-600.

Chapter 5

Increasing the Catalytic Properties of CocE Through a Structure-based Approach

Introduction

A crucial step in developing an enzyme-based therapeutic is to optimize the enzymes catalytic properties. Treating cocaine addiction, like treating many substance abuse-related diseases, requires good patient compliance and thus benefits from continuous, on-board therapeutic. Cocaine esterase, an enzyme that efficiently hydrolyses cocaine into inactive metabolites - ecgonine methylester and benzoic acid - has demonstrated great potential as a therapeutic to treat cocaine addiction through rapidly accelerating cocaine metabolism and elimination. Indeed, a thermostable form of enzyme has been successfully tested in humans as an antidote for cocaine intoxication [1]. We have since generated several forms of the enzyme with superior thermostability profiles and have tested them in models of toxicity in rodents.

While our current enzyme is arguably the most efficient to date, its actual kinetic parameters may not the most desirable for treating cocaine addiction [2]. Typical circulating cocaine concentrations found in a dosing cocaine addict might reach 50 μM in humans [3, 4]. The catalytic properties of our current enzyme would dictate that it would require 2-3 grams of enzyme on board to reduce the

cocaine to levels that are not physiologically effective, for an average 70 kg male. To avoid patient compliance issues and multiple administration protocols they formulation must either be stable in vivo for long periods (eg. 1 month), or a sustained release formulation would be required. The limited *in vivo* lifetime of biologics, which in this case is ~48 hours for the best current form of CocE, would limit our formulation to the latter, that of sustained release. A back of the envelope calculation would imply that loading a sustained release module, or even an osmotic pump, with one months worth of CocE would require approximately 30 grams of protein. Increasing the catalytic efficiency of CocE by 5-10-fold would reduce that level substantially.

Moreover, such an increase in enzyme performance would significantly reduce the cost of production of the enzyme, something that could be significant for the cocaine overdose antidote. The cost of production of protein-based therapeutics is significantly higher than for small molecule drugs. A 2008 report found that the production costs for biologics in the United States is approximately $45 per day or $16,425 per year, compared to $2 per-day and $730 per-year for more traditional, small molecule pharmaceuticals [5]. Any increase in drug efficacy or enhancement of production efficiency will therefore have a profound impact on the cost of production. Though we have optimized protein production of CocE in bacteria to gram level quantities in the laboratory and kilogram quantities for clinical trial studies, any increase the enzyme efficiency and efficacy would have a significant impact on the cost of production.

One of the most straightforward and readily available methods to improve enzyme kinetics is through site-directed mutation. One of our earlier thermostable mutant CocE enzymes, Leu^{169}Lys/Gly^{173}Gln-CocE (KQ CocE), unexpectently also displayed higher catalytic activity than wild-type [6]. The maximal velocity of KQ CocE (6500 min^{-1} for cocaine) is almost three times higher than the CocE mutant currently in clinical trials to treat cocaine addiction, Thr^{173}Arg/Gly^{173}Gln-CocE (RQ-CocE, 2500 min^{-1}).

While both KQ-CocE and RQ-CocE share the glutamine mutation at position 173, mutation of a single residue (L^{169}) seems to confer enhanced catalytic properties. Unfortunately the increase in V_{max} of KQ-CocE did not accompany an overall improvement in the enzymes catalytic efficiency, since an increase in K_M value is observed. The differences in the velocites of two mutant forms of CocE, is still encouraging, leading us to reason that we could generate other mutants with better kinetics through strategic mutation with not only better chemistry but also increased rates of substrate binding and/or product release.

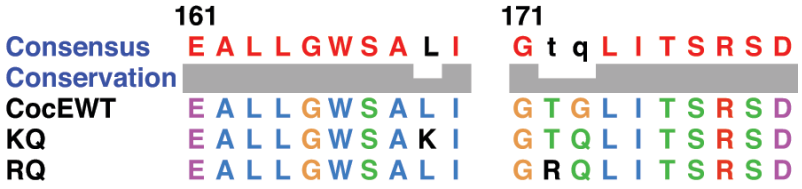

Figure 5.1: Amino acid sequence alignment of CocE mutants WT, RQ and KQ. The sequence of amino acids depicts the difference between the three forms of CocE with WT (top row), KQ (middle row), and RQ (bottom row). Residue numbers are listed above each row.

Fortunately, several previous research efforts have laid the foundation and starting point for residues to focus on based on how they may interact with

CocE's substrate or product. The several research efforts that we have used as a basis for our study are:

- *The previously published CocE structure with benzoic acid modeled in the active site (PDB: 1JU4)*
- *Our crystal structure CocE containing RTI-150 in the putative binding/desolvation site*
- *Our crystal structure of CocE in a transition state covalently bound benzoyl intermediate – positioning of the active site triad*
- *The molecular dynamics (MD) simulation of cocaine binding to CocE*

In the first structural study of CocE, Larsen *et al* reported the structure of CocE bound to benzoic, as well as the structure of CocE bound to phenylboronic acid, as a transition state analog of cocaine [7]. Together these studies provided an early model of the catalytic mechanism of cocaine metabolism. Interestingly, in their CocE-benzoic acid structure the authors reported that the benzoic acid found in the active site was actually a contaminant in the CocE preparation that remained bound during expression, purification and crystallization. These data suggest that the affinity of benzoic acid for CocE is relatively high. Considering that benzoic acid is one of two major products of cocaine hydrolysis (benzoic acid and ecgonine methyl ester), these data suggest that product release could be a limiting step in enzymatic turnover of cocaine. We thus hypothesized that lowering the affinity of benzoic acid would might speed up product release and hence increase the V_{max} for cocaine hydrolysis. We thus considered several

residues in proximity to benzoic acid in the active site that might diminish benzoic acid binding without perturbing substrate binding. Concurrent with these studies we focus on residues that coordinate the tropane portion of cocaine in an attempt to enhance substrate affinity. The combination of either two approaches, increasing product release and/or increasing substrate affinity, may contribute to lowing the K_M for cocaine by CocE. The goal would be to couple these K_M mutants with V_{max} mutants like KQ-CocE and enhance the catalytic efficiency. (Figure 4.1A)

Building off of the model containing benzoic acid, we performed a hypothetical modeling of how cocaine may sit in the active site. Positioning the benzoic acid over the partial product from the Larsen structure and then positioning the rest of the ecgonine methylester (EME) where it looks to be favorable, we were able to target several other residues that may influence the binding of cocaine or release of the EME. (Figure 4.1B)

Substrate binding site:

As described in Chapter 3, one of our attempts to generate a model for how cocaine binds to the active site includes using a non-hydrolyzable cocaine analog in an active CocE enzyme. To that end, we used two tropane-containing molecules (WIN 35,065-2 and RTI-150) without internal esters in a crystallographic study that produced a structure for each molecule with 1.8 Å resolution. Both analogues bind and inhibit CocE. The density corresponding to RTI was modeled into an electron-rich density, near where we had initially positioned cocaine. Surprisingly the position of the ester bond linking benzoic

acid to the tropane ring is approximately 11.5Å away from the active site serine. We therefore reasoned that location of RTI binding suggested by crystal structure might serve as a "docking site" where cocaine binds prior to moving into the active site. Several residues within hydrogen bonding distance to RTI in the "docking site" were subsequently mutated to interrogate each specific residue's influence on CocE kinetics.

Previous studies using MD simulation suggests that alanine at position 51 and glutamine at position 55 stabilize binding of the tropane ring of cocaine[8]. Furthermore, the investigators hypothesize, but did not test, that a glutamate substitution at this position might increase the interaction with substrate, due to hydrogen bonding between the nitrogen in the tropane ring and the acidic carboxyl side chain of glutamate, thus decreasing the K_M of the overall CocE kinetics[8]. In a collaborative effort with the Laboratory of Dr. Andrew McCammon, here at UCSD, we performed a similar course-grain MD simulation with cocaine and converged on a similar mechanism whereby the tropane ring of cocaine spontaneously moves within 3Å of both Ala^{51} and Gly^{55}. (Caliman, unpublished results).

Active site mutants and the catalytic triad:

Chapter 4 described our structure of the benzyl alcohol-bound CocE using the $Asp^{259}Asn$ mutant likely represents the first transition state of cocaine hydrolysis by CocE. Below we summarize the involvement of the residues that form the catalytic triad (Asp^{259}, His^{287} and Ser^{117}) and the proposed catalytic

mechanism in order to frame the selection and participation of candidate mutant residues that may alter catalysis.

Illustrated below is a cartoon of the catalytic triad of a CocE in relation to substrate cocaine. Highlighted are the catalytic residues Asp^{259}, His^{287} and Ser^{117} representing the acid, base and nucleophile, respectively, that are directly involved in the catalysis. The active site mutations below were designed with this classic catalytic triad of an esterase in mind but in the context of the various CocE structures now available to our laboratory. Here, His^{287} serves as the base first involved in first polarizing (*ie.* accept a proton) the nucleophile (OH of Ser^{117}) where it may attack the carbonyl carbon off the benzoyl moiety of cocaine and release the negatively charged ecgonine methyl ester. His^{287} is then deprotonated by ecgonine methyl ester. This nucleophilic attack results in the first transition state (TS1) and is depicted by our transition state structure described in chapter 4. Following stabilization of the base (His^{287}) by the acid (Asp^{259}) an incoming H_2O becomes the second nucleophile following deprotonation. The nucleophilic attack by the OH^- on the carbonyl carbon of TS1 releases yielding a tetrahedral second transition site (TS2), a structure closely resembling the phenylboronic acid-bound CocE structure (PDB: 1JU3). Finally, the protonated His^{287} donates its proton to the leaving group, in this case the oxyanion of Ser^{117}, and thus the release of benzoic acid. as the leaving group leaving and protonating the O^- of the ecgonine methyl ester.

With this mechanism in mind and utilizing the available structural information we propose to test whether mutations in surrounding residues may alter the structure of members of the catalytic triad and enhance catalytic activity.

Based on structures of the RTI-150-bound CocE and the transition state analog described in Chapters 3 and 4, respectively, we have identified several residues that may influence the binding and hydrolysis of cocaine in CocE. (Figure 4.2B) Using site-directed mutagenesis we test whether residues in the wild-type or KQ-CocE (both in the thermostabilized $Gly^{4}Cys/Ser^{10}Cys$-CocE) background that could increase or decrease their hydrophobicity or alter local charge density to the point that either product release is accelerated or substrate binding (K_M) is enhanced. The list of residues surveyed in this study, including the rationale for selecting the location of the mutant as well as the substitution is displayed in Figure 5.2.

Methods

Site-directed Mutagenesis: Oligonucleotides (IDT, San Diego, CA) were designed based on the crystal structure of the thermostable mutant CCRQ-CocE [9] and used in a modified Quickchange™ protocol (Stratagene, La Jolla, CA) to replace a specific codons in the CocE nucleotide sequence. Oligonucleotides targeting residues: F261A: 5'- G TAC GAC GGG **GCG** GTC GGC GAA TC -3'; F261W: 5' - TAC GAC GGG **TGG** GTC GGC GAA TCG - 3'; L290W: 5' - CAC AGC AAC **TGG** ACT GGT CGG - 3'; L407A: 5' - GGG ACG CTG **GCC** TTC CAC AAC - 3'; F408A: 5' - ACG CTG CTG **GCC** CAC

AAC GGA G - 3'; F408Y: 5' - ACG CTG CTG **TAT** CAC AAC GGA G - 3' were ordered from Integrated DNA Technologies (La Jolla, CA). Codons in **bold** print represent the target residue. We utilized bacterial expression vectors (pET22b) containing the thermostable mutant of CocE, CC-CocE, as a template for the mutagenesis studies [9]. The expressed protein has a Hisx6 tag at the carboxy-terminus to facilitate protein purification. Sequences for all mutant plasmids were confirmed by DNA sequencing.

Production of CocE proteins: The mutant forms of CC-CocE were expressed from pET-22b (+) plasmid in BL21 (DE3) (Novagen) bacterial cells. Cells were grown to OD_{600} = 0.6 AU, temperature shifted to 18°C, and protein expression was initiated with the addition of Isopropyl β-D-1-thiogalactopyranoside (IPTG) (Genesee Scientific). Expression continued for 16 hours, and cells were pelleted, flash frozen in liquid N_2 and stored at -80°C until purification. The cell pellet was resuspended in 1X Tris-buffered saline (TBS) and broken with two passes through a French Press (ThermoScientific). Bacterial lysates were clarified by centrifugation at 25,000x *g* and loaded onto a Ni^{2+}NTA column equilibrated with 1 x TBS at pH 7.4 @ 4°C supplemented with protease inhibitors (PIs) (3 mg/mL each of leupeptin and lima bean or soybean trypsin inhibitor). The protein was eluted using 1 x TBS with 150 mM imidazole and PIs. To facilitate disulphide crosslinking of the CocE protomers and stabilization of the CocE dimer the elute fractions were treated with 50 μM $CuCl_2$ at 4°C overnight. The entire reaction was loaded onto a Q-sepharose FPLC column equilibrated

with 50 mM Tris, pH 8.0 @ 4°C and PIs. CocE protein was eluted off with a linear gradient in a buffer containing 50 mM Tris, pH 8.0 @ 4°C, 1M NaCl and PIs. Peak fractions were analyzed with 10 % SDS-PAGE, pooled and concentrated to 10 mg/ml with Amicon concentrators (Millipore), flash frozen in liquid N_2 and stored at -80°C.

Cocaine-based activity assay: The catalytic activity of purified CCRQ-CocE mutants were analyzed using our standard absorbance-based cocaine assay, described previously [10]. Here, cocaine (Mallinckridt, Hazelwood, MO) is added a 96-well UV-permeable plate (Costar; Corning Life Sciences, Lowell, MA) as a 2X solution at 200, 100, 50, 25, 10, 5, 1 and 0.5 μM concentrations in a buffer containing 50 mM Tris-HCl, pH 8.0 @ RT. The reaction is initiated by the addition of PEG:CocE (65 ng/ml in 50 mM Tris-HCl, pH 8.0 @ RT) at a 1:1 dilution in the plate. The velocity of the reaction was measured every 10s for 20 minutes using a SpectraMax Plus 384 UV plate reader (Molecular Devices, Sunnyvale, CA) using SOFTmax Pro software (version 3.1.2). The absorbance readings were converted to change in concentration of product using Beer's law. The specific activity of the enzyme was plotted using Prism software (GraphPad Software Inc., San Diego, CA) and kinetics of the reaction (V_{max} and K_M) generated.

Results

Residues targeted for enhanced catalytic properties by mutagenesis: The list of residues targeted in this study can be found mapped on the structure of CocE (Figure 5.2). The mutants have been organized into three different categories: active site mutants, substrate binding site mutants, and putative docking-site mutants. The active site mutants were chosen for their proximity to the active site residues themselves or by their potential to alter positioning of the catalytic triad residues and influence substrate binding or chemistry. These residues include Tyr^{118}, Met^{141}, and Ser^{288} and their mutation is covered in Chapter 4.

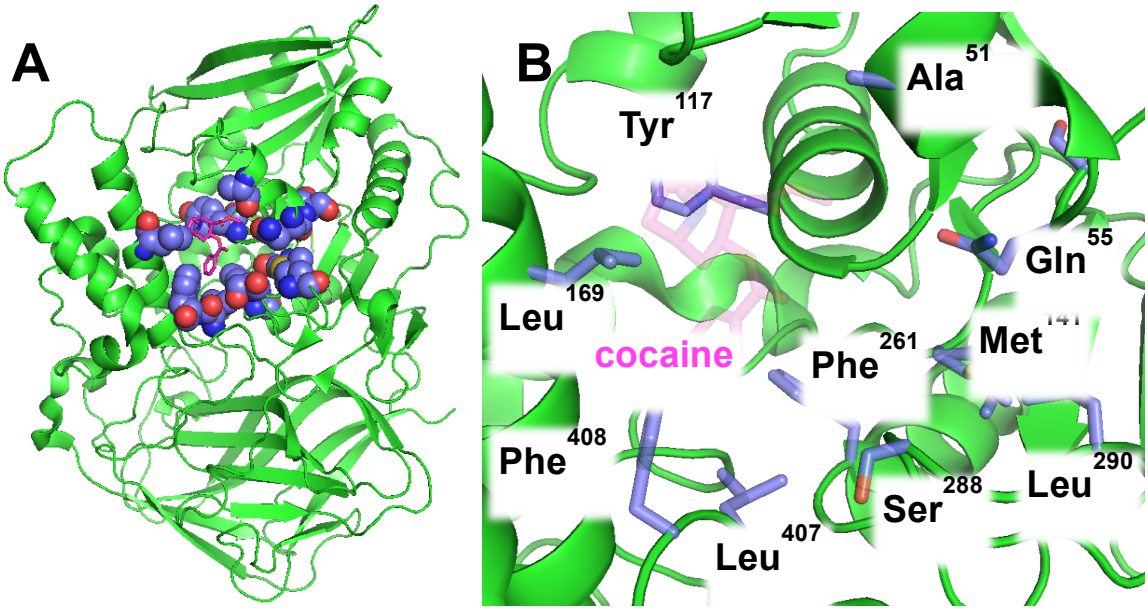

Figure 5.2: Position of all residues mutated on CocE. A) Location of the active site mutant residues mapped on the model of cocaine-bound CocE. Side chain residues are rendered as spheres and cocaine (magenta) is depicted as a stick figure. B) Close-up of A) highlighting the active site residues. Cocaine is modelled in the active site of CocE based on the structure of benzoic acid-bound CocE (PDB: 1JU4) and is rendered as

Chapter 3 covered the residues that we hypothesize will interact with substrate at the putative docking site. These residues were selected based on the crystal structure of cocaine analog RTI co-crystallized with CocE and discussed in Chapter 3, as well as from docking poses for cocaine based on MD simulations. These residues include Ala^{51}, Gln^{55}, Leu^{169}, and Ile^{170}.

The final group of residues contains substrate binding site candidate residues that were selected based on models of cocaine-bound CocE and from the x-ray crystal structures of the covalent intermediate structure discussed in Chapter 4. More specifically, we selected several residues that we hypothesize might be in position to interact with the binding of substrate to enhance its affinity or alternatively enhance the release of product benzoic acid. Residues in this group include Phe^{261}, Leu^{290}, Ile^{307}, Leu^{407}, and Phe^{408}. These mutations are presented below.

Illustrated below is a cartoon of the catalytic triad of a CocE in relation to substrate cocaine. Highlighted are the catalytic residues Asp^{259}, His^{287} and Ser^{117} representing the acid, base and nucleophile, respectively, that are directly involved in the catalysis. The active site mutations below were designed with this classic catalytic triad of an esterase in mind but in the context of the various CocE structures now available to our laboratory. Here, His^{287} serves as the base first involved in first polarizing (*ie.* accept a proton) the nucleophile (OH of Ser^{117}) where it may attack the carbonyl carbon off the benzoyl moiety of cocaine and release the negatively charged ecgonine methyl ester. His^{287} is then deprotonated by ecgonine methyl ester. This nucleophilic attack results in the

first transition state (TS1) and is depicted by acyl intermediate state 1 (AIS1) structure described in chapter 4. Following stabilization of the base (His^{287}) by the acid (Asp^{259}) an incoming H_2O becomes the second nucleophile following deprotonation. The nucleophilic attack by the OH- on the carbonyl carbon of TS1 releases yielding a tetrahedral acyl intermediate state (AIS2), a structure closely resembling the phenylboronic acid-bound CocE structure (PDB: 1JU3). Finally, the protonated His^{287} donates its proton to the leaving group, in this case the oxyanion of Ser^{117}, and thus the release of benzoic acid. as the leaving group leaving and protonating the O^- of the ecgonine methyl ester.

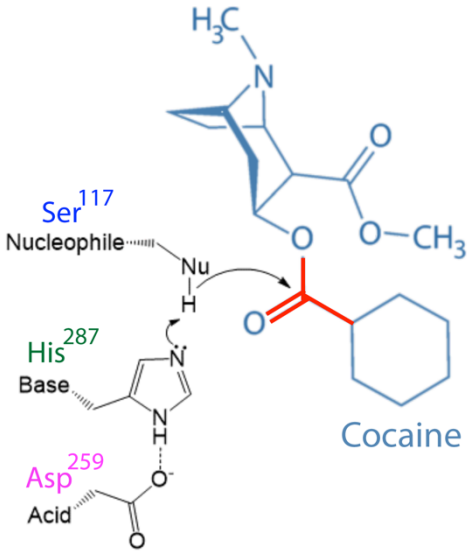

Figure 5.3: Catalytic residues involved in hydrolysis of (-)cocaine. Illustrated are the residues in the catalytic triad involved in the hydrolysis of cocaine by CocE.

Substrate binding site residues

Phe^{261}: Phe^{261} is located in the loop region at the beginning of helix E in DOM I (Figure 5.4). The phenyl ring of Phe^{261} lies 3-3.5 Å away from the phenyl ring of benzoic acid (in PDB: 1JU3) and thus a similar distance from the phenyl ring of cocaine in our cocaine-bound CocE model. Phe^{261}, as well as a set of aromatic residues including Trp^{151}, Trp^{166} and Phe^{408}, together form an extensive network of van der Waals contacts with the phenyl ring of benzoic acid and presumably the substrate cocaine.

In order to interrogate the Phe^{261}-phenyl ring interaction, several mutations were made to this residue. Substituting Phe^{261} with an alanine residue, in an attempt to eliminate the van der Waals interaction with the phenyl ring, dramatically increased the K_M for cocaine at least 320 μM. We predict that is would be an underestimation of the K_M since the highest concentration of cocaine tested in the assay is 100 μM. The enzyme does retain some enzymatic activity with projected V_{max} of 1060 min^{-1}, with the caveat that higher concentrations of substrate would be required to yield a better estimation.

Table 5.1: Kinetic constants of Phe^{261} mutants

Mutant	K_M (μM)	V_{max} (min^{-1})	Catalytic Efficiency (μM^{-1}min^{-1})
Phe^{261}Ala	>200	1100 +/- 600	NC
Phe^{261}Trp	17 +/- 2.0	2200 +/- 75	132
Phe^{261}Tyr	*ND	*ND	

*ND Not Detectable

Mutating Phe^{261} to Trp produced a mutant that displayed activity with similar kinetics to the control CocE used in this assay. Because tryptophan contains an indole ring, it can potentially contribute van der Waals interactions with substrate similar to Phe and may be the reason for this mutant's kinetics. Without structural information, again, we are not able to discern how the R-group was positioned. Interestingly, the Phe^{261}Tyr mutant displayed the most dramatic change in activity by rendering the enzyme inactive. The phenyl ring of Phe^{261} is predicted to lie perpendicular to the plane of the phenyl ring of benzoic acid or cocaine. Typically used as a conservative substitution of Tyr, Phe at position 261 however adds a hydroxyl that in the cocaine model, would protrude into the phenyl ring of cocaine and likely inhibit its binding.

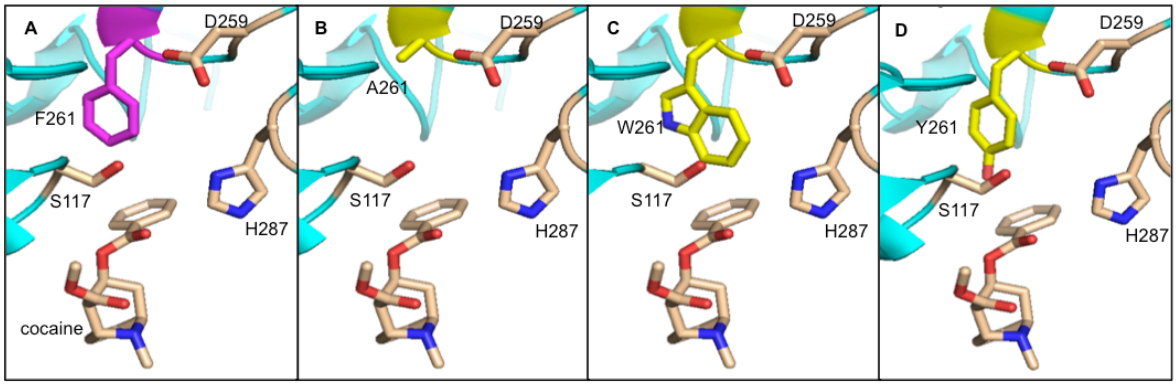

Figure 5.4: CocE residue 261 Panel A contains the native residue F261 in magenta. Mutations to residue 261 include alanine (B), tryptophan (C), and tyrosine (D). The catalytic triad is shown along with the hypothetical position of cocaine near active site residues.

Leu^{290}: Leu^{290} lies downstream of the active site His^{287}, and is located in the long loop region of β8 and β8a strands, similar to Ser^{288} (Figure 5.5). We reasoned that by increasing the hydrophobic presence of this region that together with tryptophan, through minimizing waters found in the active site and to increase the

dielectric constant in the active site. This in turn should increase the acidity of Asp^{259}, and help proton transfer and the overall chemistry of the hydrolysis reaction.

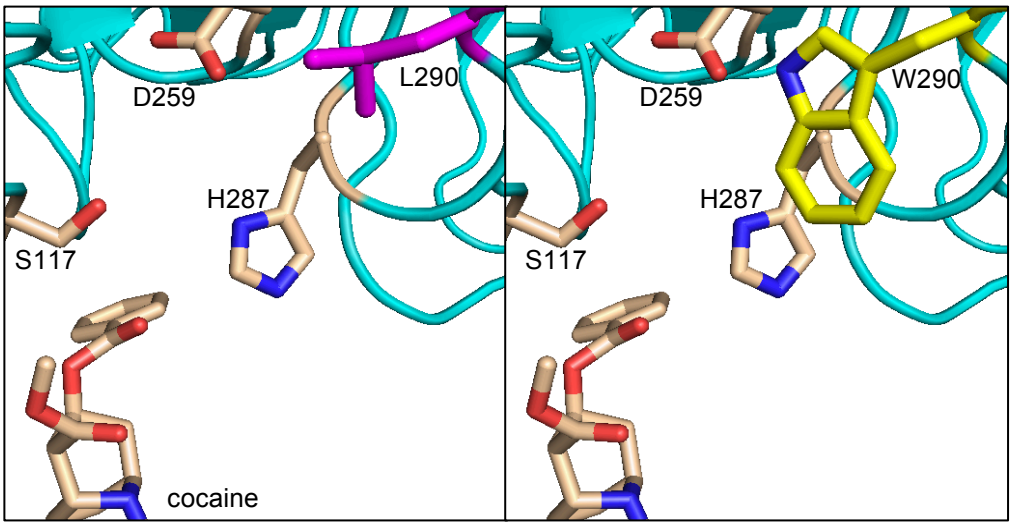

Figure 5.5: The location of Leu^{290} with respect to the catalytic triad and substrate cocaine. The left panel shows the endogenous leucine residue at position 290. The tryptophan mutation is shown in the right panel in the orientation that causes the least amount of clash with other active site residues.

Table 5.2: Kinetic constants of Leu^{290}Trp mutant.

Mutant	K_M (μM)	V_{max} (min^{-1})	Catalytic Efficiency ($\mu M^{-1}min^{-1}$)
Leu^{290}Trp	9 +/- 5.2	520 $^{+/-}$ 84	58

As depicted in table 5.2 substituting the large aromatic Trp side group at Leu^{290} appeared to subtly improve the Km of CocE for cocaine, but an accompanying decrease in the maximal velocity compared to WT-CocE. One possible explanation for this result is that this residue sits in close proximity to the backbone of Gln^{55} and Ser^{56} and thus may help to stabilize the loop-A1 helix-loop of DOM1 which forms the solvent facing region of the active site cleft. Our rationale for this mutation was originally to improve the velocity through increasing the dielectric constant around His^{287}. Our results suggest that the opposite effect may have resulted whereby we may have inadvertently altered access of His^{287} to a catalytic H_2O. Alternatively, the larger aromatic ring may have enhanced van der Waals contacts with the phenyl ring of cocaine, leading to in decrease in the K_M. This unfortunately accompanies a decrease in product (benzoic acid) release, and hence a decrease in the velocity.

Leu^{407} and Phe^{408}: Leu^{407} and Phe^{408} both are in a loop region that connects the

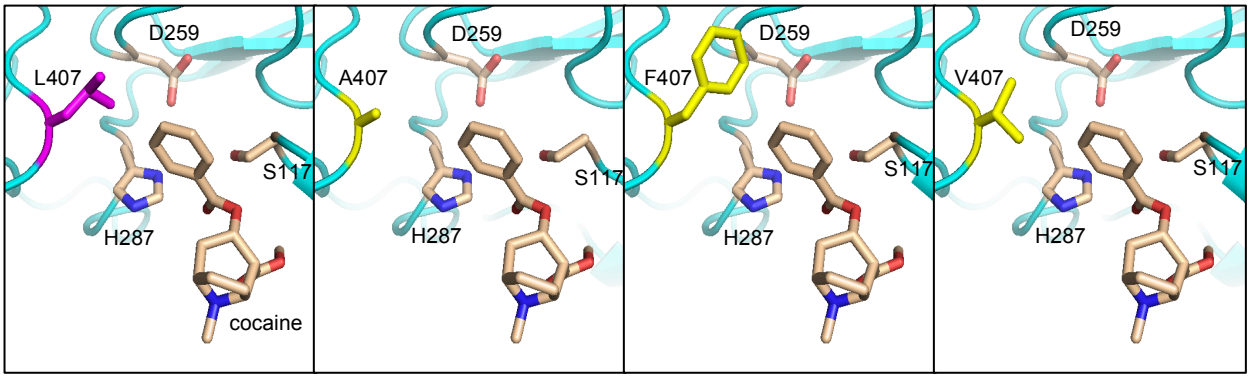

Figure 5.6: The location of Leu^{407} relative to cocaine Panel A shows the position of native residue leucine at position 407. Mutations to this residue are shown in the next three panels: alanine (B), phenylalanine (C), and valine (D).

β1 and β2 strands in DOM3 (Figures 5.6 and 5.7). Analysis of the CocE models bound to cocaine, the transition state intermediates or the product benzoic acid, suggest that Leu^{407} and Phe^{408} both interact with the benzoyl ring of cocaine (PDB: 1JU3, 1JU4 and our acyl intermediate structure). This loop inserts between DOM1 and DOM3 in CocE but also participates in the CocE's quaternary structure lying at the dimer interface to help form the hydrophobic cleft of the active site.

Table 5.3: Kinetic constants of Leu^{407} mutants.

Mutant	K_M (μM)	V_{max} (min^{-1})	Catalytic Efficiency ($\mu M^{-1} \bullet min^{-1}$)
Leu^{407}Ala	5.7 +/- 2.0	1100 +/- 40	185
Leu^{407}Phe	>200	2300 +/- 110	NC
Leu^{407}Val	8.2 +/- 5.3	500 +/- 125	61

Leu^{407}: The side chain of Leu^{407} is lies approximately 4Å away from the benzoyl ring of cocaine. Since leucine is one of the smallest of the hydrophobic residues, we sought to interrogate both decreasing and increasing the hydrophobic potentials at this position. Surprisingly, the Leu^{407}Ala mutant exhibited an improved affinity for cocaine (lower K_M~5.7 μM) but, as seen with other mutants with an improved K_M, there was an accompanying decrease in the velocity to approximately half the rate of WT-CocE. The improvement in K_M yields appears to outweigh the decrease in V_{max} and yields an overall catalytic efficiency that is the calculated so far. Similar results are observed with the Leu^{407}Val mutant an improved K_M for cocaine accompanies loss in the maximal velocity (V_{max} ~500 min^{-1}).

In contrast, increasing the overall size and hydrophobicity of residue 407 with a phenylalanine substitution leads to an enzyme with a dramatically higher K_M (>200 phenylalanine residue yields an enzyme with the poorest activity of the three mutations interrogated). Though the maximum velocity is projected to remain within the range of the standard CocE kinetics (~2500 min^{-1}), this is a projected value due to the K_M (>200 μM) falling outside of the range measurable by this assay.

A possible rational for the behavior of these substitutions at Leu^{407} may involve substrate binding and chemistry. The proximity of Leu^{407} to His^{287} may suggest that some substitutions may perturb the position of this very important catalytic residue. Similar to the argument made for the putative mechanistic influence of Ser^{288}Thr mutant His^{287} suggests that Ala and Val side chains may to too small and not capable of nudging His^{287} toward Asp^{259}, part of the catalytic triad. In this manner the velocity and not the K_M would be deleteriously affected. In contrast, a phenylalanine side chain may simply be too large and potentially lie too close to the benzoyl moiety and potentially could impair substrate binding, consistent with its deleterious effect on the K_M for cocaine.

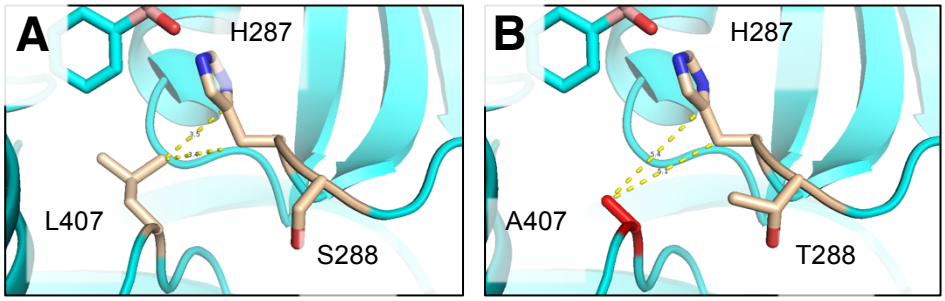

Figure 5.7: Interaction of Leu^{407} and His^{287}. A) the CH_3 group of Leu^{407} lies within van der Waals distance (3.5Å) away from His^{287} and influence its position. B) Mutation of Leu^{407} to Ala may remove these constraints (>5Å away).

Another possible explanation for the lower velocity may related to the proximity of Leu^{407} to His^{287}. As we have now observed His^{287} undergoes considerable movement during catalysis and is located within only 3.5Å of from the Leu^{407} side chain. Such close proximity may allow L^{407}, perhaps through van der Waals interactions, influence this movement and therefore catalysis. Removing the interaction through shortening the alkyl chain with an alanine and valine substitution could influence the capacity of His^{287} to serve as a general base.

Phe^{408}: Phe^{408}, like Leu^{407} lies close to both the benzoyl moiety of substrate cocaine but also within van der Waals contact of His^{287}(See Figure 5.8). Mutations designed to enhance the binding of substrate may also therefore interfere with catalysis. In the case of Phe^{408}Tyr the potential of tyrosine to π-stack on either His^{287} (depending on the charge state) and/or the phenyl ring of the substrate, the latter would decrease V_{max} and the former increase interaction with substrate.

Table 5.4: Kinetics of CocE mutants - Phe^{408}Ala and Phe^{408}Tyr

Mutant	K_M (μM)	V_{max} (min^{-1})	Catalytic Efficiency ($\mu M^{-1} \bullet min^{-1}$)
F408A	13 +/- 3.3	770 +/- 60	60
F408Y	23 +/- 4	850 +/- 50	37

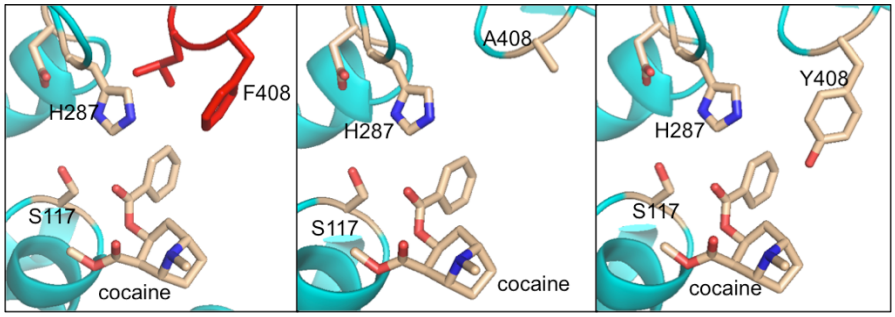

Figure 5.8: Position of Phe^{408} mutants with respect to His^{287} and the benzoyl moiety of cocaine Panel A shows the position of phenylalanine at position 408. Mutations to alanine and tyrosine are shown in the middle and right panels, respectively.

Summary of single point mutations:

Single point mutagenesis of the key residues in the active site have identified extremely interesting candidates that display enhance kinetic constants. An interesting correlation can be drawn with the mutants that display enhanced affinity for substrate, as indicated by the lower K_M. Mutants that display lower K_M value (higher affinity for substrate) also appear to have lower maximal velocities. A plausible explanation for this dichotomy may be related to the fact that improving the overall affinity for the benzoyl moiety of cocaine may also improve the affinity for the product benzoic acid. Since benzoic acid

appears to be the rate limiting step in the hydrolysis of cocaine, slowing the benzoic off-rate and hence product release will result in a decrease in the k_{cat}, or the velocity of the enzyme for substrate cocaine. Thus, mutants containing either $Leu^{290}Trp$, $Leu^{407}Ala$, $Leu^{407}V$ or $Phe^{408}Ala$ all displayed lower K_M values but lower accompanying maximal velocities, and unfortunately all with lower catalytic efficiency.

A single point mutation the targeted catalysis directly and displayed dramatic improvements in the maximal velocity was $Ser^{288}Thr$. We hypothesize that replacing the serine with the bulkier threonine would stabilize the catalytic His^{287} in a position that could interact more efficiently with the catalytic partner Asp^{259}. A better His-Asp interaction may allow the histidine residue to serve as a better general base and proton donor. This mutant enzyme exhibited the highest V_{max} and catalytic efficiency observed from a single point mutation to date, despite displaying a higher K_M than WT-CocE.

A single point mutation described in Chapter 3, $Ser^{51}Glu$, originally designed to validate whether the RTI-150-bound CocE structure represents potential docking site for cocaine, also displayed a significantly lower K_M, with a moderately low V_{max}. In this model the acidic side chain of the glutamate residue interacts with the bridging nitrogen on the tropane ring of cocaine not in the active site but in the putative cocaine docking site. This mutation, as opposed to the K_M mutants described above, should not alter benzoic acid release (~11Å away) and thus exhibit better for cocaine hydrolysis. A mutation at neighboring position 55 ($Gln^{55}Glu$) displayed similar behavior on both K_M and V_{max}. By

plotting the K_M versus the V_{max} of the single point mutants analyzed in this study, compared to CCRQ and CCKQ reveals an interesting distribution. With the exception of $Ala^{51}Glu$ and $Gln^{55}Glu$ most mutants fell along a linear correlation where improvements in K_M accompanied lower maximal velocities.

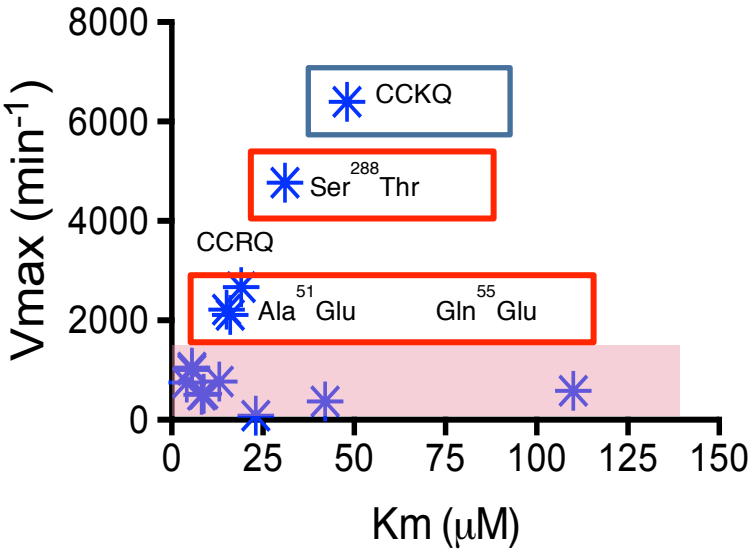

Figure 5.9: Relationship between the K_M and V_{max} of the single point active site mutants. Mutants that displayed K_M values below 200 μM were included were compared to CCRQ and CCKQ. Highlighted in red ($Ala^{51}Glu$, $Gln^{55}Glu$ and $Ser^{288}Thr$) are the single point mutants that appeared to deviate.

Analysis of CocE combination mutants:

We next determined whether combining a mutant that displays a lower K_M for cocaine with a mutant that displays higher maximal velocities, to form high activity hybrid enzymes. The one mutation showing a higher velocity in this study was $Ser^{288}Thr$ (V_{max} = 4770 min^{-1}). Three mutants had improved K_M, namely: $Ala^{51}Glu$ (K_M = 5.5 μM); $Gln^{55}Glu$ (K_M = 4.1 μM); and $Leu^{407}Ala$ (K_M = 5.7 μM). We hypothesize that combining each of these three mutations with $Ser^{288}Thr$, we would create a mutant form of CocE that would offer an improved K_M with a higher velocity – an enzyme with a superior overall catalytic efficiency.

$Gln^{55}Glu$ /$Ser^{288}Thr$: As depicted in Table 5.5, taking advantage of the superior K_M properties offered by the $Gln^{55}Glu$ mutant and the high velocity of the $Ser^{288}Thr$ mutant produced a mutant with intermediate properties that resembled the $Ser^{288}Thr$ mutant alone, with a slightly lower V_{max}. It is likely that the compromised catalytic activity of the $Gln^{55}Glu$ mutant was incorporated into the $Ser^{288}Thr$ without translating the lower K_M. Analysis of the crystal structures of the CocE models does not reveal an obvious structural rationale for the lower affinity for cocaine offered by this double mutant.

Table 5.5: Catalytic constants for K_M ($Gln^{55}Glu$) and V_{max} ($Ser^{288}Thr$) double mutants of CocE

Mutant	K_M (μM)	V_{max} (min^{-1})	Catalytic Efficiency ($\mu M^{-1} \bullet min^{-1}$)
$Gln^{55}Glu$, $Ser^{288}Thr$	29.0 +/- 2.1	3400 +/- 100	119
$Gln^{55}Glu$	4.1 +/- 0.7	750 +/-30	184
$Ser^{288}Thr$	31 +/- 9.0	4800 +/- 50	154

Ser^{288}Thr, Leu^{407}Ala: By combining the K_M mutant Leu^{407}Ala with the V_{max} mutant Ser^{288}Thr another enzyme with an intermediate activity was generated. As illustrated in Table 5.6 the Ser^{288}Thr/Leu^{407}Ala double mutant displayed activity closely resemble the single Leu^{407} mutant, with slightly higher K_M and V_{max} kinetic constants for cocaine hydrolysis. In this case the high V_{max} properties of the Ser^{288}Thr could not translate into the Leu^{407} background but did retain the low K_M (~10 μM). One possible explanation for this failure may be related to the influence of both substitutions on the position of His^{287}. The advantages gained with the Ser^{288}Thr mutation on directing His^{287} toward Asp^{259} may be counteracted by removing the His^{287}-Leu^{407} interaction and through shortening the leucine to alanine or valine.

Table 5.6: Catalytic constants for K_M (Leu^{407}Ala) and V_{max} (Ser^{288}Thr) double mutants of CocE

Mutant	K_M (μM)	V_{max} (min^{-1})	Catalytic Efficiency (μM^{-1}•min^{-1})
Ser^{288}Thr, Leu^{407}Ala	10 +/- 2.3	1200 +/- 79	120
Ser^{288}Thr	31 +/- 9.0	4800 +/- 50	154
Leu^{407}Ala	5.7 +/- 2.0	1100 +/- 40	185

Ala^{51}Glu/Ser^{288}Thr: As part of the model validation for the RTI-150 structure described in Chapter 4 we identified Ala^{51}Glu as a low K_M mutant that displayed reasonable, but diminished maximal activity (Table 5.7). This mutant, Ala^{51}Glu, displayed the one of the lowest K_M value observed in our mutagenesis studies

Table 5.7: Catalytic constants for Km ($Ala^{51}Glu$) and Vmax ($Ser^{288}Thr$) double mutants of CocE

Mutant	K_M (μM)	V_{max} (min^{-1})	Catalytic Efficiency ($\mu M^{-1} \bullet min^{-1}$)
$Ala^{51}Glu$, $Ser^{288}Thr$	70 +/- 9.7	11900 +/- 80	167
$Ser^{288}Thr$	31 +/- 9.0	4800 +/- 50	154
$Ala^{51}Glu$	5.5 +/- 0.8	920 +/- 40	167

(~5.5 mM). Combined with the V_{max} mutant, $Ser^{288}Thr$, the double mutant displayed an unprecedented maximal velocity of approximately 12,000 min^{-1}. As observed in the previously described double mutants we unfortunately did not observe a cooperative enhancement between the two mutants in the K_M. No enhancement of the K_M of $Ser^{288}Thr$ was gained by mutating Ala^{51} to Glu.

$Ala^{51}Glu/Ser^{288}Thr$ in the CCRQ and CCKQ backgrounds: Since the $Ala^{51}Glu/Ser^{288}Thr$ double mutation exhibited the best overall improvement in kinetics compared to other mutants tested, this combination of mutants was examined in our best thermostable CocE mutant backgrounds – CCRQ and CCKQ.

By combining the $Ala^{51}Glu/Ser^{288}Thr$ double mutant into either CCRQ or CCKQ backgrounds, we generated our most active mutant to date. The CCRQ background did not produce a better mutant than in CC background alone. The K_M's of both thermostable backgrounds worsened, but the improvement in V_{max} shows that the combination of mutants can produce a superior enzyme with the best catalytic efficiency.

Table 5.8: Catalytic constants for Ala^{51}Glu/Ser^{288}Thr in the CCRQ and CCKQ background

Mutant	K_M (μM)	V_{max} (min^{-1})	Catalytic Efficiency ($\mu M^{-1} \bullet min^{-1}$)
CCRQ	26 +/- 2.0	2500 +/- 240	96
CCKQ	55 +/- 10	6900 +/- 60	126
Ala^{51}Glu/Ser^{288}Thr:CCRQ	72 +/- 10	11000 +/- 100	151
Ala^{51}Glu/Ser^{288}Thr:CCKQ	88 +/- 14	14500 +/- 170	165

Discussion

By mutating individual residues on CocE we were able to generate several mutants although most with better Michaelis constants K_M and V_{max}. Single point analysis revealed three mutants, Ala^{51}Glu, Gln^{55}Glu, and Leu^{407}Ala that displayed improved K_M values and only one mutant, Ser^{288}Thr that displayed significantly higher maximal velocity, V_{max}. In combining these single mutants into double mutants, we found one combination with the best V_{max} to date (Ala^{51}Glu, Ser^{288}Thr). Finally, through inserting this combination into the most active and thermostable mutant background (CCKQ), we generated the most efficient enzyme yet developed by this laboratory. Several potential explanations for why these changes can be drawn from structural analysis of the new mutations. At the same time, we saw a definite pattern emerge in the single mutations that held true in the combination mutations, which follow the pattern of

a structural-function trade off [11-13]. Each mutant that had an improved K_M or V_{max} also showed a decrease in the other kinetic parameter. Fortunately, we were able to combine mutants to generate an improved V_{max} that with a proportionally lower penalty on K_M ($Ala^{51}Glu/Ser^{288}Thr$:CCKQ). The K_M for cocaine of $Ala^{51}Glu/Ser^{288}Thr$:CCKQ is higher than for CCKQ (K_M~50 μM) and more so than WT-CocE (K_M~25 μM) however the gain in velocity outweighs the loss.

To begin analyzing the results from this study, we should first consider the cocaine itself. The cocaine molecule has several structural elements that could potentially interact with CocE residues or the peptide backbone. The tropane ring of cocaine consists of a carbon ring containing a single nitrogen atom. The cyclical structure of tropane allows for hydrophobic interactions and the nitrogen atom can form hydrogen bonds with residues nearby. The carbonyl oxygens coming off of the two ester bonds can be hydrogen bond acceptors. The benzene ring, opposite the tropane ring, can have hydrophobic interactions, π-π stacking, and cation- π interactions. Lastly, the methyl groups attached to the nitrogen atom and the ester bond, not forming the benzoic acid, can have hydrophobic interactions. Overall, we took advantage of the multiple hydrophobic interactions by increasing ($Leu^{290}Trp$) or decreasing ($Leu^{407}Ala$) the size of the residue on CocE to interact with cocaine. We intended to increase the hydrophobic interaction in order to increase binding of substrate, and conversely, we wanted to decrease this interaction in order to facilitate product release. Unfortunately, most of the mutants that displayed a decrease in the K_M,

presumably through increasing substrate affinity, but a decrease in the V_{max}, presumably through increasing the affinity for the product and hence slowing product release even more. This is likely the reason that in two mutations, $Ala^{51}Glu$ and $Gln^{55}Glu$, we could take advantage of the interaction between the acidic glutamate residue and the nitrogen bridge on the tropane ring to increase the binding of substrate and improve K_M. Here we did not encounter large penalties on the enzyme velocity, since we were not altering the interaction and thus affinity for the product nor its release, or at least not the rate-limiting product, benzoic acid.

Looking at the results from the perspective of the enzyme, we proceeded to explore residues in two distinct regions of CocE: in the active site, based on the positioning of the active site triad and the initial structural study; and in the putative binding/desolvation site, due to our interpretation of previous structural studies described in Chapter 3 of this thesis coupled with the MD simulation performed in Huang et al (2014)[7, 14].

Our results from mutagenesis studies support that a structural-function trade off that has been found in engineering other proteins [13]. Several mutations displayed increased affinity for substrate but expressed a decrease in the maximal velocity, possibly due, as mentioned previously, to the enhanced affinity for product, benzoic acid.

Although not fully optimized the combination of $Ala^{51}Glu/Ser^{288}Thr$-CCKQ expressed an enzyme that may, however, already be useful for treatment in cocaine addiction and toxicity. The Km, albeit relatively high, is within

reasonable levels found in cocaine addicts and in over-dosing individuals, where cocaine plasma concentrations reach 25-50 mM and 50-150 μM, respectively [3, 4, 15]. We look forward to testing the effect of this combined mutant in animal studies to test its capacity to modify self-administration models of cocaine abuse as well as cocaine-induced lethality in rodents. We also look forward to analyzing the crystal structure of this mutant to both validate the proposed model for the catalytic efficiency enhancement and also utilize the structure to further enhance its catalytic properties.

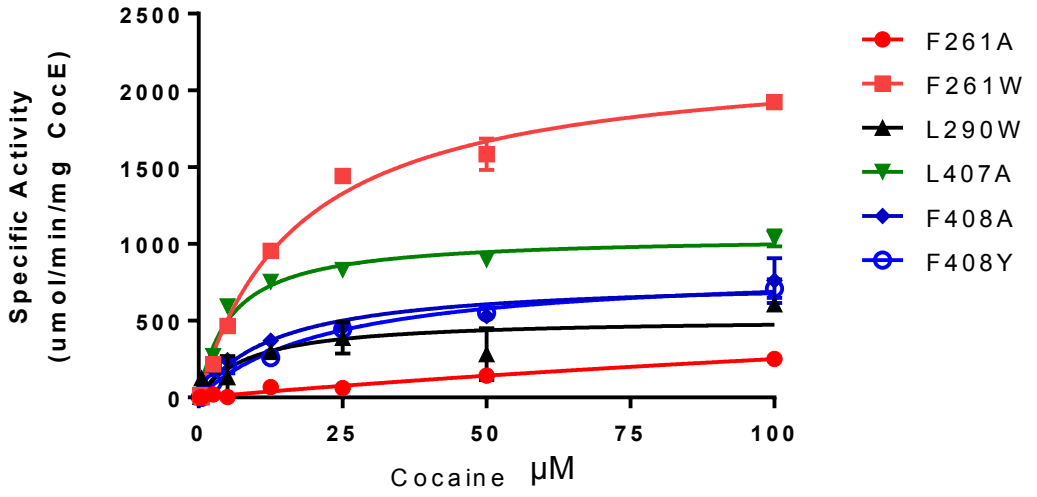

	$F^{261}A$	$F^{261}W$	$L^{290}W$	$L^{407}A$	$F^{408}A$	$F^{408}Y$
V_{max}	1100 +/- 600	2200 +/- 80	510 +/- 80	1000 +/- 90	780 +/- 70	880 +/- 80
K_M	300 +/- 200	17 +/- 2	8 +/- 4	6 +/- 2	14 +/- 4	26 +/- 6

Figure 5. 10: Michaelis-Menton plot of all single mutants covered in Chapter 5 Kinetics of all mutants with potential to interact with substrate are plotted and values for V_{max} and K_M are shown in the table below.

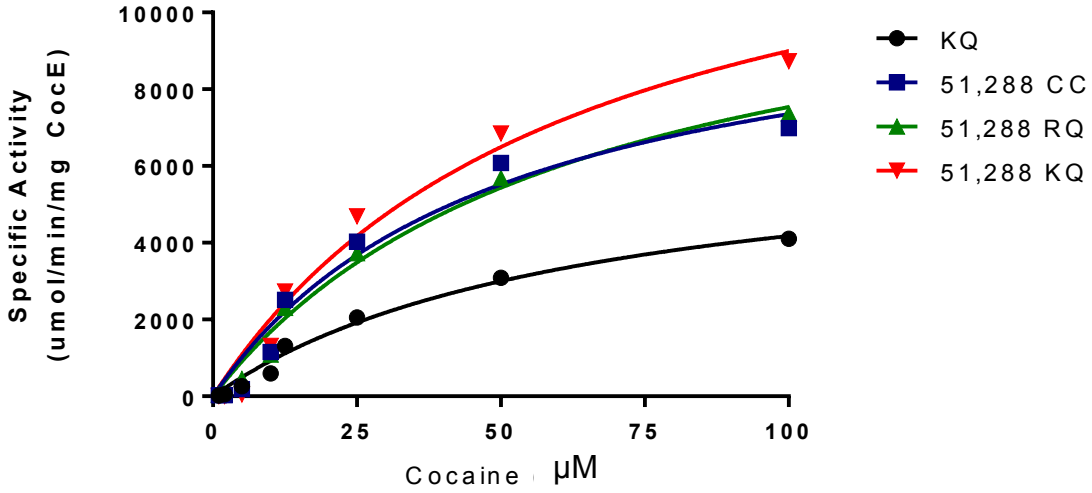

	RQ	$A^{51}E, S^{288}T$	$Q^{55}E, S^{288}T$	$S^{288}T, L^{407}A$
V_{max} (min^{-1})	2600 +/- 76	12000 +/- 80	3400 +/- 100	1200 +/- 80
K_M (μM)	24 +/- 2	75 +/- 10	29 +/- 2	10 +/- 2

Figure 5.11: CocE double mutants for increased enzyme efficiency. Single mutations A51E, Q55E, or L407A were combined with S288T in order to generate a CocE mutation with better overall enzyme efficiency. Michaelis-Menton plot is shown for each mutant compared to RQ-CocE control. Kinetic parameters for each mutant are shown below.

References

1. Nasser, A.F., et al., *A randomized, double-blind, placebo-controlled trial of RBP-8000 in cocaine abusers: pharmacokinetic profile of rbp-8000 and cocaine and effects of RBP-8000 on cocaine-induced physiological effects.* J Addict Dis, 2014. **33**(4): p. 289-302.
2. Narasimhan, D., J.H. Woods, and R.K. Sunahara, *Bacterial cocaine esterase: a protein-based therapy for cocaine overdose and addiction.* Future Med Chem, 2012. **4**(2): p. 137-50.
3. Jones, A.W., A. Holmgren, and F.C. Kugelberg, *Concentrations of cocaine and its major metabolite benzoylecgonine in blood samples from apprehended drivers in Sweden.* Forensic Sci Int, 2008. **177**(2-3): p. 133-9.
4. Grinspoon, L. and J.B. Bakalar, *Cocaine: a drug and its social evolution*. 1985: Basic Books.
5. Shapiro RJ, S.K., Mukim M. *The Potential American Market for Generic Biological Treatments and the Associated Cost Savings*. 2008; Available from: http://www.sonecon.com/docs/studies/0208_ GenericBiologicsStudy.pdf.
6. Brim, R.L., et al., *The ability of bacterial cocaine esterase to hydrolyze cocaine metabolites and their simultaneous quantification using high-performance liquid chromatography-tandem mass spectrometry.* Mol Pharmacol, 2011. **80**(6): p. 1119-27.
7. Larsen, N.A., et al., *Crystal structure of a bacterial cocaine esterase.* Nat Struct Biol, 2002. **9**(1): p. 17-21.
8. Fang, L., et al., *Rational design, preparation, and characterization of a therapeutic enzyme mutant with improved stability and function for cocaine detoxification.* ACS Chem Biol, 2014. **9**(8): p. 1764-72.
9. Narasimhan, D., et al., *Subunit stabilization and polyethylene glycolation of cocaine esterase improves in vivo residence time.* Mol Pharmacol, 2011. **80**(6): p. 1056-65.
10. Gao, D., et al., *Thermostable variants of cocaine esterase for long-time protection against cocaine toxicity.* Mol Pharmacol, 2009. **75**(2): p. 318-23.
11. Shoichet, B.K., et al., *A relationship between protein stability and protein function.* Proc Natl Acad Sci U S A, 1995. **92**(2): p. 452-6.
12. Nagatani, R.A., et al., *Stability for Function Trade-Offs in the Enolase Superfamily "Catalytic Module".* Biochemistry, 2007. **46**(23): p. 6688-6695.
13. Acton, Q.A., *Enzymes and Coenzymes—Advances in Research and Application: 2012 Edition*. 2012: ScholarlyEditions.
14. Huang, X., D. Gao, and C.G. Zhan, *Computational design of a thermostable mutant of cocaine esterase via molecular dynamics simulations.* Org Biomol Chem, 2011. **9**(11): p. 4138-43.
15. Paly, D., et al., *Plasma cocaine concentrations during cocaine paste smoking.* Life Sci, 1982. **30**(9): p. 731-8.

Chapter 6

Conclusions and Future Directions

In just under two decades, cocaine esterase went from a little known enzyme dwelling in the *Rhodococcus MB1* bacteria growing in the soil near the roots of the *Erythrozylum coca* plant to a valid candidate for treating cocaine toxicity and addiction in humans. For over ten years of that journey, we have been engineering cocaine esterase into a future therapeutic. Our earliest efforts to engineer this protein included increasing the thermostability profile of the enzyme, elucidating the metabolic profile of the enzyme, and its breakdown in circulation[1-4] (reviewed in [5]). During these studies, two different aspects of the enzyme became clear and needed to be addressed: 1) the short in vivo half-life of CocE; and, 2) increasing the overall efficiency of CocE. The research contained in Chapters 2 - 5 of this thesis addressed these issues.

The major findings of the studies in the previous three chapters can be summarized as follows:

- PEGylation of CocE occurs at a single cysteine residue (C551), and attachment of one or two additional PEG molecules per monomer will generate 24 hr further protection (>72 hr in total).

- Cocaine may temporarily bind to CocE at a site outside of the catalytic triad in a putative docking site prior to moving into the active site for hydrolysis
- CocE mutant CCKQ-Ala^{51}Glu:Ser^{288}Thr produced the best catalytic efficiency of any enzyme from our lab to date.

Combining these results to generate a PEG-CCKQ-Ala^{51}Glu:Ser^{288}Thr-CocE protein may provide the best candidate for treating cocaine addiction to date.

Though this CocE mutant offers the most desirable kinetics for breaking down cocaine *in situ*, two immediate issues need resolving. These issues are: 1) The ability of CocE to recondition away from cocaine seeking; and, 2) CocE's ability to metabolize cocaine for longer than 3-4 days.

One of the most common questions/critiques to this work is that all of our *in vivo* assays demonstrate protection against cocaine toxicity; however, we are attempting to produce a protein-based therapeutic to treat cocaine addiction. The previous research to support CocE as a tool to provide the reconditioning against cocaine seeking behavior has not been discussed in this thesis so far, but needs addressing. The study covered in Collins *et al* demonstrates the ability of RQ:CocE to alter the cocaine seeking behavior of rats that have been conditioned to seek cocaine[6]. By dosing rats with RQ:CocE, their cocaine craving decreases demonstrated their response to cocaine injection dropping to the same level as saline injection. (Figure 6.1) As the data shows, at higher

concentrations of cocaine, the reconditioning away from cocaine seeking behavior provided by CocE begins to wane.

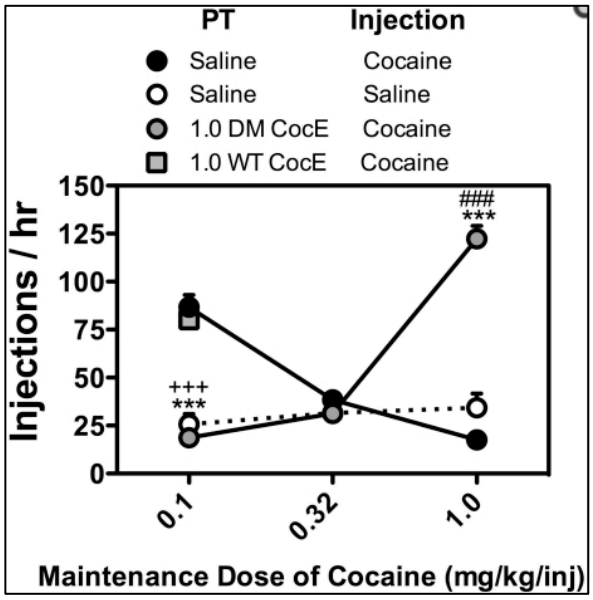

Figure 6.1: CocE can recondition rats away from cocaine seeking behavior. Rats, conditioned to self-administer cocaine, were pretreated with either saline or CocE [WT or RQ (DM)]. During an hour observation period, rats treated with RQ CoE sought cocaine at the same level as those responding to saline.

We hypothesize that having a more efficient enzyme, especially if we are able to improve the K_M value of our best mutant, Ala^{51}Glu:Ser^{288}Thr-CCKQ, then we will provide the best candidate for treating cocaine addiction. To that end, we feel that additional mutations on top of our current, optimized version could hold the key to unlocking an even more efficient enzyme and potential therapeutic. The discussion of each mutation provided a rational for the biochemistry that resulted from the mutations. By expanding the number of mutations at each position, we could further expand on this explanation and develop a more

complete model of CocE than what we currently have, in terms of catalytic efficiency and stability.

Though we have achieved a level of success in extending the *in vivo* activity of CocE using PEGylation, we hypothesize that extending limit could be achieved through coupling PEG:CocE with another method of formulation that we have tried previously.

One of the early attempts to extend the *in vivo* activity of CocE involved encapsulating PEG:CocE into the biodegradable polymer, PLGA, poly(lactic-co-glycolic acid). PLGA encapsulation has been used as a method to provide sustained release of therapeutic molecules[7, 8]. Briefly, a small molecule or protein is trapped within a millicylinder or nanoparticle of PLGA. Once the nanoparticle is inserted into the skin of an animal, the PLGA polymers begin to degrade and the target drug is released into the circulation of the animal. Release from PLGA millicylinder can proceed for up to 45 days [9].

In a collaborative effort with Steven Schwendeman (University of Michigan), we attempted to encapsulate PEG-CCKQ CocE in PLGA nanoparticles. Our efforts to obtain a nanoparticle of PEG:CocE were marginally successful. During the majority of the encapsulation experiments, the protein aggregated during encapsulation; however, on our last effort, we were able to recover soluble protein from a nanoparticle.(Figure 6.2A and B)

Unfortunately, we were unable to detect any activity in this protein. (Figure 6.2C) Though we were not able to generate any useable material, we were

encouraged by the success of the collaborating group's ability to deliver other therapeutic proteins[10]. If we are able to build on this preliminary result, we could potentially extend the protective effect of CocE from several days to several weeks.

If we are able to deliver the most effective enzyme for hydrolyzing cocaine for over a month to an addict, we believe that this therapeutic will indeed be a strong competitor to address the unmet need of an FDA approved therapeutic to treat cocaine addiction.

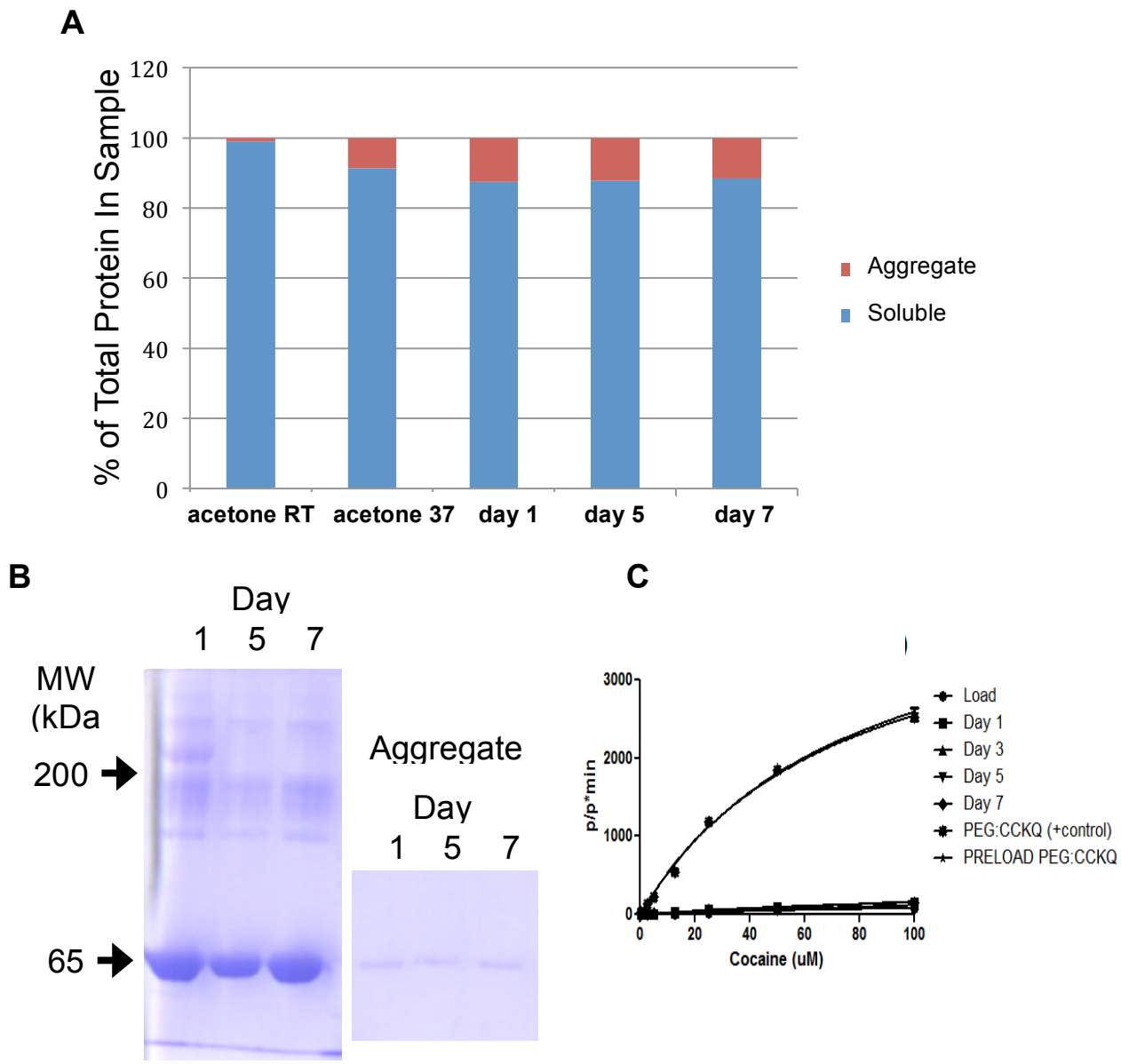

Figure 6.2 PLGA encapsulation data with CCKQ-CocE. A) Quantification of CocE that aggregated during PLGA encapsulation. Acetone RT = acetone at room temperature, acetone 37 = acetone warmed to 37°C prior to mixing with PLGA and protein mixture. B) SDS-PAGE of samples from PLGA released protein during time course. Left lanes show soluble material released, and right lanes contain aggregated material. C) CocE activity assay performed with soluble material released from PLGA millicylinder. Only PEG-CCKQ and PRELOAD PEG-CCKQ (sample prior to mixing in acetone:PLGA solution) show activity.

In summary, we feel that we have made great progress toward developing a treatment for the cocaine addiction and intoxication. We have used a structure-based approach to understand the catalytic mechanism of cocaine esterase. With these models in hand we have used the structure to designed, engineered and tested mutant forms of cocaine esterase with superior catalytic properties and stability. We will continue to take this structure-based approach to optimize and engineer this enzyme and make a safer, more efficacious treatment for this devastating disease.

References

1. Brim, R.L., et al., *A thermally stable form of bacterial cocaine esterase: a potential therapeutic agent for treatment of cocaine abuse.* Mol Pharmacol, 2010. **77**(4): p. 593-600.
2. Brim, R.L., et al., *The fate of bacterial cocaine esterase (CocE): an in vivo study of CocE-mediated cocaine hydrolysis, CocE pharmacokinetics, and CocE elimination.* J Pharmacol Exp Ther, 2012. **340**(1): p. 83-95.
3. Brim, R.L., et al., *The ability of bacterial cocaine esterase to hydrolyze cocaine metabolites and their simultaneous quantification using high-performance liquid chromatography-tandem mass spectrometry.* Mol Pharmacol, 2011. **80**(6): p. 1119-27.
4. Gao, D., et al., *Thermostable variants of cocaine esterase for long-time protection against cocaine toxicity.* Mol Pharmacol, 2009. **75**(2): p. 318-23.
5. Narasimhan, D., J.H. Woods, and R.K. Sunahara, *Bacterial cocaine esterase: a protein-based therapy for cocaine overdose and addiction.* Future Med Chem, 2012. **4**(2): p. 137-50.
6. Collins, G.T., et al., *Cocaine esterase prevents cocaine-induced toxicity and the ongoing intravenous self-administration of cocaine in rats.* J Pharmacol Exp Ther, 2009. **331**(2): p. 445-55.
7. Han, F.Y., et al., *Bioerodable PLGA-Based Microparticles for Producing Sustained-Release Drug Formulations and Strategies for Improving Drug Loading.* Front Pharmacol, 2016. **7**: p. 185.
8. Xu, Y., et al., *Polymer degradation and drug delivery in PLGA-based drug-polymer applications: A review of experiments and theories.* J Biomed Mater Res B Appl Biomater, 2016.

9. Klose, D., et al., *PLGA-based drug delivery systems: importance of the type of drug and device geometry.* Int J Pharm, 2008. **354**(1-2): p. 95-103.
10. Jiang, W., et al., *Biodegradable poly(lactic-co-glycolic acid) microparticles for injectable delivery of vaccine antigens.* Adv Drug Deliv Rev, 2005. **57**(3): p. 391-410.